



This work is licenced under the agreement „Attribution Non-Commercial No Derivatives – 2.5 Switzerland“.  
The complete text may be viewed here:  
[creativecommons.org/licenses/by-nc-nd/2.5/ch/deed.en](http://creativecommons.org/licenses/by-nc-nd/2.5/ch/deed.en)

## **Pharmaceutical Process Technology: from new materials to new technologies.**

Chapters:

**Application of cellulose type II in a pulsatile drug delivery system.**

**Influence of the drug load, liquid addition rate and batch size on the  
power consumption profile during wet granulation process.**

**Artificial Neural Network applied to pharmaceutical  
granulation process.**

### **Inauguraldissertation**

zur

Erlangung der Würde eines Doktors der Philosophie

vorgelegt der

Philosophisch-Naturwissenschaftlichen Fakultät

der Universität Basel

von

**Elaine Darronqui**

aus Santa Fé - PR, Brazil

Basel, 2010



## Attribution-Noncommercial-No Derivative Works 2.5 Switzerland

---

### You are free:



to Share — to copy, distribute and transmit the work

### Under the following conditions:



**Attribution.** You must attribute the work in the manner specified by the author or licensor (but not in any way that suggests that they endorse you or your use of the work).



**Noncommercial.** You may not use this work for commercial purposes.



**No Derivative Works.** You may not alter, transform, or build upon this work.

- For any reuse or distribution, you must make clear to others the license terms of this work. The best way to do this is with a link to this web page.
- Any of the above conditions can be waived if you get permission from the copyright holder.
- Nothing in this license impairs or restricts the author's moral rights.

**Your fair dealing and other rights are in no way affected by the above.**

This is a human-readable summary of the Legal Code (the full license) available in German:  
<http://creativecommons.org/licenses/by-nc-nd/2.5/ch/legalcode.de>

**Disclaimer:**

The Commons Deed is not a license. It is simply a handy reference for understanding the Legal Code (the full license) — it is a human-readable expression of some of its key terms. Think of it as the user-friendly interface to the Legal Code beneath. This Deed itself has no legal value, and its contents do not appear in the actual license. Creative Commons is not a law firm and does not provide legal services. Distributing of, displaying of, or linking to this Commons Deed does not create an attorney-client relationship.

Genehmigt von der Philosophisch-Naturwissenschaftlichen Fakultät  
auf Antrag von

Prof. Dr. H. Leuenberger,  
Dr. G. Betz  
Und  
PD Dr. P. van Hoogevest

Basel, den 21. September 2010

Professor Dr. Martin Spiess  
Dekan

**aos meus pais e irmã**

## ACKNOWLEDGEMENTS

I would like to express my sincere gratitude to:

First of all, thanks to The Creator and our Redeemer.

Professor Hans Leuenberger, who accepted me as a PhD student under his supervision, making all this work possible.

Coordenação de Aperfeiçoamento de Pessoal de Nível Superior – CAPES, Brazil, for to believe in this work and honor me with its maximum grant.

PD. Dr. Peter van Hoogevest, who accepted assuming the co-reference of this work.

Many thanks to Dr. Gabriele Betz, not only my thesis advisor, but the one who brought encouragement, positivity and showed the right thing to do when the wrong one was already done.

Special thanks to Mr. Stefan Winzap for his continue availability and logistic support.

Thanks to everyone that is a member, or was one, of Industrial Pharmacy Lab Group and Institute of Pharmaceutical Technology: Ms. Sonja Reutlinger, Dr. Murad Rumman, Dr. Maxim Puchkov, Dr. Maja Pasic, Dr. Vincenzo Balzano, Dr. Etienne Krausbauer, Dr. Muhanned Saeed, Mr. Miki Yamashita, Mr. Theophile Sebgo, Ms. Lizbeth Martínez, Mr. Nikos Gentis, Mr. Branko Vranic, Ms. Felicia Flicker, Dr. Ervina Hadzovic, Dr. Selma Sehic, Mr. Firas Alshihabi and many others that were present and created the perfect *atmosphere* for sharing life experiences, knowledge and their friendship.

Special thanks to Dr. Miriam Reiser and Ms. Ivana Vejnovic for, not only share the lab space with me, but also to share life moments and offer me great friendship. To Mr. Sameh Abdel-Hamid and Dr. Imjak Jeon, my colleagues in the practical teaching, for their patience, respect and great fellowship. To Dr. Krisanin Chansanroj for accompany me in new experiences and also helping me with her knowledge.

To Ms. Martina Schillinger who worked with me during her master thesis.

Thanks to Dr. Svetlana Ibric, Dr. Jelena Petrovic and Dr. Branka Ivic from Faculty of Pharmacy - University of Belgrade for the cooperative work and warm host.

To Dr. Jorgete Constantin and Dr. Osvaldo Cavalcanti, my former professors, and now life coach's.

Polyana, Francisco and Kelnner, my family in Basel, without you it would have been much more difficult. Obrigada demais!

To all my friends in Basel who made my *out-of-university life* very happy and promoted me great moments.

To all my friends in Brazil, those ones that even with big distance were always closely present, supporting me in the most varied topics. "Valeu mesmo!"

To my parents, Iria and Germano, and my sister, Silvia, for their love and support through the years.

“Post Tenebras Lux”

## TABLE OF CONTENTS

Abbreviations.....	- 9 -
<b>Thesis Summary.....</b>	<b>- 10 -</b>
<b><u>First Chapter.....</u></b>	<b><u>- 15 -</u></b>
<b><u>1 Theoretical Section.....</u></b>	<b><u>- 16 -</u></b>
1.1 Pharmaceutical powders – Excipients .....	- 16 -
1.2 Multifunctional Excipients and disintegrant aids.....	- 17 -
1.3 Cellulose derivatives: Cellulose type II.....	- 20 -
1.4 Percolation Theory in Pharmaceutical Technology .....	- 23 -
1.5 Modified (oral) Drug-Delivery Systems and the coating process.....	- 26 -
1.6 Delayed Drug Release and Chronotherapy .....	- 29 -
<b><u>2 Material.....</u></b>	<b><u>- 33 -</u></b>
2.1 Model Drug .....	- 33 -
2.2 Excipients.....	- 33 -
2.2.1 Cellulose Type II Polymorph .....	- 33 -
2.2.2 HPMC.....	- 34 -
2.2.3 Magnesium Stearate.....	- 34 -
2.3 Storage .....	- 34 -
<b><u>3 Methods.....</u></b>	<b><u>- 35 -</u></b>
3.1 Powder Characterization .....	- 35 -
3.1.1 Scanning Electron Microscopy (SEM).....	- 35 -
3.1.2 Particle Size Determination.....	- 35 -
3.1.3 Moisture Content .....	- 35 -
3.1.4 Densities.....	- 35 -
3.1.5 Hausner Ratio and Compressibility Index .....	- 36 -
3.1.6 Packing fraction and Porosity .....	- 36 -
3.2 Granulation .....	- 36 -
3.2.1 Equipment and Preparation .....	- 37 -
3.2.2 Power Consumption Measurement.....	- 37 -

3.3 Granules Characterization.....	- 38 -
3.3.1 Particle Size Determination.....	- 38 -
3.3.2 Moisture Content .....	- 38 -
3.3.3 Densities.....	- 38 -
3.3.4 Hausner Factor and Carr's Index .....	- 38 -
3.3.5 Crushing Strength of granules .....	- 38 -
3.3.6 Scanning Electron Microscopy (SEM).....	- 38 -
3.4 Tablet Compaction.....	- 39 -
3.4.1 Equipment and Process.....	- 39 -
3.5 Tablet Characterization .....	- 39 -
3.5.1 Tablet Dimensions.....	- 39 -
3.5.2 Crushing Strength (Failure Force) and Tensile Strength .....	- 39 -
3.5.3 Friability .....	- 40 -
3.5.4 Porosity .....	- 40 -
3.5.5 Scanning Electron Microscopy (SEM).....	- 41 -
3.5.6 Disintegration.....	- 41 -
3.5.7 Dissolution.....	- 41 -
3.6 Tablet Coating .....	- 43 -
3.6.1 Coating Polymers and adjuvants .....	- 43 -
3.6.1.1 Eudragit® RS 30D and RL 30D .....	- 43 -
3.6.1.2 Aquacoat® ECD 30% (Ethylcellulose Aqueous Dispersion) .....	- 45 -
3.6.1.3 Triethyl Citrate - TEC .....	- 47 -
3.6.1.4 Hypromellose (pore former) .....	- 48 -
3.6.2 Equipment and Coating Process.....	- 49 -
3.6.3 Coating Characterization .....	- 53 -
3.6.4 In vitro Drug Release Test .....	- 53 -
3.6.4.1 Mathematical Models and other release parameters.....	- 53 -
<b><u>4 Results and Discussion .....</u></b>	<b><u>- 55 -</u></b>
4.1 Characterization of Starting Materials.....	- 55 -
4.2 Granulation .....	- 56 -
4.2.1 Granules visual appearance and Crushing Strength .....	- 58 -
4.2.2 Particle Size Distribution (PSD) .....	- 59 -
4.2.3 Power Consumption .....	- 60 -
4.3 Compaction.....	- 62 -
4.3.1 Visual Appearance of Tablets' surfaces and internal structures .....	- 64 -
4.4 Coating.....	- 67 -

4.4.1	Monitoring of the coating application process and coating quality .....	- 67 -
4.4.2	Visual Appearance of coating surfaces, its homogeneous distribution and thickness .....	- 70 -
4.5	Drug Release Studies .....	- 72 -
4.6	Conclusion .....	- 85 -
4.7	Appendix .....	- 86 -
<b>5</b>	<b><u>References of chapter I .....</u></b>	<b>- 87 -</b>
	<b><u>Second Chapter .....</u></b>	<b>- 95 -</b>
<b>6</b>	<b><u>Introduction.....</u></b>	<b>- 96 -</b>
6.1	Agglomeration process and control: background.....	- 97 -
<b>7</b>	<b><u>Experimental details.....</u></b>	<b>- 102 -</b>
7.1	Materials .....	- 102 -
7.2	Methods .....	- 102 -
7.2.1	Characterization of starting material .....	- 102 -
7.2.2	Granulation design and procedure.....	- 102 -
7.2.3	Power consumption profile recording.....	- 103 -
7.2.4	Granules characterization.....	- 103 -
7.2.5	Calculations of Liquid Saturation and Power Number .....	- 104 -
<b>8</b>	<b><u>Results and discussion.....</u></b>	<b>- 106 -</b>
8.1	Characterization of starting material .....	- 106 -
8.2	Liquid Saturation .....	- 107 -
8.3	Comparison of the power consumption profiles of three different formulation mixtures: the effect of a poor water soluble drug load .....	- 110 -
8.4	Influence of the mixer bowl filling (mixer load) in the power consumption profile: scale- up invariants.....	- 113 -
8.5	Effect of the liquid addition rate on the power consumption profile .....	- 115 -
8.6	Granule size analysis .....	- 118 -
8.7	Conclusion .....	- 121 -
<b>9</b>	<b><u>References of chapter II .....</u></b>	<b>- 123 -</b>



<b>Third Chapter.....</b>	<b>- 127 -</b>
<b>10 Introduction.....</b>	<b>- 128 -</b>
Artificial Neural Networks – ANNs .....	- 130 -
Genetic Algorithms – GAs .....	- 131 -
<b>11 Materials and Methods .....</b>	<b>- 133 -</b>
11.1 Granulation materials .....	- 133 -
11.2 Characterization of starting material .....	- 133 -
11.3 Granulation Design and Procedure .....	- 133 -
11.4 Power consumption profile recording .....	- 134 -
11.5 Characterization of collected samples .....	- 134 -
11.6 Computation Methods .....	- 134 -
<b>12 Results and Discussion .....</b>	<b>- 137 -</b>
<b>13 Conclusion.....</b>	<b>- 144 -</b>
<b>14 References of chapter III.....</b>	<b>- 146 -</b>
<b>15 Thesis Outlook .....</b>	<b>- 149 -</b>

## Abbreviations

% v/v	percentage by volume
% w/w	percentage by weight
-wt	by weight
AGU	Anhydroglucose Unit
ANN	Artificial Neural Network
API	Active Principle Ingredient
BCS	Biopharmaceutics Classification System
DDS	Drug Delivery Systems
DP	Degree of Polymerization
EC	Ethylcellulose
FDA	Food and Drug Administration
GAs	Genetic Algorithms
GIT	Gastrointestinal tract
GRAS	Generally Recognized as Safe
HPMC	Hydroxypropyl Methylcellulose
MAX	Maximum value in Power Consumption measurement
MCC	Microcrystalline Cellulose
MFT	Minimum Film-forming Temperature
NMT	Not more than
PC	Power Consumption
PCM	Paracetamol
PF	Pore Former
ppm	parts per million
PQZ	Proquazone
PSD	Particle Size Distribution
rpm	rounds per minute
Sc	Crushing Strength
SD	Standard Deviation
SE	Standard Error
SEM	Scanning Electron Microscopy
TEC	Triethyl citrate
TG	Target Granules
UICEL	University of Iowa Cellulose
USP	United States Pharmacopeia
w.g.	Weight gain

## Thesis Summary

In the **first chapter** of this thesis an investigation of the influence of cellulose type II in the drug release from a coated tablet is presented. The cellulose II product can be obtained by mercerization (chemical treatment with sodium hydroxide) from cellulose I (e.g. Avicel PH102) and is suitable to be used in tableting as a multipurpose excipient. Once organic solvents have been avoided in the pharmaceutical industry it was decided to apply an aqueous coating dispersion. As this polymorphic form of cellulose also acts as a super disintegrant, carrying out an aqueous coating process could be a challenge. The model drug used was the poor water-soluble proquazone, a BCS class II drug.

First of all, the manufacture of the tablet core was already a challenge in itself due to the powder mixture being not flowable enough to be used in a rotary tablet press, in which the feed system is basically a simple hopper. To overcome this undesirable situation a wet granulation process was executed, and for monitoring the process, as well to study the powder agglomeration behavior, power consumption method was applied. The decision of to use this method as a monitoring tool during the wet granulation process originated further studies, that are shown and compose the second chapter of this thesis. The power consumption showed to be a very useful tool to monitor and control the granulation in real-time. Complete powder and granules characterization was done and is presented. Compaction studies were not the focus of this work. Nevertheless, they had been executed in other prior studies cited in the references. The tablet cores manufactured were characterized and showed to be robust enough to surpass the coating process. The initial idea of use a pan coating (a process that is known to be gentler and causes less damage to the cores) was shifted to a lab scale fluidized bed because of the load of tablets necessary to pan coating be much larger than for the fluidized bed. Tablet cores composed of high amounts of cellulose II were sensitive to the aqueous coating, which could be identified by the coating defects found. However, the process could be optimized and the source of defects eliminated adjusting parameters such as the sprayed droplets size, spray rate, bed temperature, and total solids content in coating suspension, for example. Those actions reduced the contact time between the core and water, minimizing water penetration, and thus avoiding some damage on the core surface and/or premature core disintegration. In principle, different aqueous coating systems were used: Eudragit<sup>®</sup> RS and RL and Aquacoat<sup>®</sup> ECD. The drug release studies showed that methacrylic copolymers were more flexible and kept the integrity of the reservoir, promoting a more sustained drug release through the pores. On the other hand, the ethylcellulose polymer was brittle and did rupture, promoting a burst drug release. After these results, the decision of continue further studies

with Aquacoat<sup>®</sup> ECD was taken, in order to investigate the application of the cellulose type II as a hygroscopic and expansive agent for pulsatile drug-release systems.

Many coating levels were applied in cores of three formulations (composed of different ratios of drug:excipient). The presence of a pore former (hydroxypropylmethylcellulose) in the coating layer was also analyzed. The lag time before coating rupture was shown to be directly proportional to the coating thickness and inversely proportional to the amount of pore former. It showed also to be directly dependent to the level of cellulose type II present in the cores. Higher ratios of the multifunctional excipient promoted faster, and probably larger, water uptake leading to an increase of internal osmotic pressure responsible for the separation of the coating from the core and for the core erosion. Except for a delay, the release kinetics of the drug contained in the core was not significantly influenced by the presence of the rupturable barrier, but instead for the erosion and disintegration of the core. Using model-independent approaches it could be confirmed that the release of the drug after coating rupture happened fast, in a single pulse. According to percolation theory, the tablet core consists of clusters of particles which form a network. This theory provided useful explanations to describe the composition and formation of the tablet and the distribution of the pores and particles within it. It could be concluded that use of cellulose II polymorph can be a good opportunity to develop a simple modified-drug-delivery-system, able to facilitate a rapid drug release after a lag time, and based on approved and well known excipients and also applying conventional and non-expensive processes.

On the **second chapter** of this thesis an investigation of the influence of drug load, liquid addition rate and batch size on the *power consumption profile* recorded during a high shear mixer granulation is presented. In the pharmaceutical industry the moist agglomeration process by high-shear mixing is a critical unit operation that remains more of ‘an art’ than a science-based approach. Because of the difficulties associated with the direct measurement of particle characteristics, such as particle size distribution, moisture contents and deformability, some indirect monitoring parameters have been adopted as the indicators of particle characteristics. A commonly accepted monitoring parameter in the pharmaceutical industry is the equipment power consumption technique.

The materials used in this study were the wide-spread filling microcrystalline cellulose and the poor water-soluble drug paracetamol. In all formulations hydroxypropylmethylcellulose was added as a dry binder into the mixture, and distilled water as the granulation liquid. The equipment was a lab scale high-shear mixer with 10 liters of volume. The power consumption of the mixer motor (i.e. main impeller) was measured by a transducer, converted into an electric potential signal, sampled by a multifunction card to a laptop computer, and displayed graphically by an “in process” computer calculation program.

In order to investigate the influence of drug load three formulations were designed containing different ratios of drug:excipients. For the liquid addition rate comparison, the granulation liquid was added using a peristaltic pump under constant addition speeds, two main ones, until the powder mixture become a slurry. Finally, the influence of working vessel filling in the powder agglomeration, and thereafter in energy consumption profile, was studied loading the equipment with different batch sizes. A complete starting material characterization is presented as well as a granule size analysis comparing formulations and the influence of the different compounds ratio in the behaviour of agglomerates growth kinetics. Also here, percolation theory could be applied to describe the growth behaviour and granules properties. The mass liquid saturation, expressed by the amount of liquid ( $\pi_2$ ) and the degree of saturation ( $\pi$ ), were calculated for the entire process and used to compare different moments of the granulation and also facilitate the comparison among formulations. For better understanding of the process the dimensionless Power Number ( $\pi_1$ ) which is applied to analyze process similarities between different scales was calculated too.

It was found that the powder physicochemical properties strongly affect the liquid saturation, by influencing the amount of liquid penetration and the free surface liquid which is necessary for the coalescence of primary particles and/or agglomerates, and consequently affecting the power consumption profile. Those influences also affect the rate of granule breakage wherefore affecting the energy consumption too. Thus the drug load showed to be the most influential factor on power consumption measurement. The measurement of power as defined by the parameters S3, S4, S5 was practically independent of the batch size. The granulation liquid requirement was linearly dependent of the mass loaded. The liquid addition rate made a slight impact on the total amount of water used in the process, and in the granulate growth kinetics. The granules cumulative weight fractions of the three binary-mixtures at a fixed  $\pi$ -value presented similarity but it was dependent of the proportion of the compounds. The “in process” measurement of power consumption showed to be a reliable analytical tool for monitoring the moisture content and particles agglomeration growth, thus making it a science-based real-time control.

From the data generated in the granulation studies another question arose: Would be possible *to predict* the power consumption curve? The conclusion is given in the **third chapter** of this thesis.

In a collaboration project with University of Belgrade the use of an Artificial Neural Network - ANN software to predict the characteristics of a wet granulation process was studied. The initial aim of using an expert system was to try directly predict the profile of power consumed during a granulation process; using as inputs (data used to supply the system

with information) properties of the starting material as well as process variables. After some weeks learning how to work with the artificial intelligence software, an extra time was dedicated in the first step of building a network: the data mining. In the so called 'preprocessing' step *data preparation* is carried out. That is a fundamental and very important step once that the software will *learn by observation* of the data presented to it. Which data and how to input it will make big differences in the resulted output (feature(s) that you want to predict). As inputs six formulation and process parameters were chosen, named Time (in minutes), Drug concentration, MCC concentration, HPMC concentration (all in % by weight of total formulation), Batch Size (grams) and Granulation-Liquid Added (grams). The output was the absolute power value (watts). Each of those features represents one column and the data/values were arranged in the rows and sorted in an ascending order, i.e. in a time sequence. All experiments were collated in a single excel sheet and converted to a CVS file. From the overall data an amount equivalent to 14.25% was selected for validation of the system, it corresponded to 3 experiments. As the experimental values were a time series, i.e. they are in time sequence, the order of the data is important to avoid that the software when taking a value doesn't break the sequence, leading to a misunderstanding/misinterpretation of the data. Other 3 experiments (one for each formulation) were kept out of the inputted data set in order to be used to test the trained system. After to input the data into the system evaluations over the raw data itself were carried out such as linear correlation between features, frequency histograms, clustering visualizer (Self-Organizing Map), values plotted versus samples as well as  $f(x)=y$  plots. From these tools of data mining was decided to remove the HPMC concentration as an input, once that it showed to have no influence over the output. It was due this excipient be present at the same concentration in all experiments. As the data is a time series sequence of values, in the network design step a dynamic network was selected from the software snippet library. After properly connecting all the blocks creating the network topology, the system was trained in different ways looking for the most suitable training parameters for that specific data set and specific network. The more relevant changes were found to be in the choice of how many samples to take in to account for each update of the system parameters, i.e. the batch length. Preferably the batch length should be chosen so that the full length is a multiple of the batch length. Failing to have it can result in samples being cropped. In order to avoid the samples being cut a batch length of 1 was chosen. This choice could result in slowing down the system as it results in more updates per epoch, however it can help to avoid local minima and make up the lack of precision. Another relevant point during training was the amount of times that the collection of all available samples (rows) enters the system, called *epoch*, and is the same as *iteration* (repetition). When one epoch has passed, the adaptive system has been presented with the available

data once. Many epochs are usually required to fully train the system. However for small amount of samples the system can become over-trained easily and hence not being able to execute reliable generalizations. The number of epochs was kept small. Different snippets (that are fragments of networks) were analyzed and the one that showed reduced error and better predictions was a so called Gamma-Recurrent Hybrid network (after be optimized using a genetic algorithm). After training, the system was tested using the 3 experiments left out of the inputted data set. The resulted predictions showed that the aforementioned network was able to satisfactory predict the power consumption curve of formulations containing higher amounts of excipients. For the formulation with higher drug load (90% w/w of paracetamol) the predictions were unsatisfactory. It was not possible to predict the accentuated slope, plateau and faster drop in the power consumption for that formulation. The experimental granulation process executed for the higher drug load formulation generated more irregular power consumption curves/profiles and that wide variability among the inputted samples could result in a *difficult learning* from the system, and can be the reason for the lack of network precision in predicting the behaviour of this formulation. Post-processing tools were also used to evaluate the system performance. The absolute error for the prediction of the power consumption value was 76,35; relatively small compared with other systems tested. The output prediction accuracy of +/- 201.34 was within the desired 95% confidence. A sensitivity analysis, i.e. how much the output changes if an input feature is changed at certain percentage, was done and is discussed in the results. Another way to work with the granulation power consumption using an ANN was tested. Submitting as inputs some formulation properties as drug concentration, excipient concentration, bulk density and residual moisture of the power mixture, batch size and equipment filling fraction as well as the granulation liquid addition rate, it was tested the ability of an adaptive system to predict the relevant S2, S3, S4 and S5 points of a typical Leuenberger power consumption profile. The networks that resulted in higher values in the  $R^2$  coefficient are the generalized one layer and generalized two layer. They are extensions of the standard Multi-Layer Perceptron, a basic static feedforward backpropagation neural network. The systems were trained for a very short time and using small batches. No optimization was necessary. Predicting the future output of very complex systems is a difficult task. Adaptive systems however have shown themselves, trained on the right data, quite capable of producing good predictions. They perform consistently better than more traditional methods.

## First Chapter

**Application of cellulose type II in a pulsatile drug delivery system.****Abstract**

Microcrystalline Cellulose, and its modifications, is a well known and widely used excipient in the pharmaceutical industry. Cellulose II product, that is obtained by mercerization from cellulose I polymorph, shows to behave as a multifunctional excipient, working as both a filler and super disintegrant. The objective of the presented work was to investigate the possibility to create a Pulsatile Drug Delivery System based on Rupturable Coating using the cellulose II polymorph as a hydration agent, as well as to check the behavior of this super disintegrant during an aqueous coating process. Three binary mixtures containing cellulose II and proquazone, a poor water soluble drug, were produced in different proportions. The amounts of cellulose II in the mixtures were 08, 48 and 88 percent (w/w). In all formulations 2% of Hydroxypropylmethylcellulose was added as a dry binder into the mixture. Granules in a range of 125 - 710 $\mu$ m of particle size were collected after the wet granulation of the powder mixtures using a lab scale high shear mixer and distilled water as the granulation liquid. Power Consumption method was used to monitor the granulation process. Granules were compacted into tablets using a Korsch<sup>®</sup> rotary press. The deep concaved tablet cores were coated in a bottom spray lab scale fluidized bed coater with Eudragit RS<sup>®</sup> 30D, Eudragit RL<sup>®</sup> 30D and Aquacoat ECD<sup>®</sup> 30%. Subsequently the drug release profile was analyzed. The results showed that an aqueous-based coating process is possible even in a core composed of high loads of a super disintegrant when the proper parameters are set. Special care must be taken regarding the inlet air temperature, atomizing air pressure and spray rate. The release of the drug showed to be dependent on the coating polymer type, the thickness of the coating layer and tablet core composition. A sustained drug release with no lag time was obtained using different mixtures of Eudragit<sup>®</sup> polymers. A delayed drug release, with a sigmoidal curve, and presenting different lag times according to the coating thickness, was obtained with Aquacoat. With thinner coating layers the lag time (between the tablets containing 48 and 88 percent of cellulose II) were similar, showing the influence of this excipient in the core swelling and coating disruption. These findings highlight cellulose II to be used in the development of a pulsatile drug delivery system, based on approved and well known excipients while continuing to use conventional processes.

**Keywords**

Cellulose type II, multifunctional excipient, super-disintegrant, aqueous coating, pulsatile drug delivery system, chronotherapy.



## 1 Theoretical Section

*“A drug is not given to man. What is given is a preparation containing the drug” (A.H. Beckett).*

### 1.1 Pharmaceutical powders – Excipients

Excipients are components of a finished drug product other than the active pharmaceutical ingredient (API) and are added during formulation for a specific purpose. Although listed as inactive ingredients by FDA (Food and Drug Administration), excipients generally have well-defined functions in a drug product. As with active ingredients, they may be small molecule or complex and may vary in terms of degree of characterization. They may be chemically synthesized or may be either natural source or biotechnology-derived (recombinant). In contrast to active ingredients, minor components of an excipient may have significant impact on its pharmaceutical performance (U.S. Pharmacopeia, 2007). The term ‘inert’, used alone, is not suitable anymore to describe pharmaceutical excipients.

Pharmaceutical excipients are a very diverse group of materials. They cover all the states of matter: gas, liquid, semi-solid and solid. According to Baldrick (2002) excipients include diluents, fillers and bulking agents, binders and adhesives, propellants, disintegrants, lubricants and glidants, colours, flavours, coating agents, polishing agents, fragrances, sweetening agents, polymers, and waxes. A review of the literature indicates approximately 1300 excipients used in the pharmaceutical industry. They can be used in a variety of dosage forms, and some may be used for more than one route of administration. Excipients provide a wide variety of functions, such as: to improve processability of APIs into dosage forms, tablet binding and disintegration, better API stability, solubility and bioavailability.

A large proportion of pharmaceutical API and excipients are in the powder form. The manufacture of such products involves processes such as crystallisation and size reduction followed by formulation, agglomeration, compaction and tableting. It is well-known in practice that these processes can greatly influence the chemical activity and physical properties of the final product. Thus, pharmaceutical powder technology plays a major role in the manufacturing process.

The solid-handling properties of a bulk mass are influenced by any factor that can have an effect on the particle–particle interactions of constituent particles. Factors associated with the nature of the particles and their surfaces such as size, shape, surface morphology, packing conditions, and interparticle forces must therefore be considered. To make the situation more complex, the interparticle forces can be of a number of types: mechanical

forces, surface tension, electrostatic forces, van der Waals forces, solid-bridge forces, or plastic welding forces; none of these can be readily quantified (Howard, 2002).

Two of the most common processes that a powder, or more often a mixture of different powders, undergoes in the pharmaceutical field, are the ones involved in the manufacturing of solid dosage forms, e.g., granulation and compaction. More detailed explanation about wet granulation process is given in the second chapter of this thesis, as well as Power Consumption method as a granulation process monitoring tool.

The process of compaction involves subjecting the materials to stresses causing them to undergo deformation. The reaction of a material to a deformation stress is dependent on both the mode of deformation and the mechanical properties of the material (Rowe and Roberts, 1996).

That all excipients are neither truly inert nor inactive is shown by the fact that drug-excipient interactions can considerably affect the physiological availability of many drug products (Monkhouse, 1972; Jackson et al, 2000). By either accelerating or retarding the release of the active ingredients, excipients can affect the therapeutic performance of the drug by increasing or reducing bioavailability. Indeed, the properties of the final dosage form (i.e. its bioavailability and stability) are, for the most part, highly dependent on the excipients chosen, their concentration and interaction with both the active compound and each other. No longer can excipients be regarded simply as inert or inactive ingredients, and a detailed knowledge not only of the physical and chemical properties but also of the safety, handling and regulatory status of these materials is essential for formulators throughout the world. In addition, the growth of novel forms of delivery has resulted in an increase in the number of the excipients being used, and suppliers of excipients have developed novel excipient mixtures and new physical forms to improve their properties (Rowe et al, 2006).

Such roles may reflect the definition of an excipient in the U.K. legislation on medicines as “any substance which does not contribute directly to the pharmacological action of the medicinal product otherwise than by regulation of the release of the active ingredients” (Medicines Order, 1997).

## **1.2 Multifunctional Excipients and disintegrant aids**

Functionality of an excipient refers to desirable properties that aid manufacturing and improves the quality and performance of a medicinal product, according to the International Pharmaceutical Excipients Council of the Americas and U.S. Pharmacopeia. In another

words, excipients are included in the formulation because they possess properties that, in conjunction with the processing, allow the medicine to be manufactured and to meet the required specification.

Following this thinking, “multifunctional” excipients are the ones that combine two or more functions inside a formulation usually provided by single ingredients, such as glidants, lubricants, antiadherents, binders, or disintegrants. The terms *multifunctional* and *high-functionality* excipients are quite often misused, according to Moreton. For example, a material suitable for multiple processes is not the same as saying it is multifunctional in a formulation (Rios, 2006).

Defining the functionality of an excipient may not be as easy as it seems. Many excipients are by nature multifunctional and produced in various grades. Microcrystalline cellulose (MCC) is compactable, it also wicks water and can aid disintegration without aiding compaction (Rios, 2006). It is known that its performance may change as the source of the wood pulp, the pulping process, and other factors are altered. Other typical examples are lactose, which is not only a filler but makes at the same time the formulation more hydrophilic, which is important issue concerning disintegration and dissolution of a solid dosage form; and starch that can be used in low concentrations as a disintegrant and in high concentrations as a matrix for hydrophilic long acting drug release dosage forms (Leuenberger, 2006).

There are successful histories of formulators that replaced two or more different excipients for one single multifunctional excipient, leading to a less complex formulation, fewer processing steps and lower costs (Labella and McDougal, 2006).

Excipient functionality can only be assessed in the context of a particular formulation and manufacturing process. Because functionality is linked inextricably to the formulation and process, and all formulations are different, functionality per se is a matter for the excipient user and supplier. However, certain excipient properties may relate to functionality in a more general sense and can be measured and limits can be set (Moreton, 2004 and 2006). The need for functionality tests, procedures, and acceptance criteria in an excipient monograph is generally limited, given that they are dosage form related (U.S. Pharmacopeia, 2007).

Drug bioavailability from conventional solid dosage forms is only reached when the dosage form breaks apart releasing the pharmacological active ingredient. Water penetration is a necessary first step for disintegration and the ability of some adjuvants to draw water into

the porous network of a tablet is essential for effective disintegration. Most of the adjuvants with that characteristic are called disintegrants. They help in the tablet breakup by inducing the process of desegregation of constituent particles.

Since the USP first established a disintegration standard in 1948, the search for good disintegrating agents for tablet formulations has intensified. And also the recognition of the importance of bioavailability and compendial dissolution test requirements spurred the search for new disintegrants (Chien et al, 1981).

“Superdisintegrants” (Shangraw et al., 1980) are disintegrant agents with efficient disintegrating properties at relatively low concentrations, used to promote rapid breakdown of oral solid dosage forms. Generally used at levels typically 1-10% by weight relative to the total weight of the dosage unit. Examples of superdisintegrants are sodium starch glycolate (cross-linked starch), croscarmellose sodium (cross-linked cellulose) and crospovidone (cross-linked polymer). Their disintegration efficacy is correlated with their different ability to disintegrate, i.e. a combination of various properties, including particle size, hydration capacity, swelling behaviour, swelling pressure and volume (Quadir and Kolter, 2006) and differences in the particle size generated in the disintegrated tablet (Zhao and Augsburger, 2005).

Peppas et al. (1989) attribute the difference in disintegration rate between soluble and insoluble matrices to two proposed phenomena: an interface-controlled mechanism and a diffusion-controlled mechanism. The interface-controlled phenomenon involves tablet particles breaking apart from the interface of the tablet and the diffusion-controlled phenomenon involves particles diffusing away. Although it is thought that both happen simultaneously, the degree to which disintegration depends on each system can differ. Since super disintegrants are highly hydrophilic yet insoluble in water, they would be expected to be more effective in breaking the tablet apart interfacially than controlling the diffusion per se (Augsburger et al, 2002).

The study of the effect of disintegrating agents in tablets, prepared by wet granulation is more complicated because of the action of more variables, such as the method of incorporation and position, intra- and extra-granular, of the agent in the tablet. Best compromise had been obtained by using both intra- and extra-granular agents together, so that the extra-granular agents break up the tablet rapidly to the original granules and intra-granular agent then reduces the granules into the original particles (Van Kamp et al., 1983).

In addition, during the dissolving process, soluble materials that tend to swell can form viscous barriers, which may impede further penetration of moisture into the matrix, hindering dissolution. Thus the use of multifunctional filler, that can also work as a disintegrant, and is an insoluble material can be an advantage for fast disintegration tablets.

### 1.3 Cellulose derivatives: Cellulose type II

Cellulose forms the backbone of many excipients used in marketed drug products. Cellulose is the primary constituent of wood, paper and cotton. It is a carbohydrate made up of glucose units (Figure 1.3.1); these have an empirical formula  $C_6H_{12}O_6$  and can be given a cyclic structure, sometimes designated as a beta-D-glucopyranose or anhydroglucose unit (AGU). Cellulose is built up of repeating glucose units joined by  $\beta$ -1,4-glycosidic bonds.

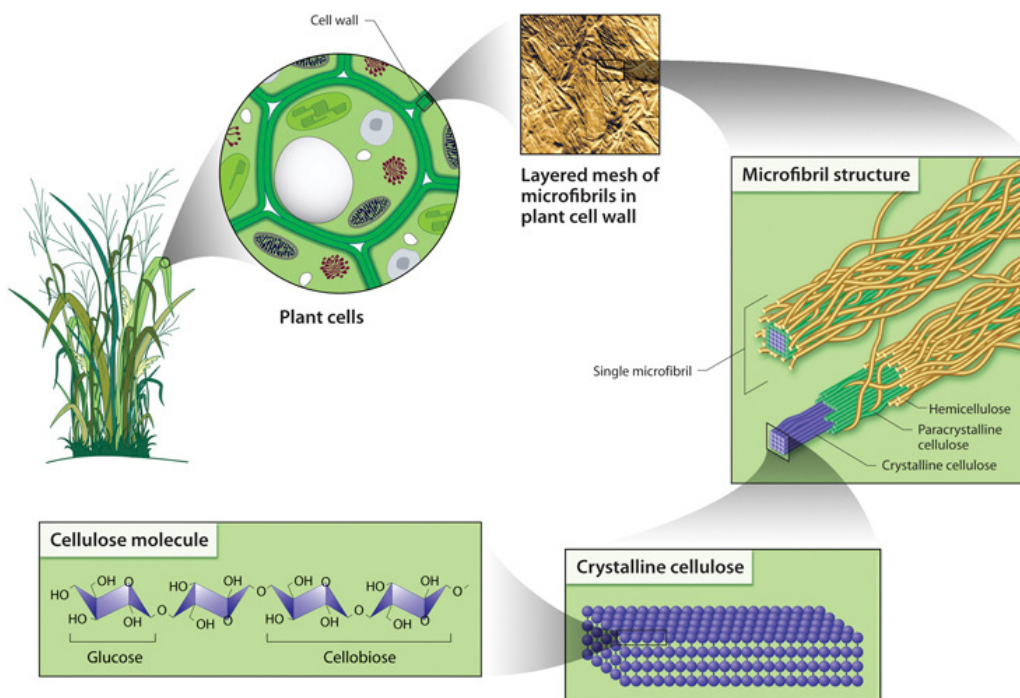


Figure 1.3.1: Cellulose Structure and Hydrolysis Challenges (Genomics: GTL Roadmap, U.S. Department of Energy Office of Science, August 2005, <http://genomicscience.energy.gov/roadmap/>)

Chain-length determination is very difficult, and average values are given, referred to the average degree of polymerization (DP), that is customarily designated as the number of AGUs in the chain. Attached to carbon atoms 2, 3 and 6 of each anhydroglucose unit is a hydroxyl group capable of undergoing chemical reactions (Bolhuis and Chowhan, 1996).

The cellulose fibres in the starting material are composed of millions of microfibrils (Figure 1.3.1). In the microfibrils, two different regions can be distinguished: a paracrystalline region, which is an amorphous and flexible mass of cellulose chains, and a crystalline region, which is composed of tight bundles of cellulose chains in a rigid linear arrangement (Bolhuis and Chowhan, 1996).

Whereas inorganic compounds often crystallize in one particular crystal system, organic compounds have the capability of crystallizing in several different (*poly*) forms (*morphs*), and this phenomenon is denoted *polymorphism*. The molecules may be in different lattices, because their orientation is different in the two different polymorphs (Cartensen, 2001).

As different polymorphic forms display diverse physicochemical properties (solubility, wettability, melting point etc.), the polymorphic form can play an important role in the quality of a drug product (bioavailability and stability, shelf life). In contrast with the polymorphism of drugs, little attention is dedicated in the study of polymorphism of excipients, despite the impact of this variable on the quality of the drug product.

It is known that cellulose can exist in four polymorphic forms, namely cellulose I, II, III and IV. The polymorphic forms can be interconverted according to Figure 1.3.2 mostly by certain chemical and thermal treatments. Among the allomorphs of cellulose, the major forms are cellulose I (native cellulose) and cellulose II (most regenerated or mercerized from native cellulose) (Zugenmaier, 2001).

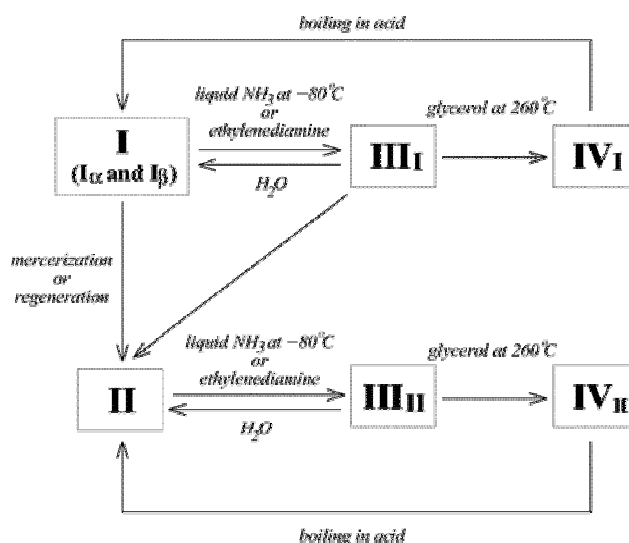


**Figure 1.3.2:** Polymorphism of cellulose and their conversions (from Kono, 2004)

Native cellulose can exist in a crystalline or non-crystalline state, as described above. Crystalline cellulose has at least two distinct allomorphs, the cellulose I and II. Both are found naturally synthesized in nature; however, the metastable cellulose I is by far the most prevalent. There are two known suballomorphs of cellulose I (cellulose I $\alpha$  and cellulose I $\beta$ ) and usually they coexist together within a given microfibril. Cellulose II is the most thermodynamically stable form, which has an additional hydrogen bond per glucose residue. Cellulose which has undergone solubilization, then re-precipitation (e.g. mercerization) is cellulose II. Cellulose I can be converted directly to cellulose II; however, the opposite cannot happen (Brown, 1999, 2004).

Microcrystalline cellulose (MCC), cellulose I powder, is widely used in pharmaceuticals, primarily as a binder/diluent in oral tablet and capsule formulations where it is used in both wet-granulation and direct-compression processes. In addition to its use as a binder/diluent, microcrystalline cellulose also has some lubricant and disintegrant properties that make it useful in tableting. It is also used in cosmetics and food products. Microcrystalline cellulose is a purified, partially depolymerized cellulose that occurs as a white, odourless, tasteless, crystalline powder composed of porous particles. It is commercially available in different particle sizes and moisture grades that have different properties and applications. Microcrystalline cellulose is manufactured by controlled hydrolysis with dilute mineral acid solutions of  $\alpha$ -cellulose, obtained as a pulp from fibrous plant materials. Following hydrolysis, the hydrocellulose is purified by filtration and the aqueous slurry is spray-dried to form dry, porous particles of a broad size distribution. Several different grades of microcrystalline cellulose are commercially available that differ in their method of manufacture, particle size, moisture, flow, and other physical properties (Galichet, 2006). As an effect of controlled hydrolysis (in MCC manufacture), the amorphous fraction has largely been removed, yielding aggregates of the more crystalline portions of cellulose fibres (Bolhuis and Chowhan, 1996).

Kumar et al. (2002) had investigated, for the first time, the use of sodium hydroxide treated cellulose powder as a direct compression excipient. They found that cellulose-derived powders (e.g. MCC, powdered cellulose (PC) and low crystallinity powdered cellulose (LGPC)), when soaked in an aqueous solution of sodium hydroxide (conc.  $\geq$  5N) and subsequently precipitated by ethanol, result in a material (hereinafter referred to as UICEL – University of Iowa Cellulose), that can be compressed into a tablet, with or without the aid of a binder. The resulting tablet rapidly disintegrates in water, suggesting that UICEL can be used as a direct compression excipient, especially in the design and development of fast-disintegrating tablets due its highly effective disintegrant activity. The powder X-ray diffractogram peaks, as well as the FT-IR (*Fourier-transform infrared*) spectra, of UICEL are

indicative of the presence of the cellulose II lattice and low crystallinity. The degree of crystallinity of UICEL ranged between about 47 and 57% (Kumar et al., 2002).

Lower degree of crystallinity causes more hydroxyl groups to be accessible for interaction with water molecules. The cellulose chain arrangements, and consequently, the hydrogen bonding network, in UICEL compared to Avicel® PH-102 may also contribute to its increased affinity for water molecules (Kumar et al., 2002).

In further comparative evaluations of powder properties and compression behaviour of cellulose type II (referred as UICEL, UICEL-A/102, MCC Sanaq Rapid) and cellulose type I (most cases Avicel® PH-102) it was concluded that cellulose II lattice has lower degree of polymerization and lower crystallinity, however shows higher true density, bulk density, tap density, Carr's index and Hausner ratio values. Compared to Avicel® the cellulose II powders were denser, shows improved flow, less ductile and more elastic; while showed much faster disintegrating properties (Kumar et al., 2002; Reus-Medina et al., 2004; Reus-Medina and Kumar, 2007b; Rumman, 2009). Ishikawa and co-workers also found that cellulose II is more hydrophilic and with a larger internal surface area of the fibres compared with other cellulose polymorphs (Ishikawa et al., 1997).

A modified cellulose type II was also prepared and investigated in order to improve its binder properties, without adversely affecting the rapid disintegration characteristics. After reaction of UICEL-A/102 with glutaraldehyde the product (referred as UICEL-XL) had a lower degree of polymerization, higher crystallinity, lower bulk and tapped density, higher porosity, less elastic, and it is more compressible and compactable, keeping similar fast disintegration, compared with the starting UICEL-A/102 (Reus-Medina and Kumar, 2007a).

The original idea proposed by Iowa group (Reus-Medina and Kumar, 2006) of the application of cellulose II polymorph as a multifunctional excipient for direct compression, acting as an all-in-one filler/binder/disintegrant, was supported by other investigations (Lanz, 2006; Müller, 2008; Rumman, 2009; Balzano, 2009).

#### **1.4 Percolation Theory in Pharmaceutical Technology**

In general the starting material for tablets is a mixture of particulate material consisting of a certain amount of fine drug powder and of appropriate amounts of excipients. A tablet formulation can be considered a *complex system* and percolation theory is a tool to a better understanding the behaviour of such a system.



Percolation theory (Stauffer, 1994) deals with the random occupation of a chosen (one-, two-, three-dimensional,  $n$ -dimensional) lattice, real or virtual, by different items (e.g. trees of a forest, atoms, molecules, nanoparticles, coarse particles, etc.). Generally, it deals with the number and properties of clusters. It is assumed that the spaces/sites are randomly occupied by the particles, of a drug for example, thus the unoccupied sites may be empty, i.e. pores, or may be occupied by an other material, e.g. an excipient. This random occupation of particles forms clusters (Leuenberger, 1999; Leuenberger et al, 1996). Such a system can be described in general as a binary one, i.e. for a better understanding, a drug formulation can be analysed as a two-component, i.e. drug/matrix carrier-system (Holmann and Leuenberger, 1980; Leuenberger, 2006).

It is generally accepted that an oil-in-water (O/W) emulsion has totally different properties to a water-in-oil emulsion (W/O), as we have either water or oil as a continuous phase. It is astonishing that many people do not make a distinction between a drug-in-excipient (D/E) and an excipient-in-drug (E/D) powder system. In the case of a poorly wettable drug and a hydrophilic filler such as lactose the formulation becomes non-robust close to the critical concentration, where the component starts to percolate (Leuenberger, 2005).

It is possible to distinguish between random *site* and *bond* percolation phenomena. In the case of bond-percolation, a group of particles is considered to belong to the same cluster only when bonds are formed between neighbouring particles. The bond probability  $p_b$  can play an important role, and can assume values between 0 and 1. When  $p_b = 1$ , all possible bonds are formed and the tablet strength is at its maximum. In order to form a stable compact it is necessary that the bonds percolate to form an 'infinite' cluster within the ensemble of powder particles filled in a die.

In site-percolation a cluster may be considered as a single particle or a group of similar particles which occupy bordering sites. The formation of clusters is a function of the occupation probability  $p$  of the lattice. In a square lattice, Figures 1.4.1 and 1.4.2, can be found an occupation probability below (Fig. 1.4.1) and above (Fig. 1.4.2) a critical concentration  $p_c$ , i.e. the percolation threshold, point where a continuous network is formed. Below  $p_c$  only isolated clusters exist, however, exactly at the critical concentration an 'infinite cluster' is formed spanning the whole lattice from left to right and from top to bottom. Thus in a *two-dimensional* lattice only one component can percolate.

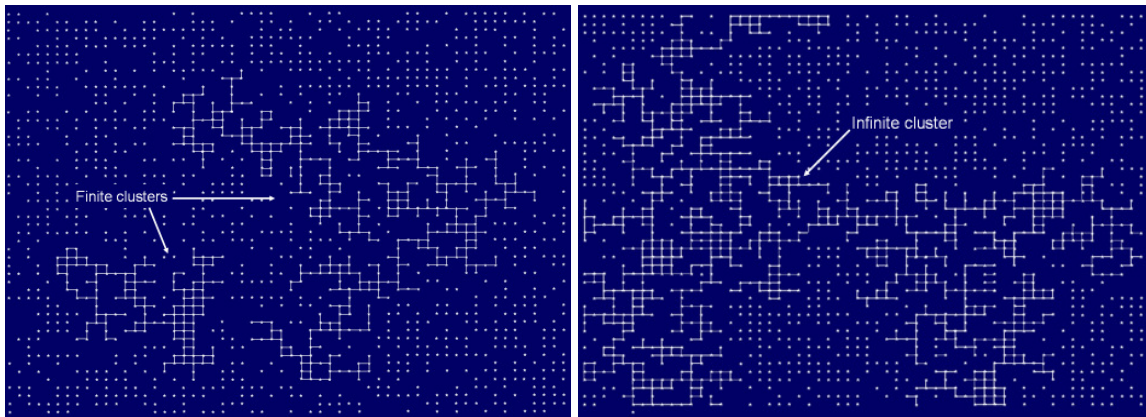


**Figure 1.4.1 (at left):** Square lattice (site-percolation, i.e. random occupation of lattice sites) with an occupation probability  $p$  below the critical concentration, i.e. percolation threshold  $p_c$ . The points represent occupied sites, empty sites are ignored. Two clusters are marked by lines. **Figure 1.4.2 (at right):** Square lattice (site-percolation) with an occupation probability  $p$  above the critical concentration, i.e. percolation threshold  $p_c$ . An 'infinite cluster' is marked by lines.

In a *three-dimensional* lattice two components can percolate at the same time, and two percolation thresholds,  $p_c$ , can be defined: a lower threshold,  $p_{c1}$ , where one of the components just begins to percolate, and an upper threshold,  $p_{c2}$ , where the other component ceases to have an infinite cluster. Below the lower or above the upper percolation threshold, the clusters of the corresponding components are finite and isolated. In site percolation of a binary powder mixture,  $p_c$  corresponds to a critical concentration ratio of the two components. The critical volume-to-volume ratios depend on the type of percolation and the type of lattice. In the case of a real powder system the geometrical packing is a function of the particles size, shape and distribution. At a percolation threshold some property of a system may change abruptly or may suddenly become evident (Leuenberger, 1999; Leuenberger et al, 1996).

When the formation of a tablet inside a die, the granules represent clusters of primary particles and primary particles are considered as clusters of molecules.

Holman (1991) also shown that the percolation theory, in combination with the principles of mechanics, adequately describes the relationships between resistance to volume change and the area of interparticulate contact below and above the percolation threshold, in other words, the mechanical properties of the material under compression. Among others, he identified the percolation threshold of the pores,  $p_{ca}$ , which signifies the transition from a particulate system to a continuum one (Holman, 1991).

The percolation theory was successfully used to interpret water uptake, disintegration time and intrinsic dissolution rate of tablets consisting of binary mixtures (Luginbühl and

Leuenberger, 1994), as well as to describe the percolation effects in matrix-type controlled drug release systems allowing a more rational design of such systems (Leuenberger et al., 1995).

Caraballo et al. (1996) studied for the first time the existence and behavior of the percolation thresholds in ternary pharmaceutical tablets. They demonstrated that a multicomponent system can be reduced to a binary one by using a discriminating property and the percolation theory is able to be applied to an increasing number of pharmaceutical systems giving a better explanation of these systems than 'classical theories' (Caraballo et al., 1996).

### **1.5 Modified (oral) Drug-Delivery Systems and the coating process**

The term *drug delivery* covers a very broad range of techniques used to get therapeutic agents into the human body.

In recent years there has been great interest in the development and use of tablets which should be swallowed and thereafter slowly release the drug in the gastrointestinal tract. Such tablets are denominated in various ways, such as slow release, extended release, sustained release and prolonged release. They are often also referred to as controlled-release preparations. This latter term is somewhat misleading, as all tablets, irrespective of their formulation and use, should release the drug in a controlled and reproducible way (The nomenclature for prolonged-release preparations is subject to some debate and no harmonized worldwide system exists) (Alderborn, 2007).

According to FDA definition, *Modified Release (MR) Dosage Forms* are dosage forms whose drug-release characteristics of time course and/or location are chosen to accomplish therapeutic or convenience objectives not offered by conventional dosage forms such as a solution or an immediate release dosage form. Modified release solid *oral* dosage forms include both delayed and extended release drug products (FDA, 1997).

From an extended release, also known as sustained release system, the drug is released slowly at a nearly constant rate (or alternatively as a series of pulses). If the rate of release is constant during a substantial period of time, a zero-order type of release is obtained, i.e.  $M = kt$  (where  $M$  is the cumulative amount of drug release and  $t$  is the release time). For delayed release tablets the drug is liberated only some time after administration. After this period, of lag time, the release is normally rapid (Alderborn, 2007).

These techniques for drug delivery are capable of regulating the rate of drug delivery, sustaining the duration of therapeutic action, and/or targeting the delivery of drug to a specific tissue. These advancements have already led to the development of several novel drug delivery systems that could provide one or more of the following benefits (Chien and Lin, 2002):

1. Controlled administration of a therapeutic dose at a desirable rate of delivery.
2. Maintenance of drug concentration within an optimal therapeutic range for prolonged duration of treatment.
3. Maximization of efficacy-dose relationship.
4. Reduction of adverse side effects.
5. Minimization of the needs for frequent dose intake.
6. Enhancement of patient compliance.

Oral modified release forms most commonly involve either dispersing the drug into a polymeric matrix, or encapsulating the drug containing core or granules with a rate-controlling membrane. *Film coating* is a popular technique to modify the release of a drug from the dosage form. As shown in figure 1.5.1, it involves the deposition, usually by a spraying method, of a thin film of a polymer formulation surrounding the surface of a tablet core, capsule or multiparticulate core.

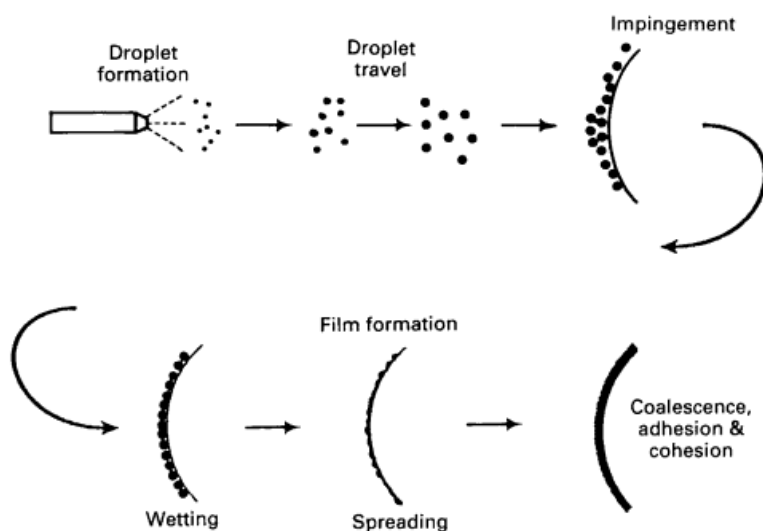


**Figure 1.5.1:** Schematic representation of the stages in spray film coating (Aulton and Twitchell, 1995).

*Modified-release film coatings*, also known as ‘functional’ coatings, can be categorized as either for delayed-release or extended-release coatings, according to the design or polymer applied.

Currently, the majority of film-coating processes involve the application of a liquid coating formulation where the major component (the solvent/vehicle) is removed by means of a drying process that is concurrent with the application of that coating solution/suspension. Film-coating formulations typically comprise of polymer, plasticizer, solvent/vehicle, pore former (when necessary), and colourants.

In general, film coatings have two main functions. Coatings intended to be applied on immediate-release products should have good solubility in aqueous fluids to facilitate fast release and dissolution of the drug. However, film coatings used to modify the rate of drug release tend to have limited or no solubility in aqueous media. Polymers solubility, viscosity, permeability and mechanical properties are imperative factors in the choice of the polymer to be used. The same factors can also be applied to the plasticizer choice.

For many years, the liquid component of coatings was a volatile solvent, such as alcohol or other quick-drying substances like methylene chloride. While solvent-based coatings performed well in many respects, they presented problems in handling, operator safety, recovery, and odour. They could even make the finished tablets smell like solvent, which is not a desirable property. Solvent-based coatings are still used in some applications, but water-based, or aqueous, coatings have largely replaced them. It does not present all that troubles and it is environmentally friendly as well. As a result, coating has become much more challenging, because water-based coatings are much less forgiving. The coating must be applied and the water removed before it can jeopardize the integrity of the tablet. The key to tablet coating is to get the surface slightly wet and immediately dry (Tousey, 2005).

The water penetration into the core depends on a complex set of interacting factors related to the coating process, the formulation of the coating liquid and the tablet core. Most pharmaceutical solid dosage formulations contain disintegrants. Modern disintegrants, often referred to as superdisintegrants, act by rapid uptake of water followed by rapid and, for some, enormous swelling up. Superdisintegrant particles compressed into the surface of the tablet may get activated prematurely on contact with droplets of aqueous film coating solution resulting in very fast and excessive water penetration into the core and uneven surface of the coated product (Levina and Cunningham, 2005).

## 1.6 Delayed Drug Release and Chronotherapy

Another alternative terms used to describe delayed release are pulsatile or sigmoidal release. Ideally, with a pulsatile release system, the drug is released rapidly and completely after a defined lag time of no drug release (Figure 1.6.1). In recent years, pulsatile release systems have gained increasing interest.

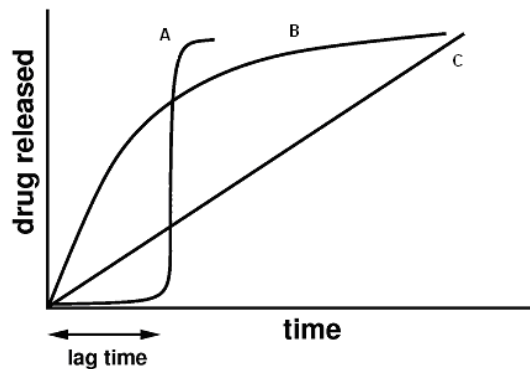


**Figure 1.6.1:** Drug release profiles: (A) pulsatile, (B) and (C) conventional extended release.

The application of pulsatile release systems can be advantageous to adapt a drug therapy to chronopharmacological needs or to target a drug to a specific site in the gastrointestinal tract (GIT), e.g., to the colon. Besides one-pulse systems, can be done multipulse systems that release the drug in subsequent pulses.

These drug delivery systems (DDS) can be classified in site-specific and time-controlled systems. Drug release from site-specific systems depends on the environment in the GIT, e.g., on pH, presence of enzymes, and the pressure in the GIT. In contrast, time-controlled DDS are independent of the biological environment. The drug release is controlled only by the system. Time-controlled pulsatile delivery has been achieved mainly with drug-containing cores, which are covered with release-controlling layers. The cores serve as reservoirs, which protect the core from the environment, e.g., water, acidic pH, and enzymes, until the drug is released after the lag phase. The coatings can erode/dissolve, rupture, or alter their permeability at the required time (Bussemer and Bodmeier, 2003).

When the integrity of the coating is destroyed, the core then disintegrates immediately and burst releasing all or most of the drug at a specific site. By controlling parameters in the device, such as the core composition, carrier material in the coating, film thickness and particulate matter, the location and time of release of the drug can be carefully controlled.

A well time-controlled pulse, or series of pulses, is currently attracting great interest and several investigations have been done. Some examples of pulsatile DDS are Pulsincaps and hydrophilic sandwich (Stevens, 2003 and Nayak et al., 2009), modified pulsincap systems (Patel and Patel, 2009), systems containing a swellable core material (Lerner and Penhasi, 2003), multiple-unit formulations (Roy and Shahiwala, 2009), press-coated tablets (Conte, 1993), rupturable coated hard gelatin capsules (Bussemer et al., 2003), self-exploding microcapsules (De Geest et al., 2009), multitude of multicoated particulates (Percel et al., 2006), magnetic hydrogel nanocomposites for remote control (Satarkar and Hilt, 2008), “tablets in capsule” device (Li et al., 2008), incorporation of disintegrants in pH-responsive polymer coatings (Schellekens et al., 2008), system based on swelling and osmotic pumping mechanism (Zhang et al., 2003), among others.

Very few products are already found in the market, e.g. Verelan<sup>®</sup> PM XL release capsule (hypertension treatment), InnoPran<sup>®</sup> XL tablet (hypertension treatment), Moxatag<sup>™</sup> tablet (infections treatment), Covera<sup>®</sup> HS (hypertension treatment), Uniphy<sup>®</sup> (bronchodilator), Ritalin<sup>®</sup> LA (psychostimulant drug).

A challenge in the development of pulsatile drug delivery system is to achieve a rapid drug release after the lag time. Often, the drug is released over an extended period of time. Pulsatile drug delivery offers advantages such as extended day-time or night-time activity, reduced side-effects, reduced dosing frequency and dose size, improved patient compliance and lower treatment costs.

Many individuals take their medications at times of the day that are convenient or easy to remember (in the morning, at lunchtime, or before bed, for example). Instead, an approach called Chronotherapy takes into account your body’s rhythms to tailor the timing and dosage of your drugs so that they work better and produce fewer side effects. The term “chrono” basically refers to the observation that metabolic events undergo rhythmic changes with time. And chronotherapeutics refers to a treatment method in which *in vivo* availability is timed to match rhythms of disease.

If a multiple dosage regimen requires a dose to be administered ‘four times a day’ it is unlikely that a dose will be administered at exactly 6-hourly intervals around the clock. Instead, the four doses are likely to be administered during the ‘waking’ hours of each day. The significance feature of both these dosing schedules is that the patient will experience an overnight no-dose period of 12 hours. Such periods will result in substantial decrease in the amount of drug in the plasma and body, and may also cause problems in maintaining

therapeutic steady-state plasma concentrations of drug in the body after the first overnight no-dose period (unless the therapeutic range of the drug is sufficiently large to accommodate the fluctuations in drug concentration associated with overnight no-dose periods). The potential problems associated with overnight no-dose periods are even further complicated by patients who forget to take one of their daytime doses (Collett, 2007).

The human body follows multiple natural rhythms to regulate physiological functions and behaviour. The most important one for chronotherapy is circadian rhythm, your body's daily biological clock that follows the sun's 24-hour cycle and regulates sleeping and waking. Circadian rhythm also affects important biological processes such as hormone secretion, cell growth, and metabolism. Scientists have also discovered that biological rhythms (chronobiology) play a role in disease and its treatment, since these rhythms cause symptoms to vary throughout the day. Consequently, chronotherapy times administration of a drug so that its peak concentration in the blood occurs around the time of day when the symptoms are worst, not necessarily because the drug works any better at that time. For example, symptoms of allergic rhinitis, a condition that affects the mucus membranes of the nose and includes seasonal allergies (hay fever), are often worst in the morning when histamine levels in the body are elevated. That is why some allergists recommend that individuals take a long-acting antihistamine drug at bedtime so it will be in their systems when they wake up (Johns Hopkins Health Alert, 2009). Chronotherapeutic diseases include asthma, cardiovascular diseases, glaucoma, rheumatoid arthritis and cancers (Khan et al., 2009)

If symptoms of a disease display circadian variation, drug release should also vary over time. Drug pharmacokinetics can also be time-dependent; therefore, variations both in a disease state and in drug plasma concentration need to be taken into consideration in developing drug delivery systems intended for the treatment of disease with adequate dose at appropriate time. Various technologies such as time-controlled, pulsed, triggered and programmed drug delivery devices have been developed and extensively studied in recent years for chronopharmaceutical drug delivery. Time-controlled or pulsed-release formulations are preferable, especially in the treatment of early morning symptoms (Sajan et al., 2009). Conventional controlled release drug delivery systems are not designed to complement the circadian rhythm. In order to achieve optimal success, drug release should coincide with the body's circadian rhythm and ought to occur after predetermined time delays.

While it seems logical to simply change dosing schedules to account for the chronobiology of disease states, patient time structure, and chronokinetics and dynamics of medications



as a means to improve therapeutic impact and safety, this approach requires faithful patient adherence. This can be difficult, especially in poorly motivated or uneducated patients, or patients requiring treatment with many different medications for co-existing morbid conditions (Smolensky and Peppas, 2007). Thus the common theme underlying these delivery modes is increased therapeutic efficiency as well as increased patient compliance.

It can be concluded that pulsatile drug delivery systems offer a solution for delivery of drugs exhibiting chronopharmacological behaviour, extensive first-pass metabolism, necessity of night-time dosing, or absorption window in GIT. A variety of systems based on single or multiple units are developed for pulsatile release of drug. Most systems perform quite well *in vitro*; their performance *in vivo* has often not been tested. One major challenge will be to obtain a better understanding of the influence of the biological environment on the release performance of pulsatile delivery systems in order to develop simple systems based on approved excipients with a good *in vitro-in vivo* correlation (Gothoskar et al., 2004).

Thus, despite of the potential therapeutic benefits of the *modified drug delivery systems*, still remaining a lack of manufacturing reproducibility and efficacy mainly due to their complicated manufacturing procedures and the large number of process variables caused by multiple formulation steps. Added to that is the use of new or expensive excipients what has been strongly limiting the number of marketed products. All major components of the modified drug delivery systems should have a pharmacopeia monograph or have GRAS status and present no regulatory issues regarding the composition of the dosage form itself.

## 2 Materials

### 2.1 Model Drug

Proquazone (1-isopropyl-7-methyl-4-phenyl-2(1*H*)-quinazolinone);  $C_8H_{18}N_2O$ ; CAS Registry Number: 22760-18-5; molecular weight 278.35; melting point 137-138°C; log P (octanol-water) 3.020;  $pK_a$  1.1; presented as a yellowish powder; soluble in chloroform, insoluble in water; with a contact angle  $> 90^\circ$ . Solubility in acid medium of 1.42 g/L (measured at pH 1.0 - 0.1N HCl). It can be classified as a BCS class II drug, which is characterized by a high permeability and a low solubility (Lanz, 2006; Von Orelli, 2004; O'Neil, 2006; U.S. Nat. Lib. of Med.; NCBI).

It has a total surface free energy of 21.0 mN/m (polar contribution: 3.7 mN/m, and non-polar contribution: 17.3 mN/m) according to Owens and Wendt (Owens and Wendt, 1969). Proquazone (PQZ) is an NSAID that had been used in musculoskeletal and joint disorders (Sweetman, 2007), as well as in children with juvenile rheumatoid arthritis (Lempiäinen and Mäkelä, 1985). The drug was kindly provided by Sandoz Ltd., Basel, Switzerland (nowadays Novartis Pharma AG). Batch n° 87.327.

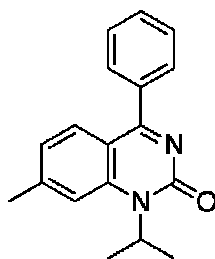


Figure 2.1: Chemical formula of proquazone

### 2.2 Excipients

#### 2.2.1 Cellulose Type II Polymorph

In this study the polymorphic form type II of cellulose was used. It was kindly provided by Pharmatrans Sanaq, Switzerland, in two batches: MCC SANAQ Rapid Type II (Lot. no. 126-T03) and MCC SANAQ Burst (Lot. no. 120-34).

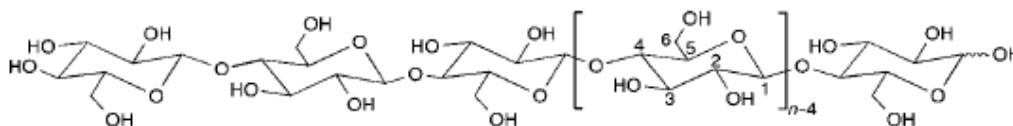


Figure 2.2: Chemical formula of cellulose

Empirical formula:  $(C_6H_{10}O_5)_n$

Manufacturing: Powdered cellulose, manufactured by mechanical processing of  $\alpha$ -cellulose pulp from fibrous plant materials.

Properties: White, odorless, tasteless powder of various finesses, ranging from a free-flowing, dense powder to a coarse, fluffy, non-flowing material. Insoluble in water, dilute acids and most organic solvents.

### **2.2.2 HPMC**

Hydroxypropylmethylcellulose is an odorless and tasteless, white or creamy white fibrous or granular powder. Used as coating agent; film-former; rate-controlling polymer for sustained release; stabilizing agent; suspending agent; tablet binder; viscosity-increasing agent. Concentrations between 2% and 5% w/w may be used as a binder in either wet- or dry-granulation processes. High-viscosity grades may retard the release of drugs from a matrix system (Rowe et al., 2006); therefore a low-viscosity grade was used as a binder for wet granulation (Methocel<sup>®</sup> E5 Premium LV, Dow Chemical).

### **2.2.3 Magnesium Stearate**

The European Pharmacopeia describes magnesium stearate as a mixture of magnesium salts of different fatty acids consisting mainly of stearic acid and palmitic acid and in minor proportions other fatty acids. Magnesium stearate is a very fine, light white, precipitated or milled, impalpable powder of low bulk density. Flowability: poorly flowing, cohesive powder. It is primarily used as a lubricant in capsule and tablet manufacture at concentrations between 0.25% and 5.0% w/w (Rowe et al., 2006). Magnesium stearate (Lot. no. 84808), kindly donated by Novartis Pharma, Switzerland.

## **2.3 Storage**

All starting materials were stored at room temperature in their original packaging, protected from light and humidity.

## **3 Methods**

### **3.1 Powder Characterization**

#### **3.1.1 Scanning Electron Microscopy (SEM)**

Scanning Electron Microscopy pictures were taken at the Center of Microscopy from the University of Basel, ZMB-UniBasel. (Scanning Electron Microscopy, Philips XL 30 FEG ESEM. Philips, Eindhoven, Netherlands). Sample preparation was consisted of to fix the samples over aluminium holders and sputtering them with gold to achieve conductivity.

#### **3.1.2 Particle Size Determination**

The particle size distribution was analyzed by laser diffraction scattering (MasterSizer X Long Bed, Malvern Instruments, UK). The measurement was performed using the Manual Dry Powder Feeder for cellulose type II and the liquid sample unit for a dispersion (water:tween 80) of Proquazone. The process system and the resulted data analysis were operated by MasterSizer X Software (version 2.19, Malvern Instruments, UK). The function “polydispers” was activated and the “Frauenhofer” model was chosen (following Malvern recommendation), and obscuration value was kept between 15-25% for all measurements. The measurements were carried out 5 times for each sample.

#### **3.1.3 Moisture Content**

Loss on drying was determined thermogravimetrically (Mettler-Toledo LP16M, Mettler Instruments, Switzerland). Before and immediately after granulation, as well as right before compaction, specimens of 1 to 2 g were heated up at 105°C for 20 minutes. The loss of moisture was calculated in percent by weight.

#### **3.1.4 Densities**

True density  $\rho_t$  was determined using a Helium Pycnometer (AccuPyc 1330, Micromeritics Instruments Corporation, USA). A known weight of the samples was placed into the sample cell. Helium was used as a measuring gas and values were expressed as the mean of five parallel measurements. The apparatus determined the sample volume on the base of the displaced gas mass, and then it calculated the true density dividing the sample weight by the sample volume. The Pycnometer repeated automatically the measurement five times for each sample, and the final true density was calculated as an average of the five results.

Bulk and Tapped Density ( $\rho_{\text{bulk}}$  and  $\rho_{\text{tap}}$ , respectively) were determined according to U.S. Pharmacopeia 31, using the apparatus Type STAV 2003, Engelsmann AG, Germany. 100g of powder or granules were poured into a glass cylinder and their bulk volume (50-250ml) was read immediately. Then the sample was tapped 250 times, until to complete 1250 taps, or the difference between succeeding measurements was less than 2%, in order to check the respective tapped volume.

Both bulk and tapped density were calculated using the following equation:  $\rho = m/V$

where:  $\rho$ : Bulk or tapped density [g/ml]

$m$ : Weight of the sample [g]

$V$ : Bulk or tapped volume [ml]

### 3.1.5 Hausner Ratio and Compressibility Index

Hausner Ratio and Compressibility Index (also called Carr's Index) are simple, fast, and popular methods of predicting powder flow\* characteristics. They were calculated and scaled according to European Pharmacopoeia 5.3.

$$\text{Hausner Ratio} = \frac{\text{Tapped Density}}{\text{Bulk Density}} \quad (1)$$

$$\text{Compressibility Index} = \frac{\text{Tap Density} - \text{Bulk Density}}{\text{Tap Density}} \times 100 \quad (2)$$

\*The *flow through an orifice* technique could not be done, because the cohesive forces between the relatively small particles of the starting materials perturbed its free flow.

### 3.1.6 Packing fraction and Porosity

The constant of proportionality,  $k$ , is known as the *packing fraction* or *fractional solids content*. And it is equal the proportion  $\rho_{\text{bulk}}/\rho_t$  (bulk density/true density).

Powder porosity ( $\varepsilon$ ) was calculated using the powder true and bulk densities, according to the formula:

$$\varepsilon = [1 - \rho_{\text{bulk}}/\rho_t] \times 100.$$

## 3.2 Granulation

A wet granulation method was used. It has the advantage of improved uniformity of content for low concentration, potent drugs, and of enhanced batch to batch reproducibility of the process. The granulation also improves the flowability of the powder and the hardness of the obtained tablets.

### 3.2.1 Equipment and Preparation

A lab scale Diosna<sup>®</sup> P10 high-shear mixer (Dierks & Söhne, Osnabrück, Germany) with a volume of 10L was used. Three main formulations containing the cellulose type II polymorph and Proquazone (PQZ) in different proportions were produced, as shown in Table 3.2.1. The percentage of drug was 10%, 50% and 90% (w/w). In all formulations 2% of Hydroxypropylmethylcellulose (HPMC) was added as a dry binder into the mixture, and the granulation liquid was distilled water. The granulation liquid was added using a peristaltic pump under constant addition speeds. The total amount of blend was mixed for 5 minutes inside the mixer with an impeller speed of 430 rpm. After the mixing time, the liquid addition and the power consumption measurement were started simultaneously. The process was stopped when samples with the desired granules diameter were collected.

**Table 3.2.1:** Formulations prepared containing different proportions of drug and excipient.

Starting materials	percentage per weight (% w/w)		
Proquazone	10	50	90
Cellulose type II	88	48	08
HPMC	02	02	02

### 3.2.2 Power Consumption Measurement

An “in process” computer calculation program was used to record the power consumption (P.C.) profile during all granulation experiments. It was used as a monitoring tool in a way to facilitate the visualization of the mixture liquid saturation and powder cohesion inside the mixer vessel. The power consumption of the mixer motor (i.e. main impeller) is determined by the electric current consumption of the motor according to the equation  $P = U \times I$ , where  $P$  is the power (W),  $U$  the electric potential (V), and  $I$  is the electric current (A). The product of electric potential (V) times electric current (A) is measured by a measuring transducer (Sineax Type PQ 502, 0–2kW, Camille Bauer AG, Switzerland). The power consumption is converted into an electric potential signal between 0 and 10V, 10V corresponding to 2 kW and sampled by an I/O Multifunction DAQ-Card, to a laptop computer and displayed graphically by the Recorder Software (produced in co-operation with Pharmatronic Ltd, Switzerland).

### **3.3 Granules Characterization**

#### **3.3.1 Particle Size Determination**

The wet granulates were dried in a dish dryer (Heraeus Instruments) at 40°C for around 10 hours before sieve analysis be carried out in ISO-norm sieve oscillator type equipment (Rietsch, Germany), using eight selected sieves ranged from 1000 µm to 90 µm mesh screen. A particle-size distribution was calculated by the ratio of sieves cumulative weight and total sample mass. In this work, the desired granules particle size used for posterior compression was set between 125 to 710µm (i.e., cumulative samples from sieves 125 to 500µm) in order to keep more homogeneity among the particles and avoid the presence of fines.

#### **3.3.2 Moisture Content**

Determined as previously described for powder characterization in section 3.1.3.

#### **3.3.3 Densities**

Determined as previously described for powder characterization in section 3.1.4.

#### **3.3.4 Hausner Factor and Carr's Index**

Determined as previously described for powder characterization in section 3.1.5.

#### **3.3.5 Crushing Strength of granules**

The mechanical strength of a material is associated with its resistance to fracturing, attrition and deformability.

The crushing strength (hardness), of the granules produced from the three powder mixtures, was measured by a force tester (Programmable Universal Tester for tensile and compression forces, FMT-310, Alluris, Germany). The measurements were carried out in samples consisted of 20 to 40 isolated granules, for each formulation. An average value, and its standard error, was calculated.

#### **3.3.6 Scanning Electron Microscopy (SEM)**

Determined as previously described for powder characterization in section 3.1.1.

### **3.4 Tablet Compaction**

The manufacture of biconvex-faced tablets was chosen in a way to guarantee a more efficient and robust coating process, avoiding or minimizing tablet damage during tumbling inside the coating pan, and/or fluid bed container walls attrition, as well as to avoid sticking between tablet's surfaces.

#### **3.4.1 Equipment and Process**

Tablets were compressed using a 6 station rotary tablet press (Phamapress PH100, Korsch, Germany), equipped with 8mm concave-faced punches (R= 5.5) with edge. Granules were mixed with 0.1% (w/w) of Magnesium Stearate for 3 minutes in a Turbula blender (Type T2A, W. A. Bachofen, Switzerland) before compression. No glidant was used, as well as very few lubricant, to prevent any interactions that could influence the drug release. The machine was loaded pouring the material through a steel conical hopper. During operation, the speed of the turret rotation was fixed at 19 rpm, and the depth of the filling material and the thickness of the tablets were manually adjusted for each formulation to keep similar tablet characteristics, such as porosity, for all tablet formulations. The tablet weight was fixed at 200mg.

### **3.5 Tablet Characterization**

#### **3.5.1 Tablet Dimensions**

The thickness (or total height), the length/height of the edge and the diameter of the biconvex tablets were measured by a digital caliper (Digimatic® Caliper CD-15CPX, Mitutoyo Corporation, Japan). The tablets weight was measured with an analytical balance (XS 204, Mettler Toledo, USA). The measurements were carried out from samples consisted of 10 tablets for each preparation. (In the Appendix of this chapter an explanatory figure about the biconvex tablet dimensions is presented)

#### **3.5.2 Crushing Strength (Failure Force) and Tensile Strength**

The resistance of tablets to capping, abrasion or breakage under conditions of storage, transportation and handling before usage depends on its mechanical properties. The mechanical strength of a tablet also provides a measure of the bonding potential of the materials.

The crushing strength ( $S_c$ ) is the compressive stress required to cause a solid to fail by fracture; in essence, it is the resistance of the solid to a pressure placed upon it. Using a



tablet hardness tester (8M, Dr. Schleuniger Pharmatron AG, Switzerland),  $Sc$  was measured from samples consisted of 10 tablets for each formulation. The apparatus measures the diametrically applied force required to break the tablet.

A non-compendial method of measuring the mechanical strength of tablets that is now widely used is the tensile strength. The breaking load of a powder compact subjected to diametral loading ( $Sc$ ) can be converted into a tensile strength ( $\sigma_t$ ) value by the application of the expression:

$$\sigma_t = \frac{10Sc}{\pi D^2} \left( \frac{2.84t}{D} + \frac{0.126t}{W} + \frac{3.15W}{D} + 0.01 \right)^{-1}$$

where  $Sc$  is the crushing strength (or breaking load),  $D$  is the tablet diameter,  $t$  is the total tablet thickness and  $W$  is the central cylindrical core thickness (edge height). The above expression is only valid for convex-faced tablets (Pitt et al., 1989; Haririan and Newton, 1999; Newton et al., 2000).

### 3.5.3 Friability

The  $Sc$  provides a measure of tablet strength while friability ( $F$ ) is a measure of tablet weakness.

Friability was measured according to the standard friability test USP 31, using a friability tester (Erweka TAP, Erweka, USA) at the rotation speed of 25 revolutions per minute for 100 revolutions. Each batch was consisted of not less than 6.5 g (total weight) of tablets. The uncoated tablet samples were carefully dedusted prior and after testing, when the weight loss after tumbling could be determined.

### 3.5.4 Porosity

It has been shown that penetration of water into a tablet is proportional to its mean pore diameter or porosity (Singh et al., 1968; Ganderton, 1969). Generally short disintegration times are associated with rapid fluid penetration (Ganderton and Shotton, 1961; Nogami et al., 1969).

The porosity of the tablets was calculated according to the following equation:

$$\varepsilon = [1 - \rho_{app}/\rho_{gran}] \times 100.$$

where:  $\varepsilon$ : porosity of the compact (% v/v)

$\rho_{app}$ : apparent density of the compact [g/cm<sup>3</sup>]

$\rho_{\text{gran}}$ : true density of granules [g/cm<sup>3</sup>] used for tableting.

The apparent density of the compact was calculated dividing the weight of the tablet by its volume:

$$\rho_{\text{app}} = m/V$$

where:  $m$ : weight of the tablet [mg]

$V$ : geometric volume of the tablet [mm<sup>3</sup>]

The apparent density of the compact was calculated using the average of the weight and geometric volume of 5 tablets. For the calculations of the geometric volume see Appendix.

### 3.5.5 Scanning Electron Microscopy (SEM)

Surface roughness and internal structure morphology of the tablets were assessed using SEM images. The method was previously described in the section 3.1.1.

### 3.5.6 Disintegration

For a drug to be absorbed after oral administration of a solid dosage form, it must first be dissolved, and the first important step toward this condition is usually the break-up of the tablet; a process known as disintegration. The disintegration test is a measure of the time required, under a given set of conditions, for a group of tablets to disintegrate into particles which will pass through a 10 mesh screen.

The disintegration time was determined in a disintegration tester Sotax DT3 (Sotax, Allschwil/Basel, Switzerland) with a basket-rack assembly without disk. The disintegration medium was consisted of 900 ml of distilled water and hydrochloric acid 0.1N, maintained at 37°C ±1. The tablets were considered disintegrated when no residue of the units remained in the basket, except for fragments of coating layers. For each formulation six tablets were tested and the time taken to complete the disintegration was recorded. The results were expressed as average of the six measurements.

### 3.5.7 Dissolution

Dissolution is the process by which a solid solute enters a solution. In the pharmaceutical industry, it may be defined as the amount of drug substance that goes into solution per unit time under standardized conditions of liquid/solid interface, temperature and solvent composition. Dissolution behaviour of drugs has a significant effect on their pharmacological

activity. Solid dosage forms may or may not disintegrate when they interact with gastrointestinal fluid following oral administration, depending on their design (Figure 3.5.1). For disintegrating solid oral dosage forms, disintegration usually plays a vital role in the dissolution process since it determines to a large extent the area of contact between the solid and liquid. However it is well known that considerable dissolution of the drug can take place before complete disintegration of the dosage form, a phenomenon which depends largely on the mechanism of disintegration and certain physicochemical properties of the drug, such as its solubility. This could be important when considering the motility of the drug or dosage form, and the release of the drug at specific sites, in the gastrointestinal tract (Amidon et al., 1995).

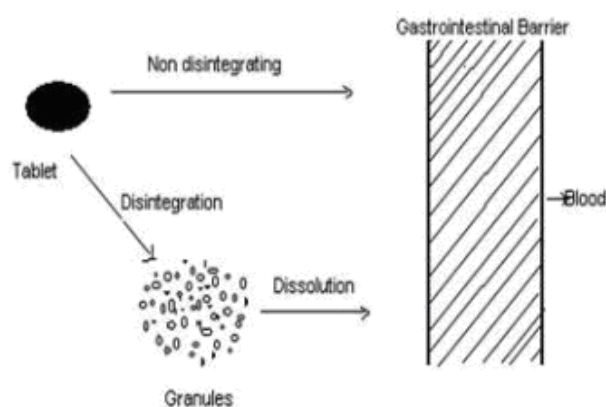


**Figure 3.5.1:** schematic representation of disintegrant and non disintegrant tablets.

No official method for the measurement of proquazone is found in the literature. Thus the selection of the medium was done based on the work of Lanz (2006) and Van Orelli (2004). The dissolution test was performed after tableting and coating ( $n=6$ ), using a dissolution apparatus (Sotax AT7, Sotax AG, Basel) equipped with an automatic sampling unit. The dissolution procedure was performed with a USP Paddle (apparatus II) method. The speed of the paddles was set to a constant speed of 100 rpm. Different dissolution mediums were tested: hydrochloric acid 0.1M, phosphate buffer pH 6.8 and phosphate buffer pH 6.8 + 1% Sodium Lauril Sulfate, all with volume of 1000 ml, maintained at  $37 \pm 0.5^\circ\text{C}$ . The concentration of PQZ was quantified with a UV spectrophotometer (Lambda 25, PerkinElmer, Inc. Fullerton, USA), using 1mm cells, at the maximum wavelengths ( $\lambda_{\text{max}}$ ) of 299 nm (for HCl) and 285 nm (for the buffer), and compared to the calibration curve of PQZ in the same mediums. For controlled-release dissolution test, the USP Method B was chosen. 1000 mL of acid media was placed for 2h followed by total replacement of pH 6.8 phosphate buffer. Sink conditions (defined in this study as the total drug concentration dissolved in the medium should not be significant higher than 10% of its total solubility)

were maintained throughout the experiments except for the formulation containing 90% (w/w) drug that represents 12.6% of its total solubility.

## **3.6 Tablet Coating**

### **3.6.1 Coating Polymers and adjuvants**

In order to investigate the influence of cellulose type II in the drug release from a coated system, different polymers were tested: Eudragit<sup>®</sup> RS 30D, Eudragit<sup>®</sup> RL 30D and Aquacoat<sup>®</sup> ECD 30%. Afterwards Aquacoat ECD<sup>®</sup> 30% was selected for further experiments.

#### **3.6.1.1 Eudragit<sup>®</sup> RS 30D and RL 30D**

Eudragit<sup>®</sup> RS and RL are methacrylic copolymers with trimethylammonioethyl methacrylate as functional group, available in aqueous dispersion with 30% polymer content.

They provide time-controlled release of active ingredients independently of the pH of gastric fluids. The drug release occurs by diffusion and is tailor-customized by varying film thickness and polymers ratio. Both are water insoluble, swellable film formers based on neutral methacrylic acid esters with a small proportion of trimethylammonioethyl methacrylate chloride (functional ionic group).

With Eudragit<sup>®</sup> RL, the molar ratio of the quaternary ammonium groups to the neutral ester groups is 1:20 (corresponding to about 50 meq./100g), with Eudragit<sup>®</sup> RS this ratio is 1:40 (corresponding to roughly 25 meq./100g).

Since quaternary ammonium groups determine the swellability and the permeability of the films in aqueous media, Eudragit<sup>®</sup> RL, which contains more of these groups, forms more permeable films with little delaying action. By contrast, and owing to the reduced content in quaternary ammonium groups, films of Eudragit<sup>®</sup> RS swell less easily and are only slightly permeable to active ingredients. Given coherent film coatings and an adequate layer thickness, it is therefore possible to slow down drug diffusion very noticeably.

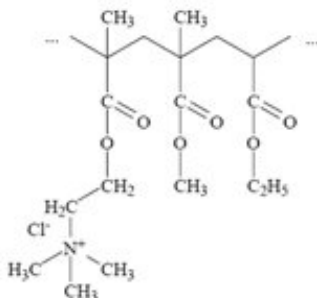
Eudragit<sup>®</sup> RS and RL polymers can be mixed in any ratio to produce films with intermediate permeability. In order to obtain films of adequate flexibility, 20% plasticizer on dry polymer substance has to be added to the dispersions of Eudragit<sup>®</sup> RS and RL.

During processing special attention should be given to the process temperature, it has to be well controlled and kept down to avoid sticking, since the Eudragit<sup>®</sup> polymers are soft.

**Eudragit® RS 30D** (Lot n° G070118011, Evonik Röhm, Germany)

Physical properties: It is a milky-white liquid of low viscosity with a faint characteristic odour.

Chemical structure:



Product Form: Aqueous Dispersion 30% (w/w)

Targeted Drug Release Area: Time controlled release, pH independent

CAS number: 33434-24-1

Chemical/IUPAC name: Poly(ethyl acrylate-co-methyl methacrylate-co-trimethylammonioethyl methacrylate chloride) 1:2:0.1

INCI name: Acrylates / Ammonium Methacrylate Copolymer

Monographs:

Ph. Eur.: Ammonio Methacrylate Copolymer, Type B

USP/NF: Ammonio Methacrylate Copolymer Dispersion, Type B - NF

JPE: Aminoalkyl Methacrylate Copolymer RS

GMP standard: The Joint IPEC – PQG Good Manufacturing Practice

Guide for Bulk Pharmaceutical Excipients 2006 and

USP-NF General Chapter <1078>

Drug Master File: # 1242

Molecular weight information: approx. 32,000 g/mol

Alkali Value: 19,4 mg KOH/ g Polymer

Minimum Film Forming Temperature (MFT): ~45 °C

**Eudragit® RL 30D** (Lot n° G070516084, Evonik Röhm, Germany)

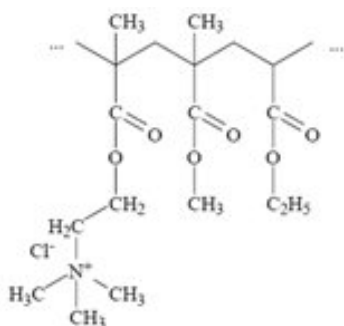
Physical properties: It is a milky-white liquid of low viscosity with a faint characteristic odour.

Product Form: Aqueous Dispersion 30% (w/w)

Targeted Drug release Area: Time controlled release, pH independent

CAS number: 33434 – 24 – 1

Chemical structure:



Chemical/IUPAC name: Poly(ethyl acrylate-co-methyl methacrylate-co-trimethylammonioethyl methacrylate chloride) 1:2:0.2

INCI name: Acrylates / Ammonium Methacrylate Copolymer

Monographs:

Ph. Eur.: Ammonio Methacrylate Copolymer, Type A

USP/NF: Ammonio Methacrylate Copolymer Dispersion, Type A - NF

JPE: Aminoalkyl Methacrylate Copolymer RS

GMP standard: The Joint IPEC – PQG Good Manufacturing Practice

Guide for Bulk Pharmaceutical Excipients 2006 and

USP-NF General Chapter <1078>

Drug Master File: # 1242

Molecular weight information: approx. 32,000 g/mol

Alkali Value: 32,3 mg KOH/ g polymer

Minimum Film Forming Temperature (MFT): ~ 40 °C

*(from Eudragit® Application guidelines)*

### 3.6.1.2 Aquacoat® ECD 30% (Ethylcellulose Aqueous Dispersion)

Aquacoat ECD is a low viscosity, nanosized, 30 percent by weight, aqueous dispersion of ethylcellulose polymer. Ethylcellulose (EC) is a hydrophobic coating material used in a variety of coating applications.

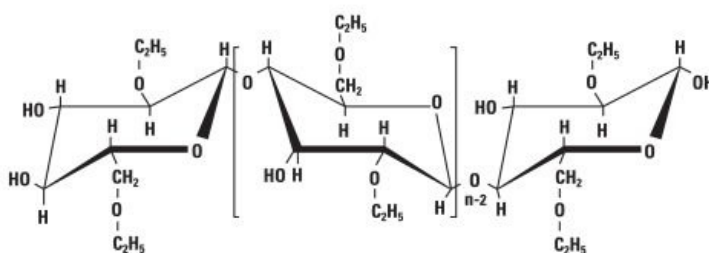
It offers dissolution rate control, stability and reproducibility, which are pH independent. Drug release happens by diffusion through the film layer, being a function of wall thickness and surface area. The drug release profile can be tailored by adjusting the coating level, plasticizer type, level of plasticizer, and by adding soluble polymers (pore formers) such as HPMC.

Aquacoat ECD is a solvent-free pharmacoepial coating product, low viscous and non-tacky features, with monographs in the US National Formulary and the book of Japanese Pharmaceutical Excipients (“Aqueous Ethylcellulose Dispersion” NF/JPE).

For sustained release applications, additional heating is necessary to cure the polymer coating. This is a necessary step for aqueous polymer coatings to ensure that the film coating is fully coalesced, resulting in reproducible release profiles. It is recommended curing at 60 °C for two hours.

**Aquacoat® ECD 30%** (Lot n° JN06817063, FMC BioPolymer, USA)

Chemical structure:



Ethylcellulose is derived from cellulose, and like cellulose, the backbone of its molecule is based on repeating β-anhydroglucose units. Specific properties of the various ethylcellulose polymers are determined by the number of anhydroglucose units in the polymer chain and the degree of ethoxyl substitution.

**Product Specifications**

CAS number: 9004-57-3

Ethylcellulose: 24.5 - 29.5%

Sodium lauryl sulfate: 0.9 - 1.7%

Cetyl alcohol: 1.7 - 3.3%

Total solids: 29-32%

Loss on drying: 68.0 - 71.0%

pH: 4.0 - 7.0

Hydrogen peroxide: NMT 50 ppm

Heavy metals: 0.001%

Viscosity: NMT 150 cP\*

Specific gravity: 1.025 - 1.040

Particle size: Submicron, 85% of particles < 0.5 μm

Total aerobic microbial count/gm: NMT 100 cfu/g\*\*

Total yeast and mold count/gm: NMT 20 cfu/g\*\*

Glass Transition Temperature: 129-133°C (ethylcellulose powder)

Minimum Film Forming Temperature (MFT): ~ 40 °C

Properties: Odorless, tasteless, white to light tan-colored. No ammonia used.

\* centipoise

\*\*colony-forming units-granulocyte

*(from Aquacoat® Application guidelines)*

### 3.6.1.3 Triethyl Citrate - TEC

TEC is used to plasticize polymers in formulated pharmaceutical coatings. It has hydrophilic characteristics.

Plasticizers are non-volatile, high-boiling liquids used to impart flexibility to otherwise hard or brittle polymeric materials. They are high-boiling to avoid loss from the polymers by volatilization. Plasticizers produce partial neutralization of the secondary valence bonds of the polymer molecules which become less strongly bound to each other, changing its physical properties, e.g., tensile strength is lowered, elongation and flexibility are increased, and softening temperature and brittle temperature are lowered (Citroflex, 2005).

Plasticizers soften and swell the polymer latex spheres which aid deformation and coalescence, and lower the film forming and glass transition temperatures. The glass transition temperature,  $T_g$ , is the temperature at which the polymer undergoes marked changes in physical properties. Higher amounts of plasticizer will even accelerate film formation.

For most of applications, excluding specific tailored ones, it is recommended that plasticizers be added at 20-25 percent of the latex solids level (grams plasticizer/grams solid x 100 = 25%) (FMC guidelines).

As a general rule it can be stated that the use of hydrophilic plasticizers produces coatings with higher permeability and faster dissolution, whereas lipophilic ones reduce permeability and dissolution speed (Eudragit guidelines).

**Citroflex® 2** (Lot n° N86154, Morflex, Inc., USA)

Chemical Name: 2-Hydroxy-1,2,3-propanetricarboxylic acid; triethyl ester.

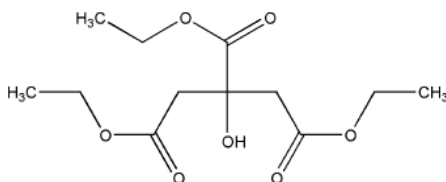
CAS number: 77-93-0

Triethyl citrate is a clear, odorless, practically colourless, oily liquid.

Viscosity (dynamic): 35.2 cP at 25°C



Structural Formula:



**Typical Properties:**

Acid value: 0.02

Melting Point: -45 °C

Water Solubility: 5.7 g/100 ml (25 °C)

Boiling Point: 288 °C

Flash Point: 151 °C

Molecular Weight: 276.32

Solubility: soluble 1 in 125 of peanut oil, 1 in 15 of water. Miscible with ethanol (95%), acetone, and propan-2-ol.

Among others materials, TEC as a derived from citric acid, is most often chosen as plasticizer for its global regulatory acceptance and compatibility with most of the generally useful polymers. Triethyl citrate is especially recommended as a solvent plasticizer for cellulose acetate and other cellulosic derivates. It enhances the grease resistance of formulations because of its limited oil solubility (Citroflex, 2005).

**3.6.1.4 Hypromellose (pore former)**

Hypromellose, also known as hydroxypropylmethylcellulose (HPMC), is water-soluble cellulose ether, and had been shortly described in section 2.3.2.

Depending upon the viscosity grade, concentrations of 2-20% w/w are used for film-forming solutions to film-coat tablets. Lower-viscosity grades are used in *aqueous* film-coating solutions. As a hydrophilic polymer it can be used as a pore former in mixtures with hydrophobic polymers.

Since it is nonionic, hypromellose will not complex with metallic salts or ionic organics to form insoluble precipitates.

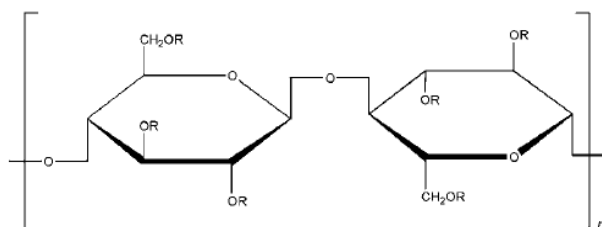
**Methocel™ E3 Premium** (Lot n° 850 721 1E, Dow Chemical, USA)

Chemical Name: Cellulose hydroxypropyl methyl ether. (Hypromellose 2910)

CAS number: 9004-65-3

Formula Weight: 59.08708

Structural Formula:



where R is H, CH<sub>3</sub>, or CH<sub>3</sub>CH(OH)CH<sub>2</sub>

### Typical Properties:

Acidity/alkalinity: pH = 5.5–8.0 for a 1% w/w aqueous solution.

Ash: 1.5–3.0%, depending upon the grade and viscosity.

Auto-ignition temperature: 360 °C

Density (bulk): 0.341 g/cm<sup>3</sup>

Density (tapped): 0.557 g/cm<sup>3</sup>

Density (true): 1.326 g/cm<sup>3</sup>

Melting point: browns at 190–200 °C; chars at 225–230 °C.

Glass transition temperature: 170–180 °C.

Nominal viscosity (cP): 2.4–3.6, for *Methocel E3 Premium LV* (for 2% (w/v) aqueous solutions measured at 20 °C.)

Methoxyl content (%): 28–30

Hydroxypropyl content (%): 7–12

Specific gravity: 1.26

Solubility: soluble in cold water, forming a viscous colloidal solution; practically insoluble in chloroform, ethanol (95%), and ether, but soluble in mixtures of ethanol and dichloromethane, mixtures of methanol and dichloromethane, and mixtures of water and alcohol.

Moisture content: hypromellose absorbs moisture from the atmosphere; the amount of water absorbed depends upon the initial moisture content and the temperature and relative humidity of the surrounding air.

Stability: Stable material. Solid is combustible, incompatible with strong oxidizing agents.

### 3.6.2 Equipment and Coating Process

The tablet cores were coated in a bottom spray lab scale fluid bed (Aerocoater™ Strea-1™ Classic, Aeromatic-Fielder AG, Switzerland) equipped with a stainless steel container, an appropriate perforated plate and without a boost tube.

Tablets were preheated and gently dedusted, applying pressured air, prior the coating process.

As illustrated in the figure 3.6.2, the coating solution was sprayed onto the semi-finished products. The solution was fed using peristaltic pump and the coating nozzle atomizes it inside the product container. Subsequent drying fixed the particles and generated the final products.

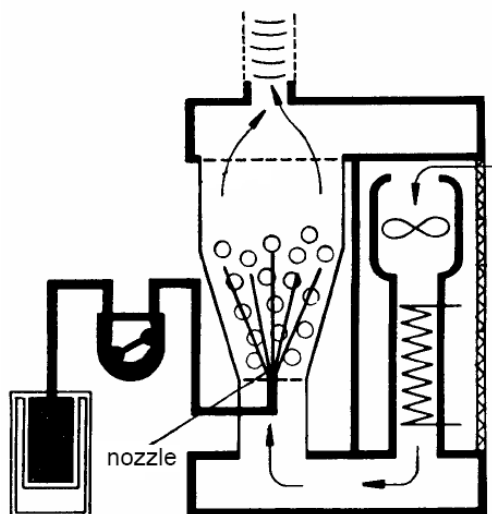


**Figure 3.6.2:** schema of the fluid bed used for coating.

A flashlight was used during the coating process to look into the container and check the tablets fluidization and nozzle cleanness.

The composition of the spray suspensions are summarized on Table 3.6.1 and Table 3.6.2.

Process parameters were optimized according to the coating polymer used, and set under the following parametric conditions:

**Coating polymer:** Eudragit® RS 30D and RL 30D

**Polymer combinations:** Eudragit® RS was applied lonely, aiming different coating thickness, and also with addition of 50% Talc (anti-tacking agent). Eudragit® RL was applied lonely, aiming different coating thickness. Two different combinations of RS and RL were also tested: ratio RS:RL = 70:30 and 50:50.

**Plasticizer:** TEC; set constant for all applications in 20% calculated on the dry polymer basis.

**Total of Solids in the Spray Suspension:** 25% (mass), except for one experiment it was 20%.

**Preparation:** Eudragit® products were agitated for 1h (at least) before its use in the coating suspension preparation. All adjuvants, including the plasticizer, were first poured in the diluent liquid and homogenized. After, the adjuvants suspensions were added to the Eudragit® suspension and stirred for at least 30 minutes.

**Load/Mass of tablets:** 50 -100 grams

**Desired weight gain:** 3 – 10%

**Inlet temperature (°C):** 35-45

**Bed temperature (°C):** 30-40

**Atomizing Air (bar):** 0.5-1

**Spray rate (g/min):** 3.5-6

**Coating solution temperature:** Room Temperature

**Fan speed (Air Flow):** the air flow rate was adjusted in order to promote an accurate number of particles revolutions with the air turbulences. The entire charge should be fluidised during the entire process, to guarantee an acceptable heat and mass transfer between air and product.

**Spray Time:** adjusted according to the desired load of coating to be added.

**Drying time:** 3 - 6 minutes

**Curing conditions:** Enteric Eudragit formulations usually do not show curing effects. For the mixtures of RS and RL a curing time of at least 3h at 40°C was applied.

The coating suspension was gently stirred during the entire coating process to prevent sedimentation. During first experiment trials the loss of coating suspension in the container walls and tube connections was calculated and, afterwards, an excess was applied in the following experiments to compensate it.

**Table 3.6.1:** Composition of the Eudragit® suspensions sprayed

<i>Mixtures</i>	Mix 1	Mix 2*	Mix 3	Mix 4	Mix 5
<i>Substances</i>	[% w/w]	[% w/w]	[% w/w]	[% w/w]	[% w/w]
Eudragit® RS	69.44	39.25	-	34.72	48.61
Eudragit® RL	-	-	69.44	34.72	20.83
TEC	4.16	2.33	4.16	4.16	4.16
Talc	-	5.90	-	-	-
Water	26.40	52.52	26.40	26.40	26.40
Total	100	100	100	100	100

\* Total of solids in the spray suspension was 20%.

After drying or curing, the coated tablets were stored in a desiccator; protected from light, moisture, crushing, and mechanical shocks.

**Coating polymer:** Aquacoat ECD 30%

**Pore Former:** Methocel E3 Premium; without (w/o), and added in concentrations of 3% and 6% calculated considering the amount of coating polymer used on a dry basis (by weight).

**Plasticizer:** TEC; set constant for all applications in 25% calculated on the dry polymer basis.

**Total of Solids in the Spray Suspension:** 25% (mass)

**Preparation:** Aquacoat product was mixed at least for 1h before its use in the coating suspension preparation. The plasticizer was then added to the Aquacoat suspension and mixed for at least 30 minutes before adding any other ingredients. The pore former was primary mixed with a portion of water until it got completely dissolved. After, the pore former was added to the coating suspension and stirred for plus 20 minutes at minimum.

**Load/Mass of tablets:** 50 -100 grams

**Desired weight gain:** 3 – 10%

**Inlet temperature (°C):** 65 - 85

**Bed temperature (°C):** 55-70

**Atomizing Air (bar):** 0.55

**Spray rate (g/min):** 4.3 – 4.5

**Coating solution temperature:** Room Temperature

**Fan speed (Air Flow):** the air flow rate was adjusted in order to promote an accurate number of particles revolutions with the air turbulences. The entire charge should be fluidised during the entire process, to guarantee an acceptable heat and mass transfer between air and product.

**Spray Time:** adjusted according to the desired load of coating to be added.

**Drying time:** 3 - 6 minutes

**Curing conditions:** 2 hours at 60°C in a tray dish dryer (according to MFT for Aquacoat ECD).

The coating suspension was gently stirred during the entire coating process to prevent sedimentation. During first experiment trials the loss of coating suspension in the container walls and tube connections was calculated and, afterwards, an excess was applied in the following experiments to compensate it.

**Table 3.6.2:** Composition of the Aquacoat® suspensions

<i>Mixtures</i>		Mix 1	Mix 2	Mix 3
<i>Substances</i>		[% w/w]	[% w/w]	[% w/w]
Aquacoat®	ECD	66.66	65.09	63.60
	30			
	TEC	5.00	4.88	4.77
	Methocel E3 Prem	-	0.59	1.16
	Water	28.34	29.44	30.47
	Total	100	100	100

After curing, the tablets were stored in desiccators; protected from light, moisture, crushing, and mechanical shocks.

### 3.6.3 Coating Characterization

Visual inspection of the coated tablets surface was carefully carried out to verify the non-existence of coating defects. A conventional lab bench microscope (Laborlux S, Leitz, Germany) coupled with a digital camera system (Leica DC 200, Leica Microsystems AG, Germany) was also used to characterize the uncoated and coated tablet surface.

Scanning Electron Microscopy pictures, as described in section 3.1.1, were taken from the whole tablet surface. A vertical fracture in the tablet was done in order to assess the coating-core adherence, and to verify the homogeneous distribution of the coating layer over the tablet surface (with special attention to the tablet edges). The thickness of the coating layer could be measured by the SEM pictures, and also estimated from the increase in tablet weight after coating (coating level in % (w/w)). The uniformity of mass, or weight variation, was measured using an analytical balance and selecting not less than 10 units.

### 3.6.4 In vitro Drug Release Test

The drug release test was performed following the procedure previously described in section 3.5.7 (Dissolution).

#### 3.6.4.1 Mathematical Models and other release parameters

To study drug release mechanisms and compare drug release profiles various approaches are possible. The pharmaceutical industry and the registration authorities do focus, nowadays, on drug dissolution studies. The quantitative analysis of the values obtained in dissolution/release tests is easier when mathematical formulas that express the dissolution

results as a function of some of the dosage forms characteristics are used. In some cases, these mathematic models are derived from the theoretical analysis of the occurring process. In most of the cases the theoretical concept does not exist and some empirical equations have proved to be more appropriate. A water-soluble drug incorporated in a matrix is mainly released by diffusion, while for a low water-soluble drug the self-erosion of the matrix will be the principal release mechanism. To accomplish these studies the cumulative profiles of the dissolved drug are more commonly used in opposition to their differential profiles. To compare dissolution profiles between two drug products model dependent (curve fitting), statistic analysis and model independent methods can be used (Costa and Lobo, 2001).

Model-independent methods are easy to apply but they contribute with little information to clarifying the release mechanism and should be associated with each other or with some model-dependent approach. Examples are simple statistical methods (ANOVA) and ratio test. The last ones are relations between parameters obtained from the release assay, normally used to compare two assays at the same time point, e.g.  $T_{85\%}$  and  $T_{15\text{min}}$ .

The  $t_{x\%}$  parameter corresponds to the time necessary to the release of a determined percentage of drug (e.g.,  $t_{20\%}$ ,  $t_{50\%}$ ,  $t_{85\%}$ ) and sampling time corresponds to the amount of drug dissolved in that time (e.g.,  $t_{20\text{min}}$ ,  $t_{50\text{min}}$ ,  $t_{90\text{min}}$ ). Pharmacopeias and most of guidelines frequently use these parameters, among others, for comparisons between profiles and as acceptance limits.

The lag time of pulsatile release tablets is defined as the time when the outer ethylcellulose coating starts to rupture. It was determined visually during dissolution test and also estimated from the drug release profiles. For the calculation of  $T_{x\%}$  and  $T_{x\text{min}}$  the lag time was reduced from the total time, i.e., the time was counted after the coating rupture and beginning of the drug release.

## 4 Results and Discussion

### 4.1 Characterization of Starting Materials

The physical properties of the two main compounds and their powder mixtures, in three different ratios, are compiled in Table 4.1.

**Table 4.1:** Characterization of Starting Materials

	cellulose Type II	PQZ	Powder Mix1 (10%-wt. drug)	Powder Mix2 (50%-wt. drug)	Powder Mix3 (90%-wt. drug)
Mean particle size ( $\mu\text{m}$ )	120.31	16	-	-	-
D(v, 0.1)* ( $\mu\text{m}$ )	23.78	6.69	-	-	-
D(v, 0.9)** ( $\mu\text{m}$ )	305.60	27.29	-	-	-
Loss on Drying (%)	5.30	0.39	4.58	3.19	1.09
True Density ( $\text{g}/\text{cm}^3$ )	1.543	1.230	1.509	1.403	1.294
Bulk Density ( $\text{g}/\text{cm}^3$ )	0.641	0.323	0.526	0.393	0.266
Tapped Density ( $\text{g}/\text{cm}^3$ )	0.781	0.396	0.654	0.596	0.410
<i>K</i> (packing fraction)	0.42	0.26	0.35	0.28	0.21
Powder Porosity (%)	58	74	65	72	79
Hausner Ratio	1.22	1.22	1.24	1.51	1.54
Compressibility Index	17.95	18.55	19.47	33.98	35.11
Other Properties (Rowe et al., 2006; Lanz, 2006)	hygroscopic	Hydro- phobic	--	--	--

\* 10% of volume distribution is below this value.

\*\* 90% of volume distribution is below this value.

The hydrophobic property of PQZ was confirmed by its very low residual moisture, 0.39% under loss on drying. Very low moisture can also hinder flow since it is more likely to develop electrostatic charging (Howard, 2006; Hearn, 2002). Cellulose type II presented much higher moisture content, 5.30%. This property can be an indicator of the cellulose hygroscopicity and wettability. In the powder mixtures, increased amounts of cellulose type II elevated the moisture content proportionally.

The *Compressibility Index* and *Hausner ratio* showed that the powder mixture of 90%-wt. PQZ had a very poor ability to flow. The 50%-wt. PQZ formulation presented a poor flowability and 10%-wt. drug a passable one. For poorer flowing materials, there are



frequently greater interparticle friction and interactions, being more cohesive and hence less free-flowing powders. This phenomenon could be clearly noticed during the experiments execution when the powder mixtures were not able to proper flow and fill the dies in the press machine in an attempt of direct compaction. Consequently a granulation process was required to overcome the poor flow problem.

The fractional solids content,  $k$ , was much higher for the cellulose powder compared with PQZ, and proportionally higher among the mixtures with increased amounts of cellulose. The opposite happened with the porosity values. The smaller particle size material, PQZ, showed lower densification tendency compared with larger particle size of cellulose, since it produced more void space in the powder bed under the same experimental conditions. The densities values also expressed that behaviour. Probably caused by the broad difference in PQZ particles size plus its static electricity, both affect its packing geometry that became more loosely.

Figure 4.1 shows the long fibres (aggregated and non-aggregated) that provide UICEL particles with a high contact area. Unlike cellulose, proquazone powder is composed of small and very small particles, some flakes shaped and with smoother surface and edges, and forming a kind of aggregated structure among the very broad range of particles sizes. PQZ also showed to be a microfine powder (90% of particles smaller than  $45\mu\text{m}$ ), reinforcing its cohesiveness, with very high surface-to-mass ratio.

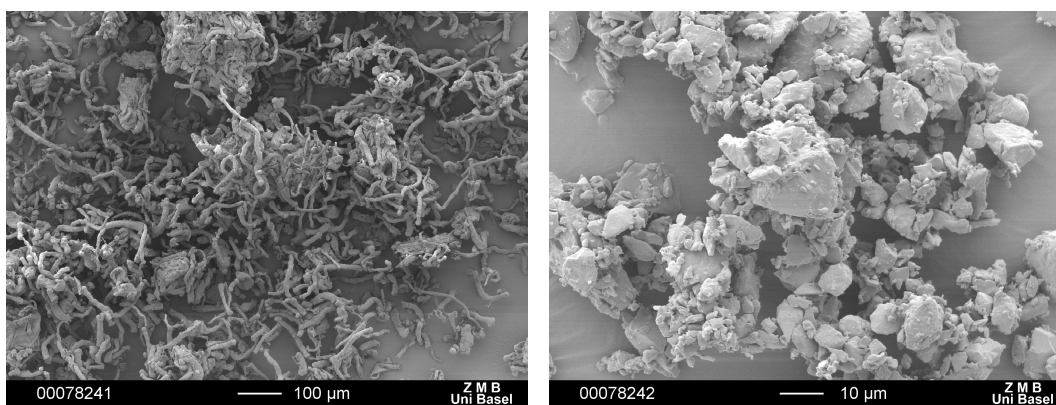


**Figure 4.1:** SEM pictures of UICEL (left) and Proquazone (right).

## 4.2 Granulation

The physical properties of the granules produced from the different powder mixtures are compiled in Table 4.2.

**Table 4.2:** Granules Characterization

	Granules Mix1 (10%-wt drug)	Granules Mix2 (50%-wt drug)	Granules Mix3 (90%-wt drug)
Median particle diameter ( $\mu\text{m}$ )	282	460	555
Loss on Drying (%)	7.95	5.24	1.20
True Density ( $\text{g}/\text{cm}^3$ )	1.483	1.389	1.287
Bulk Density ( $\text{g}/\text{cm}^3$ )	0.400	0.417	0.500
Tapped Density ( $\text{g}/\text{cm}^3$ )	0.435	0.444	0.546
Porosity (%)	73.0	70.0	61.0
Hausner Ratio	1.09	1.07	1.09
Compressibility Index	8.00	6.25	8.50
<i>K</i> (packing fraction)	0.27	0.30	0.39
Crushing Strength (N) (Error - SE)	21.08 (1.38)	16.78 (1.74)	9.40 (1.10)

The granules moisture content was increased proportionally to the amount of cellulose II in the formulation. The moisture content of a material can affect its mechanical properties generally by acting as an internal 'lubricant' facilitating the slippage and plastic flow (Khan et al, 1981; Dawoodbhai and Rhodes, 1989).

The granulate porosity appeared to increase with the enlargement in the starting material particle size. The lower porosity of the 90%-wt. drug granulate compared with others may be attributed to its wider particle size distribution and the ability of the fine particles to fill in the voids between the larger particles.

Higher bulk density and packing fraction, smaller porosity, can all be indications of more dense granules. The granules with high content of drug behaved exactly the opposite of the drug bulk powder bed. The presence of water in the environment, acting as a binder and as an electrostatic isolator, together with the binder itself (HPMC), probably was able to improve the drug interparticulate contacts and hence to improve the superficial interparticulate bonding; with the fine particles again filling the void spaces.

Bulk and tapped densities are also correlated with particles size and shape. The median granules diameter was bigger for granules of higher drug concentrations, and their shape were more spherical with smoother surfaces, as can be seen in the figure 4.2.1.

The *compressibility index* and *Hausner ratio* were similar among the different granulates. All presented excellent flow character.

#### 4.2.1 Granules visual appearance and Crushing Strength

It is well known that the material morphology affects its flow and packing properties (Howard, 2002; Brittain, 1989). As well as the mechanical strength of the granules can affect the strength of the tablets (Alderborn et al, 1987). Figure 4.2.1 shows the surface roughness of the granules, which was increased with the increase in cellulose II concentration. In another words, increasing the particle size of the starting material, the surface of the granules became rougher. This granule characteristic plus its “hardness” will influence in the inner part of the tablet core and its surface as well.

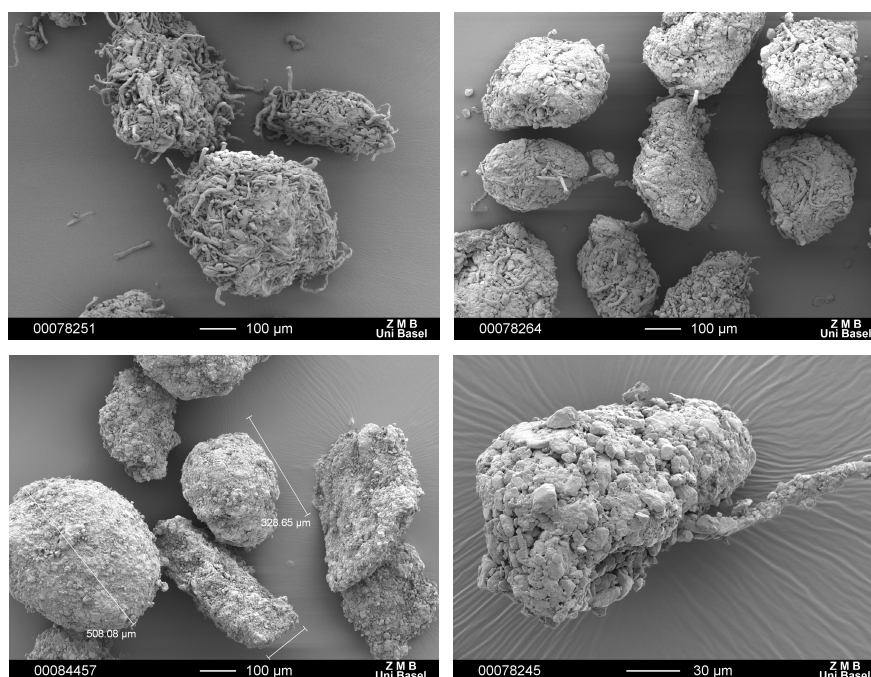


**Figure 4.2.1:** SEM pictures of granules with 10% drug (top left), 50% drug (top right) and 90% drug (bottom left and right).

A high difference in the agglomerates topological ruggedness could be qualitatively evaluated from the SEM images. Shape, particle structure and the propensity of the material to fragment or deforming can change the volume reduction behaviour of the agglomerate (Alderborn, 1996). That could be verified by the values found for the packing fraction and crushing force. Comparing all granulates, granules composed of 90%-wt. PQZ showed to have higher packing fraction and smaller crushing strength. Increasing amounts of cellulose II decreased the packing fraction and increased the crushing strength, proportionally to the amount of cellulose fibres present in the granules. That probably happened due to the tendency of irregular-shaped particles to produce open structures and loosely packing.

The granules produced with 90%-wt. of the very fine proquazone powder (with its flat and smooth surface and edges) showed to have higher propensity to fragment or deform, i.e.,

they were weaker under an external pressure, what was revealed by the smaller values of the crushing strength test. This can be a result of an insufficient binder addition for that high drug load formulation and a brittle behaviour. Nonetheless, during the crushing strength test for the granules made of 90%-wt. drug, it was observed that the particles (i.e., the individual granules tested) did not broke apart in little pieces but instead they changed their shape becoming flattened ones. It had been reported by Benbow (Benbow, 1983) that when the particles sizes are markedly reduced, a transition from a brittle to a plastic behaviour takes place. In another study, the compression of sodium chloride showed that particles above 33  $\mu\text{m}$  in diameter fractured under compression, while particles below this size did not show any fragmentation but deformed plastically under compression (Roberts et al., 1989). The relative *standard deviation* of the crushing force measurements was approximately 9, 16 and 20% (for the formulations of 90, 50 and 10 percent-wt. drug, respectively), which is very high and due to the fact that the granules themselves differ in size.

#### 4.2.2 Particle Size Distribution (PSD)

In the figure 4.2.2 is possible to compare the cumulative particle size distribution of the three formulations. It is noticed that the formulation with higher content of cellulose II had a smaller range or spread of equivalent diameters than the other two formulations. The PSD of granulates made of 50%-wt. drug showed to follow the distribution of granulates made of 90%-wt. drug more than the 10%-wt. drug ones. It can be interpreted that the influence of PQZ in the agglomeration process was more significant than the cellulose type II for that formulation. Furthermore, the volume of drug (55.48%) was bigger compared with the volume of cellulose II (42.46%).

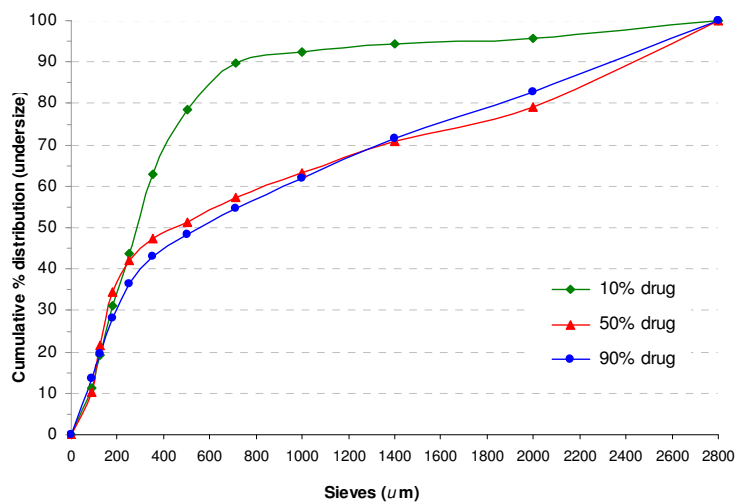


**Figure 4.2.2:** Cumulative percental frequency *undersize* distribution curves. The 3 formulations are distinguished by the symbols in the legend (%-wt. of drug).

### 4.2.3 Power Consumption

Monitoring tool which provides a real-time visualization of the powder liquid saturation as well as changes in powder agglomeration/cohesion inside the mixing vessel. Examples of power consumption measurements are shown in the figures 4.2.3, 4.2.4 and 4.2.5. Profiles were more similar in experiments of formulations with higher content of the cellulose material. The total amount of water applied was increased proportionally to the increasing of cellulose II in the mixtures (data not shown). It can be concluded that for the progressive liquid saturation of the system, and the agglomeration of the particles, the cellulose II powder was a material with high influence. The *cohesion path* showed to be driven by its hygroscopic properties. However, the final granulate characteristics, such PSD, was markedly influenced by the drug content, as explained above.

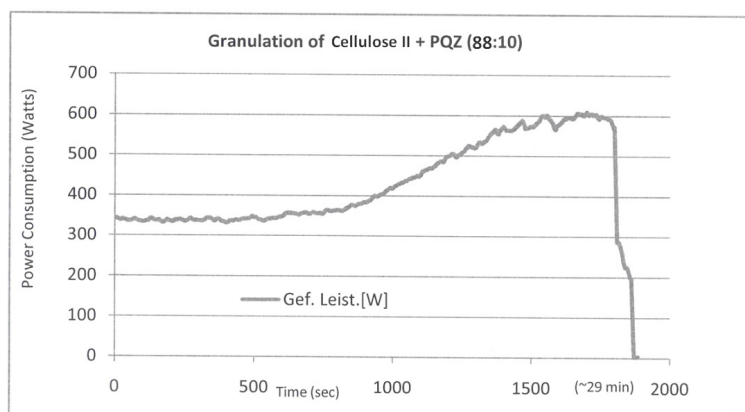


**Figure 4.2.3:** Power consumption measured during a granulation of a mixture containing cellulose type II:proquazone (88:10) (w/w).

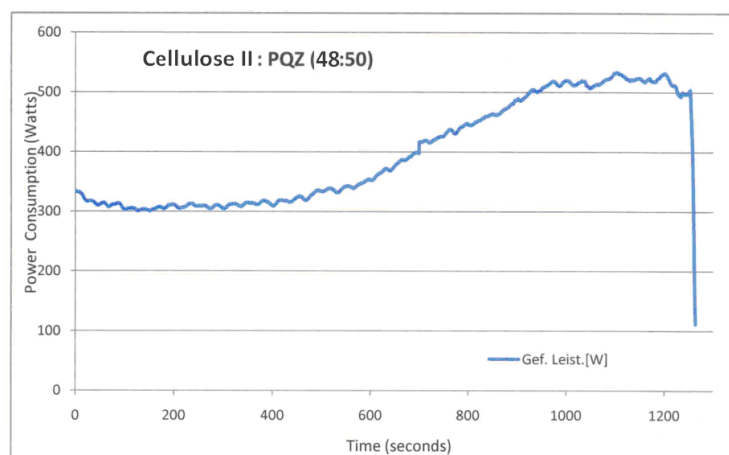


**Figure 4.2.4:** Power consumption measured during a granulation of a mixture containing cellulose type II:proquazone (48:50) (w/w).

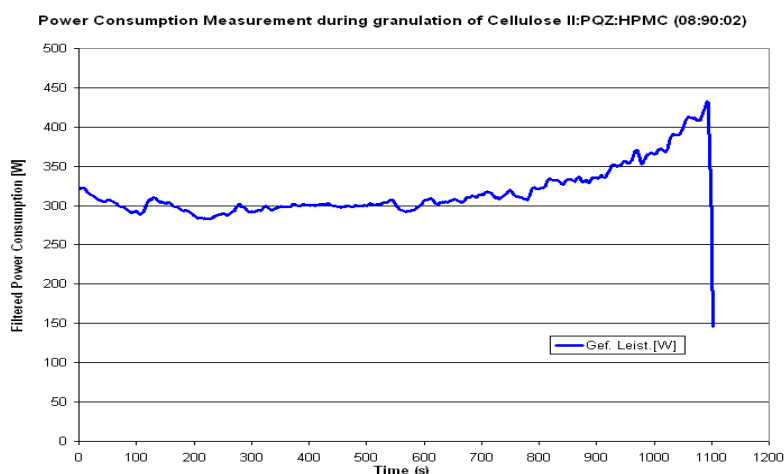


**Figure 4.2.5:** Power consumption measured during a granulation of a mixture containing cellulose type II:proquazone (08:90) (w/w).

The maximum absolute value of energy consumed was decreased with the increase of PQZ in the formulation. Considering that power consumption measurement is strongly correlated with the fluidity of the powders inside the mixer vessel and its contact with the vessel walls (adhesion was not avoided) and impeller blade, the results showed that the higher drug load formulation presented smaller adherence and resistance to impeller movement. Looking at the granules SEM images can be assumed that the attrition or friction among the particles and against the equipment surfaces was minimized by the higher sphericity and smoother surface for granules of 90%-wt. drug. A brittle or crumb behaviour for the *still green* granulates, during granulation, could have influenced the power consumption as well. Moreover, the true density of the 90%-wt. PQZ mixture and its resulted granulates were small than other formulations.

For reason of data mining a plot was generated showing the correlation between the properties of the starting powder mixtures, their respective produced granules properties, with the power consumption measured during granulation (Figure 4.2.6). The blue columns represents a positive correlation and the red ones a negative correlation.

From the plot can be seen that the amount of PQZ, the powder porosity, the generated granules size, bulk density and packing fraction had a negative influence over the power consumption.

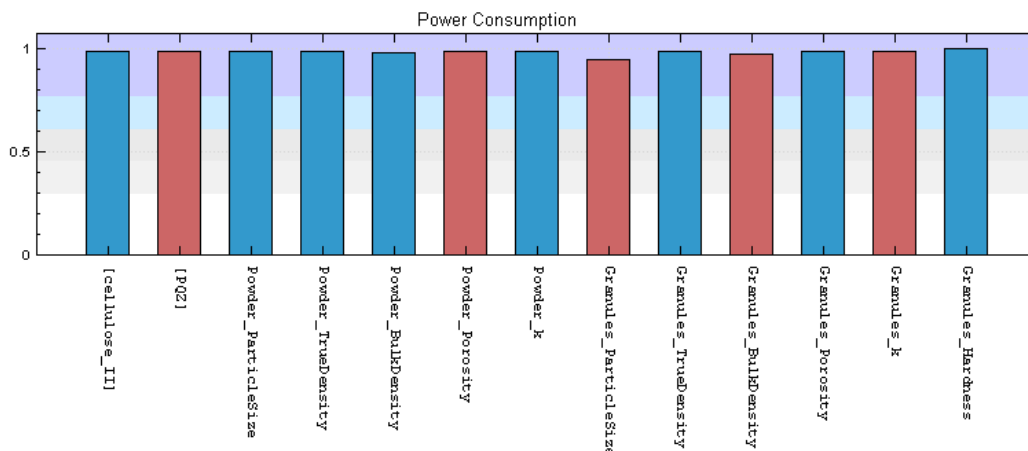


**Figure 4.2.6:** correlation between powder properties, their respective produced granules properties, with the power consumption. Plot generated by Synapse program (Peltarion Synapse version 1.3.5), software for artificial neural networks.

### 4.3 Compaction

The properties of the tablets manufactured from the three different granulates are compiled in Table 4.3.1.

**Table 4.3.1:** Tablets properties

	Formulation 1 (10%wt drug)	Formulation 2 (50%wt drug)	Formulation 3 (90%wt drug)
Weight (mg)	205	200.8	204.9
Geometric Volume (mm <sup>3</sup> )	157.67	169.52	174.56
Surface area (mm <sup>2</sup> )	153.68	159.39	162.53
Ratio W/D*	0.17	0.19	0.22
Density of tablet (mg/mm <sup>3</sup> )	1.305	1.185	1.165
Porosity (%)	13	15.5	10.0
Friability (%)	0.09	0.02	0.02
Crushing Strength (N)	42.40	50.00	55.88
Tensile Strength (N/mm <sup>2</sup> )	2.24	2.04	1.87
Disintegration Time (water)	50 sec.	8 min.	> 2h
Disintegration Time (HCl 0.1M pH 1.2)	<i>immediately</i>	5 min.	50 min.

\* (W/D is the ratio of cylinder length/disc diameter)

As a rule of thumb, it is normally assumed that a decreased original particle size increases the tablet strength (Alderborn, 1996). Besides, under the applied compression force, granules usually fragment along failure planes created between primary particles (Wikberg, 1991). The result is the formation of smaller fragments during compression of granules made of small particles. Consequently, by this de-agglomeration, a high superficial area that can be available for bonding is expected. And a core with small pore volume would be created during compression of those granules. The tablets core made from the 90%-wt drug granulates held these characteristics.

The friability test showed that the tablets were robust enough to resist the tumbling inside the coating equipment. Also the porosity of the tablets appeared to be appropriate, once those very high porous tablets tend to soak up the first application of solution, eroding the core and preventing the coating polymer from spreading uniformly across the surface of every tablet in the batch.

In Figure 4.3.1 the crushing strength and tensile strength of the tablets are plotted as a function of the crushing strength of the granules. A reduction in the granules crushing strength (i.e., interpreted here as its fragmentation or deformation propensity) was correlated with an increased crushing strength and a decreased tensile strength of the compacts.

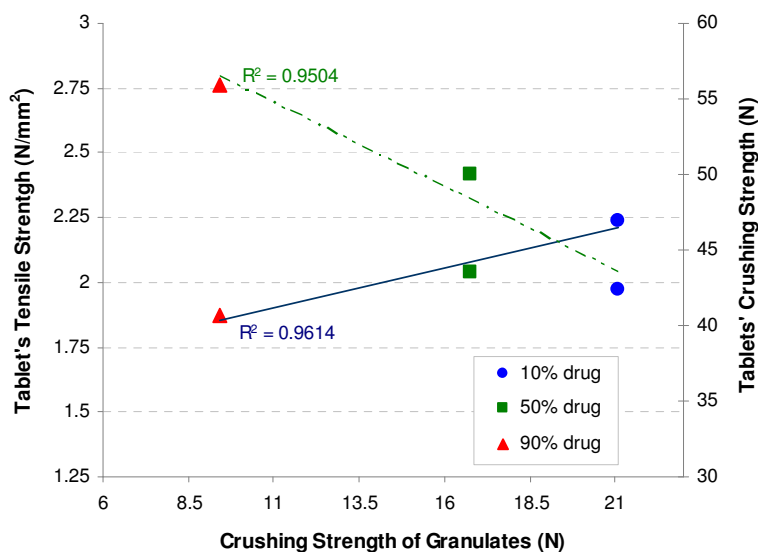


**Figure 4.3.1:** Tablets tensile strength and crushing strength (second axis) as a function of the granules crushing strength, for the three formulations. The dashed line represents the trendline for the tablet crushing strength.



These findings might be explained by the phenomenon that tablets obtained from 90%-wt drug formulations can be described as large agglomerates consisting of a large number of small particles agglomerated together.

Hard granulates are better able to withstand compression forces and they are less deformable. Thus, the harder granules of 10%-wt drug formulation were found to produce fragile tablets. It is known that the bonding force of the intergranular bonds and the structure of the intergranular pores will be significant for the tensile strength of the tablets (Alderborn, 2007). These same granulates containing higher amounts of cellulose II generated tablets with stronger tensile strengths.

From the plot, it can be assumed that probably because the poorly compactable properties of proquazone the tensile strength decreased with increased amounts of drug.

Cellulose powders appear to exhibit little or no swelling, yet takes water into its network quite rapidly. Furthermore, longer fiber length could improve the efficiency of capillary uptake of water into the dosage form matrix, due to its greater particle size. That could be seen by the short disintegration times for the tablets with higher amounts of cellulose type II. (Further possible reasons for the fast disintegration properties of cellulose II are given in the theoretical section).

Due to the addition of excipients have been done by dry-mixing with the drug powder, prior to granulation, the cellulose type II was probably incorporated intragranularly. This mode of incorporation promotes disintegration of the tablets in finer particles compared with extragranular incorporation.

#### **4.3.1 Visual Appearance of the tablets surfaces and its internal structures**

Irregularities in the tablet surface can interfere in the quality of the coating. Very porous tablet surface prevent the coating from proper adhering to it. Also consistent hardness of the tablet surface enables the coating to 'lock' into the surface. If too soft, the impingement of the solution can erode the tablet, and the opposite, too hard, can not allow the solution to adhere and the coating will peel away (Tousey, 2005).

SEM images of the inner part of the tablets' core and their surfaces are shown in the figures 4.3.2 and 4.3.3.

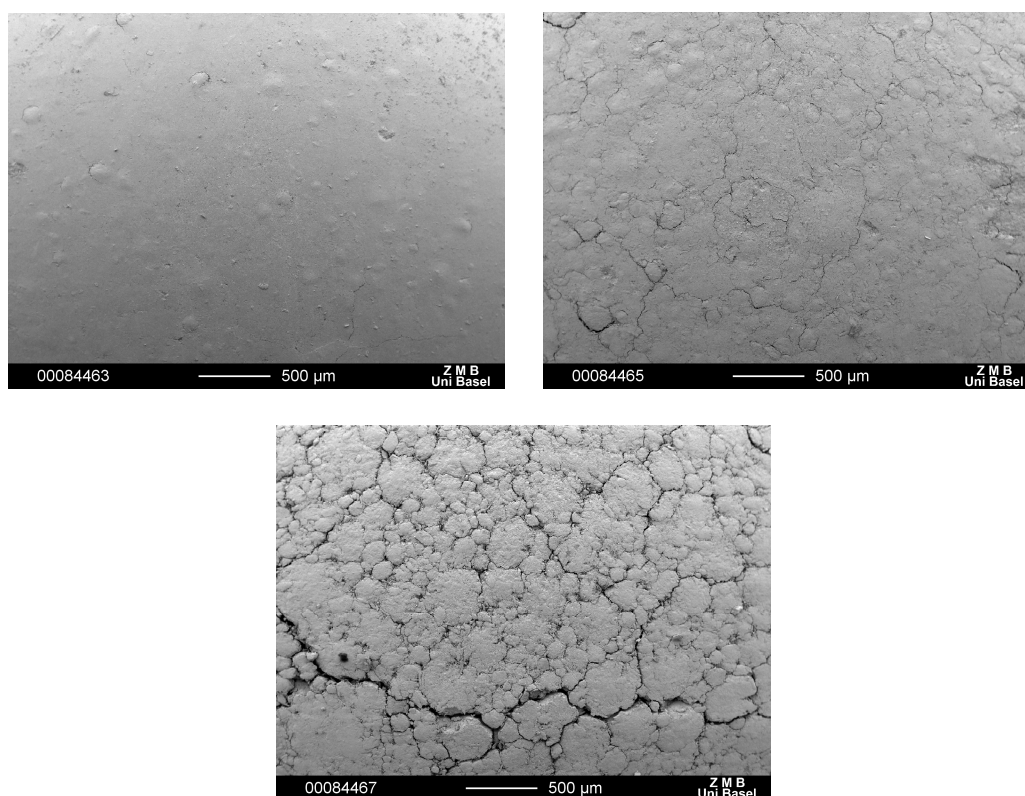


**Figure 4.3.2:** SEM pictures of the tablets' surfaces. Tablet with 90%-wt drug (top left), 50%-wt drug (top right) and 10%-wt drug (bottom).

As expected, due to the softness of the granules with higher amounts of PQZ, the tablets produced from these granules shown smoother surfaces, practically with no cracks or fissures. Few lumps or protuberances are noticed. As the amount of cellulose was increased into the formulation, the cracks or fissures appeared to spread and the primary granules could be easily detected on the surface, separated by dips between them.

These findings were similar to the work of Narayan and Hancock, where the highly irregular shape and surface morphology of the MCC particles was related to the prevention of close packing during compression and contributed to the high roughness of the compact surface. They also found that ductile materials seemed to produce compacts with rough surface while brittle powders seemed to produce smooth compacts (Narayan and Hancock, 2003).

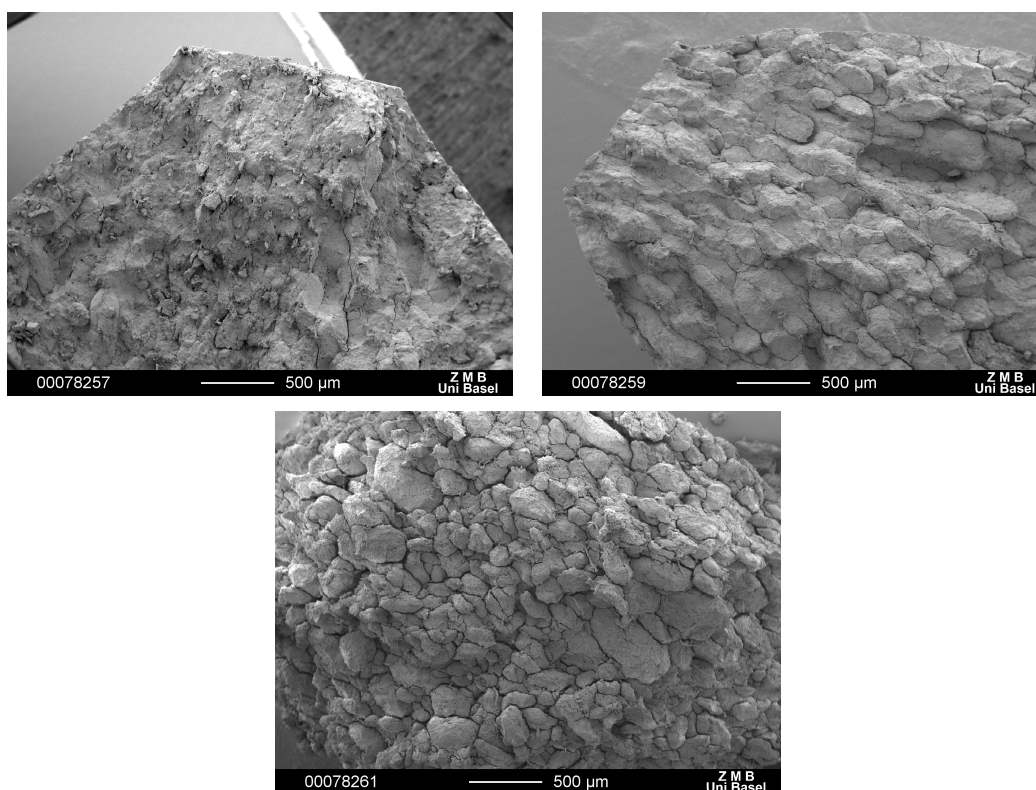


**Figure 4.3.3:** SEM pictures of the internal structures of the tablets. Tablet with 90%-wt drug (top left), 50%-wt drug (top right) and 10%-wt drug (bottom).

In the internal structure of the tablets made of 90%-wt proquazone drug, the core looks like a totally embedded mass, originated by the deformation of the granulates, which ones are not anymore clearly visible. This *internal view*, and also the surface roughness, can be well correlated with the tablet physical characteristics such its hardness. Tablets with closer packing/arrangement of the particles showed to be harder due to the particles have no space for motion.

In the 50%-wt drug formulation some granules still visible and *channels*, void spaces, between them are present. For the formulation of 10%-wt drug, the edges of the granules are clearly visible and there are many channels in all places. Granules were only partially deformed in the inner part of the tablet and at the surface they still visible too. The void spaces present in these tablets were forming channels all around inside the core, in another words, they were percolating through the entire system.

According to Beckert et al. (1996) when compressing pellets into tablets, their deformation depends on their hardness. The variations found in the internal structure of the tablets strengthen the affirmation that hardness and deformability of the original particles are co-dependents and inversely proportional.

In all SEM images it was possible to notice that in the region of the tablets edges the material appears more compressed, with less noticeable granules limits and pores, probably a consequence of compressing using deep concave punches.

It was also taken a SEM image of a tablet (direct compressed) made exclusively with cellulose type II powder. Figure 4.3.4 shows very clear the long cellulose fibres that promote a very porous and rough surface.

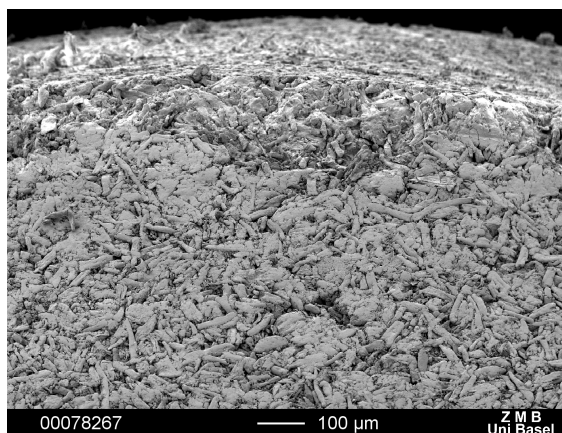


**Figure 4.3.4:** SEM image of the surface of a direct compressed tablet made of cellulose type II.

## 4.4 Coating

### 4.4.1 Monitoring of the coating application process and coating quality

Since spraying, coating distribution, and drying all take place at the same time, tablet coating is a dynamic, complex process that is affected by many variables.

In the beginning of this study, it was not sure if it would be possible to carry out an aqueous coating over a tablet core composed of high amounts of filler which is also considered as a disintegrant (the cellulose type II). The reason lies in the possibility of erosion of the tablet due to water absorption and/or a soft or friable tablet. Just one broken tablet inside the coating equipment can distribute particles to all the other tablets and spoil their appearance, as well as jeopardize the function of the coating. A special attention was taken in order to avoid the over-wetting of the cores.

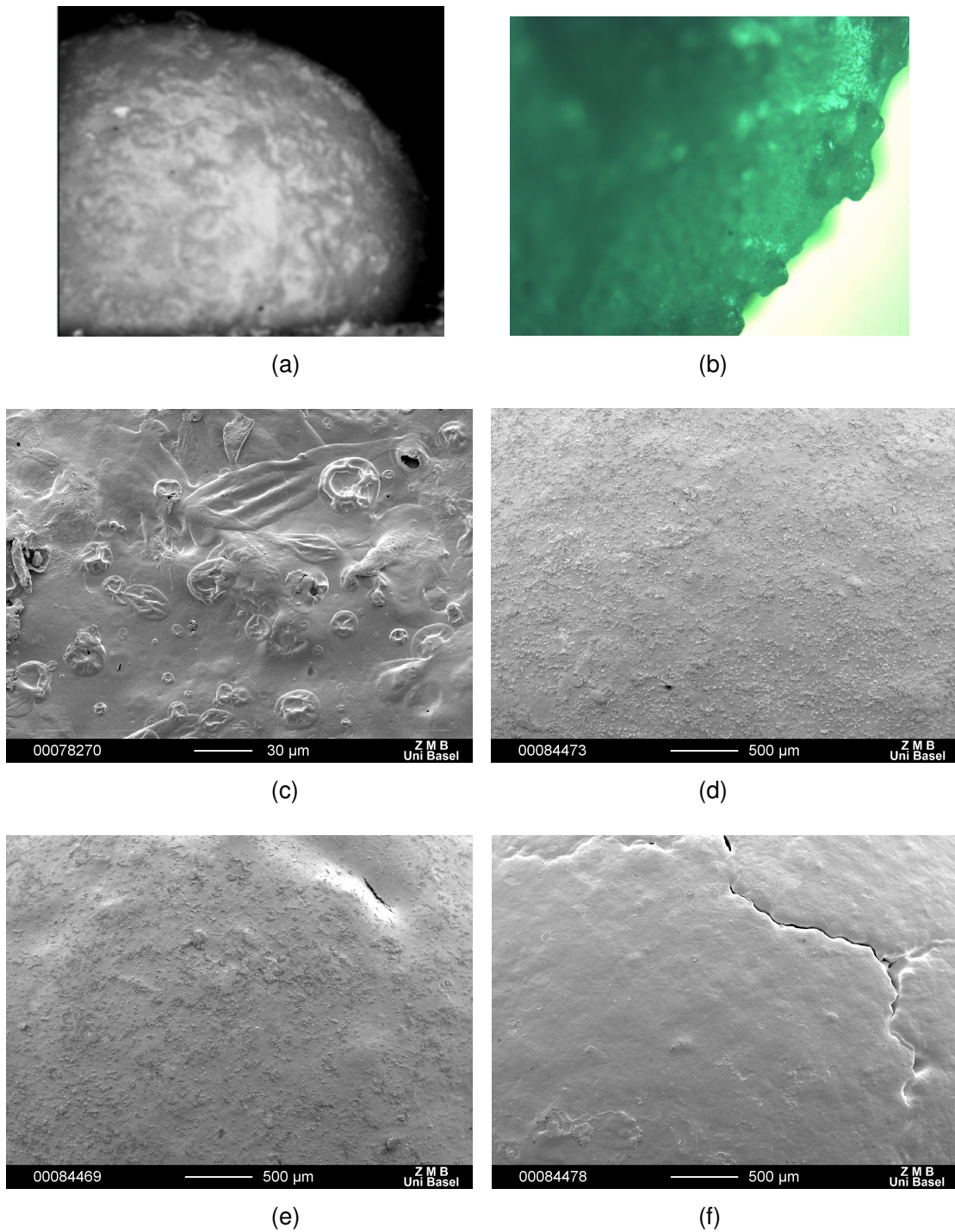
Thin coatings, with percentage of weight gain not bigger than 10%, were chosen in order to reduce the application time and core exposure to water. Coating solutions must be formulated to have a sprayable solution viscosity. To maintain that condition, a low viscosity HPMC grade, in small concentrations, was successfully used. The low viscosity of Methocel E3 Premium permits high solids content in the coating solution, thus less water can be used

and later on be removed. The goal was to enable the coating equipment to evaporate the water at the same rate as it is introduced into the process.

Figure 4.4.1 shows coating defects found during the experimental trials done during the optimization of the coating process. Some of the possible causes of these defects could be the overwetting of the core, high atomization pressure, low bed temperature, high percentage of solids, high loading volume, and weak cores. The reason could also be an inadequate coating solution.

In some cases the coating solution penetrates the surface of the tablet, often at the crown where the surface is more porous, causing localized disintegration of the core and disruption of the coating. The defect is often alleviated by increasing the drying (inlet air) temperature and decreasing the spray application rate, although in a minority of cases increasing the viscosity of the coating solution by increasing polymer concentration may be necessary to slow the rate of penetration of the solution into the tablet surface (Rowe, 1997).

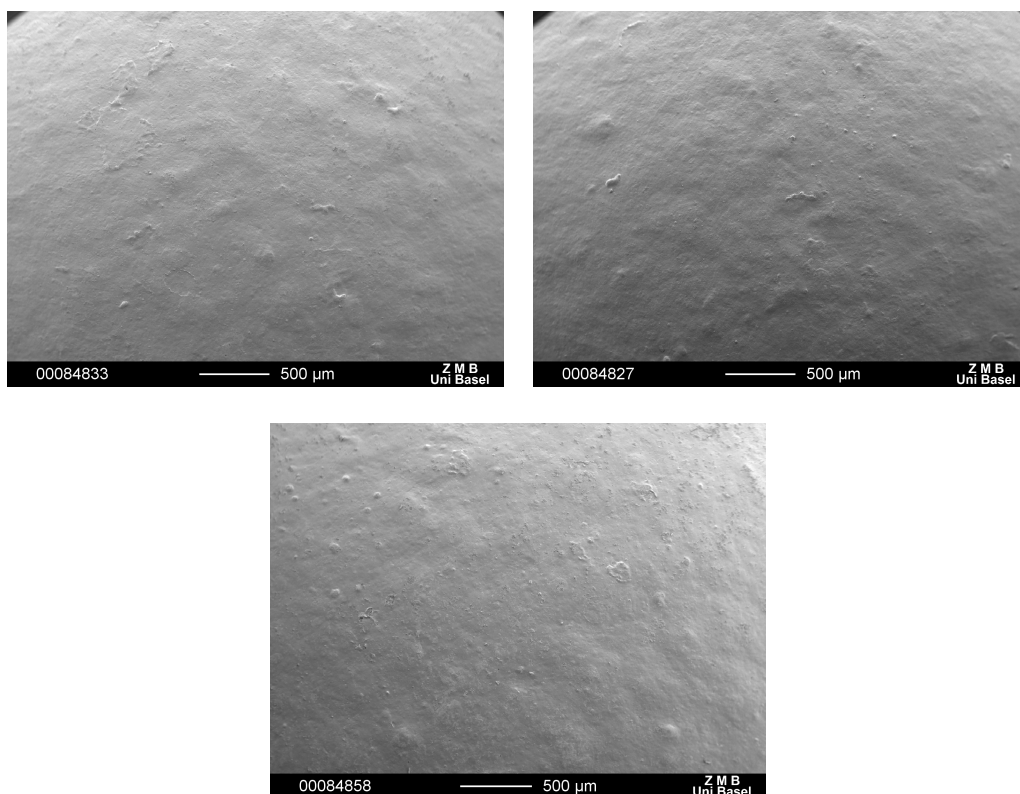
As shown in the Figure 4.4.2, the defects mentioned above could be overcome taking the following actions: reducing the spray rate at the beginning of application; the bed temperature was increased in order to reduce the time for water evaporation (bed temperature is a critical step in coating process, and should be adjusted according to the coating formulation. Some polymers, as Eudragit® ones, are soft polymers and can 'over'melt after application, consequently causing tablets sticking); the atomized air pressure was reduced as well as the loading volume of tablets. The spray pattern was optimized in order to enhance the fineness of the scattering by the proper adjustment of the nozzle aperture. Even with the reduction in the initial spray rate, the total time of spraying was kept as shorter as possible, followed by the drying step (with increased air flow ventilation to promote higher fluidization).



**Figure 4.4.1:** Coating defects found during trial experiments. (a) and (b) different views of *orange peel* defect with high roughness; (c) cratering and/or blistering; (d) particulate contamination; and (e) and (f) fissures and cracks are visible.

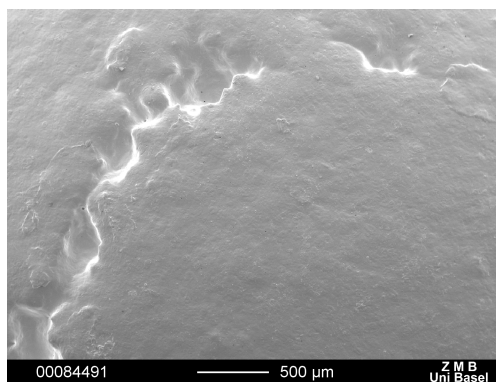
#### 4.4.2 Visual appearance of the coated surfaces, its homogeneous distribution and thickness

Figure 4.4.2 shows examples of surfaces of coated tablets, after the coating process optimization. The cross section images of the film-coated tablets, shown in Figure 4.4.4, were taken to assess the homogeneous distribution of the coating over the entire tablet surface, as well as its thickness, specially in the edges of the tablets where the chance of defects are higher.



**Figure 4.4.2:** SEM pictures of coated tablets surface. Tablet with 90%-wt drug and coating of 3% P.F. with 3.29% w.g. (top left); tablet of 50%-wt drug, 3% P.F., 5.70% w.g. (top right) and tablet of 10%-wt drug, 6% P.F., 9.39% w.g (bottom).

Defects in the tablet core, as fissures or dips, could be overcome by the application of the coating polymer, as shown in the Figure 4.4.3.



**Figure 4.4.3:** SEM image of a fissure in the surface of the tablet totally coated by the polymer.

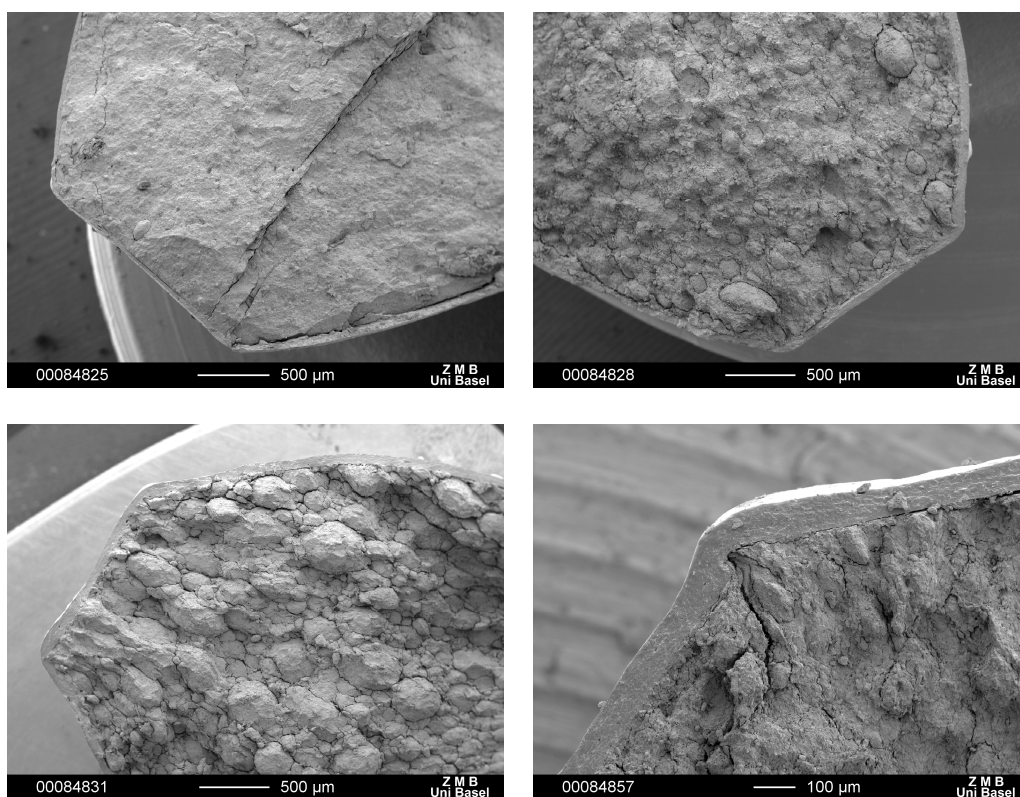


**Figure 4.4.4:** cross section SEM images of the film-coated tablets showing the homogeneous distribution of the coating layer. Tablet with 90%-wt drug (top left); 50%-wt drug (top right) and 10%-wt drug (bottom left). All coatings have 3% P.F. and 5.70% w.g. Detail of a tablet edge (bottom right).

In addition to check the coating distribution, the SEM photos enabled to measure the thickness of the coating layers. The thickness did not show be reduced on the edges, but it was homogeneous all around the tablet surface.



Almost all coating experiments, using ethylcellulose, had their SEM images taken. For those experiments without SEM photos the coating thickness was estimated by weight variation, i.e., the weight gained after coating. The results are compiled on table 4.4. The values in micrometers represent an average of at least 10 measurements taken from different points of the coating layer. The values showed a good connection between gained weights and layer width.

**Table 4.4:** Coating thickness expressed in percentage of tablet weight gain and by micrometers ( $\mu\text{m}$ ) measured from the SEM images.

Tablet weight gain after coating (%)	Coating thickness ( $\mu\text{m}$ )
9.39	99.38
9.00	118.30
8.07	97.00
6.57	77.42
5.75	88.23
5.70	52.48
3.80	44.20
3.29	44.55

#### 4.5 Drug Release Studies

The dissolution profile of the uncoated cores, for the three formulations, can be seen in the Figures 4.5.1.a, b and c. Different dissolutions media were tested in order to find the most discriminatory one: HCl 0.1N, phosphate buffer pH 6.8 and phosphate buffer pH 6.8 + 1% surfactant (sodium lauryl sulfate - SLS).

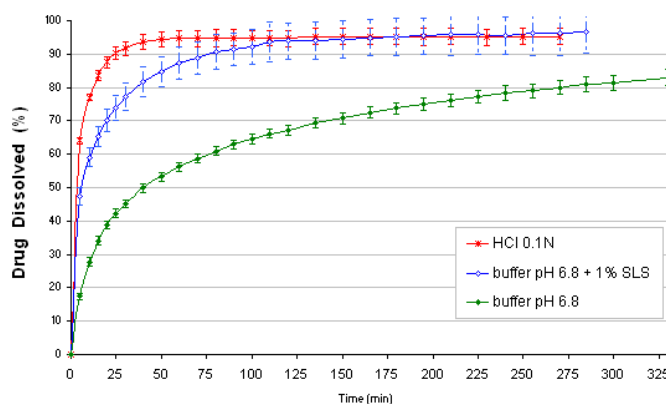


**Figure 4.5.1 a)** Dissolution profiles of uncoated tablets composed of 10%-wt drug in different mediums. (Mean  $\pm$  SD, n= 6)

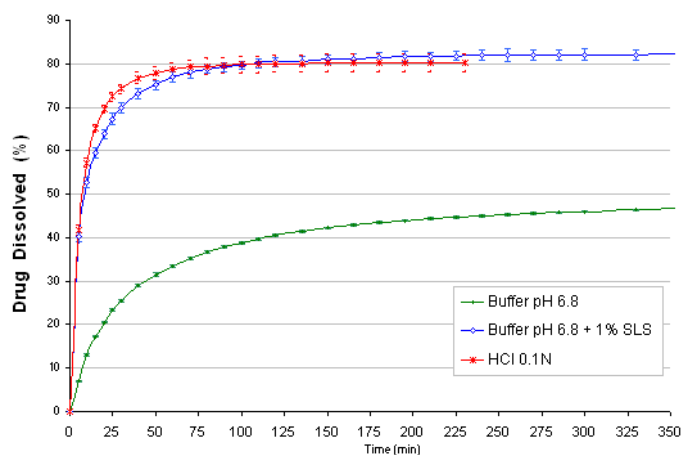


**Figure 4.5.1 b)** Dissolution profiles of uncoated tablets composed of 50%-wt drug in different media. (Mean  $\pm$  SD, n= 6)

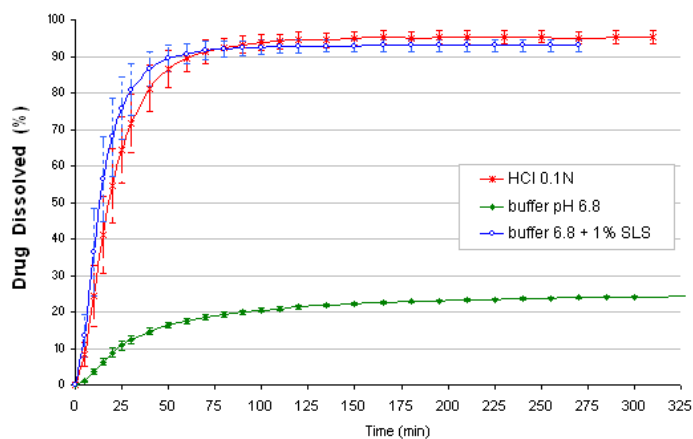


**Figure 4.5.1 c)** Dissolution profiles of uncoated tablets composed of 90%-wt drug in different media. (Mean  $\pm$  SD, n= 6)

Proquazone solubility was considered an important variable influencing the drug dissolution in the three dissolution media. Hydrochloric acid 0,1N showed to represent better the drug release after core disintegration. A proper solubilisation of PQZ in the buffer medium was only possible with the addition of surfactant. The presence of a surfactant in the aqueous media enhances the wetting of particles by lowering the advancing contact angle. Ethylcellulose is known to be pH-independent, however it was shown (Bodmeier and Paeratakul, 1991) that the commercial available ethylcellulose pseudolatex, Aquacoat<sup>®</sup>, presented a pH-dependent drug release in coated beads; having an increased release in simulated intestinal fluids, caused by the presence of the anionic surfactant that gets complete ionized at increased pH's.

Thus, looking for the most discriminative way to show the fast release of the drug from the inner parts of the tablet (i.e. the rupture of the coating membrane and the burst disintegration of the core, caused by the cellulose type II) with fewer variables that could possibly influence it, the HCl media was chosen for further tests.

The delayed-release (DR) dissolution testing, according to USP Method B, was carried out and compared with the acidic media 0.1N HCl. The results are plotted in the Figures 4.5.2.a and 4.5.2.b. The tablets tested belong to the same formulation and manufacturing batch.

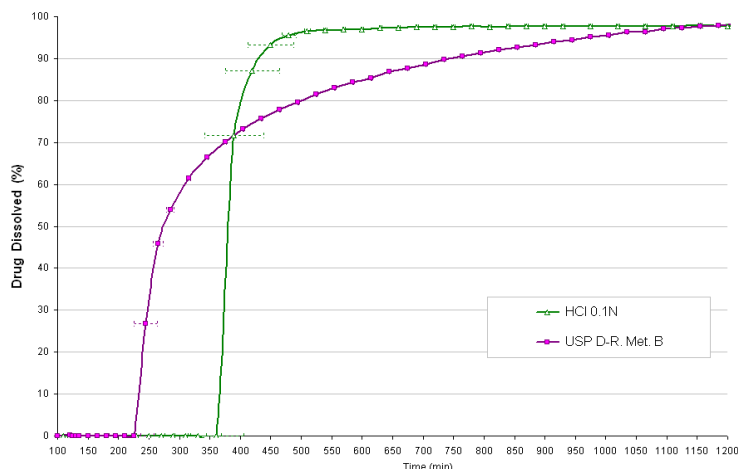


**Figure 4.5.2.a:** Dissolution profiles of tablets composed of 10%-wt. drug and 9.39% of weight gain after coating with Aquacoat<sup>®</sup> ECD + 6% of Pore Former (Mean  $\pm$  SD, n= 6). The two mediums are named in the legend.

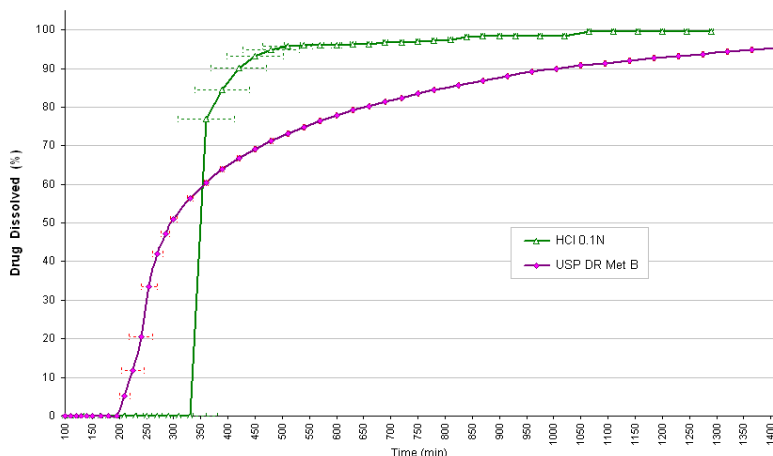


**Figure 4.5.2.b:** Dissolution profiles of tablets composed of 10%-wt. drug and 6.57% of weight gain after coating with Aquacoat<sup>®</sup> ECD + 6% of Pore Former (Mean  $\pm$  SD, n= 6). The two mediums are named in the legend.

The drug release profiles were in agreement with Bodmeier and Paeratakul (1991), showing a pH-relation for the commercial available ethylcellulose pseudolatex, Aquacoat<sup>®</sup> ECD. The premature rupture of the coating layer in the buffer media compared to the acidic one, probably happened due to the presence of the ionized surfactant, enhancing the water permeation throughout the membrane. The neutral pH media showed again not to be adequate for proquazone dissolution test once the drug takes very long time to achieve total dissolution. The aim was to choose a medium that shows the functionality of the delivery system in release all the drug in a short time.

Tablets coated with Eudragit<sup>®</sup> polymers showed a dissolution profile absent of lag time and with a prolonged release, examples are in the figure 4.5.3. When Eudragit<sup>®</sup> RS was applied alone the drug release was smaller than 5%, therefore is not shown.

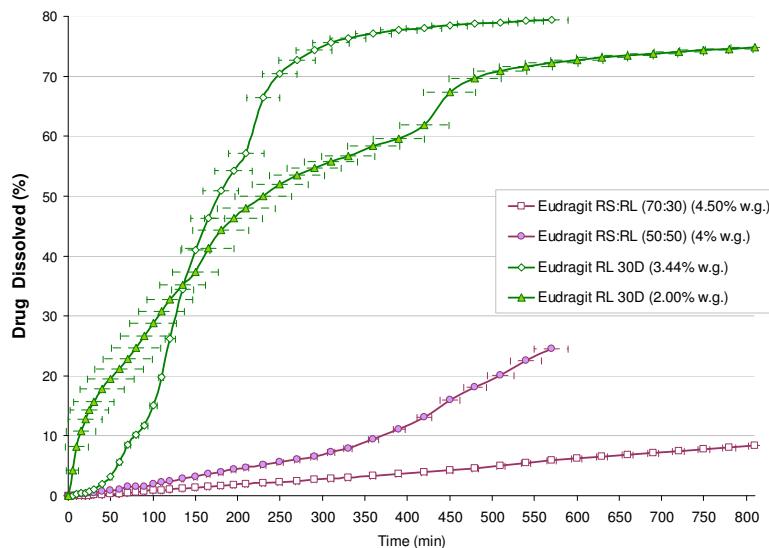


**Figure 4.5.3:** Dissolution profiles of tablets composed of 50%-wt. drug and different weight gains (w.g.) after coating with Eudragit<sup>®</sup> Polymers in different proportions (Mean  $\pm$  SD, n= 6).

A water-insoluble, but water-permeable, polymeric membrane resists the environmental degradation according to its thickness. Once in contact with the fluids the soluble component present in the layer starts to be dissolved away. This produces a microporous membrane and the drug can be delivered in a controlled manner by a combination of drug dissolution in the core and diffusion through the pore channels. This mechanism of release could be noticed when Eudragit<sup>®</sup> polymers were applied as coating membrane. With the water permeation through the membrane into the reservoir the system became swollen/turgid and the coating membrane was flexible, swellable, enough to keep the integrity of the reservoir and the drug was released through the pores without the rupture of

the system. In this case the membrane served as a rate-controlling barrier to modulate the release of drug from the system.

Almost no drug release was noticed from tablets coated exclusively with Eudragit® RS. Because quaternary ammonium groups determine the swellability and the permeability of the film in aqueous media, Eudragit® RL (which contains more of these groups) forms more permeable films with little delaying action. By contrast, films of Eudragit® RS (with reduced content in quaternary ammonium groups) swell less easily and are only slightly permeable to active ingredients (as explained in the materials and methods section).

For Eudragit® coatings the penetration of the dissolution media into the core, causing the tumescence of the system, could be clearly visualized and measured using an analytical balance and a calliper (see table 4.5.1).

**Table 4.5.1:** Percentage of weight gain and dimensional changes caused by water wicking (after 5h exposure) from the tablet core coated exclusively with Eudragit RS 30D (5% of weight gain).

Tablet Composition (% by weight)	Original Weight (g)	Final Weight (g)	% in weight increase	Original Thickness (mm)	Final Thickness (mm)	Original Diameter (mm)	Final Diameter (mm)
10% PQZ	212.1	515.8	143.19	4.78	8.60	8.12	10
50% PQZ	211.2	357.5	69.27	4.80	6.64	8.13	9.35
90% PQZ	207.4	214.4	3.38	4.94	5.03	8.20	8.27

Films prepared from ethylcellulose dispersions resulted in very weak and brittle films when compared to the acrylic films. Pseudolatex-cast ethylcellulose films showed lower puncture strength and elongation values when compared to those of the solvent-cast films. Curing of the pseudolatex-cast ethylcellulose films had minimal effects on their mechanical properties (O'Donnell and McGinity, 1997).

For the tablets coated with ethylcellulose polymer, see Figures 4.5.4.a, b and c, the coating layer was burst/broken by the expanding core. These cores developed an internal osmotic pressure, leading to a fast separation from the coating; what could be noticed visually during the disintegration and dissolution tests. The drug was released from the core after the rupture of the surrounding polymer layer, caused by a pressure build-up within the system. This pressure necessary to rupture the coating was achieved by the presence in the core of the hygroscopic super-disintegrant. Thus, resulting the film rupture followed by a rapid drug release.

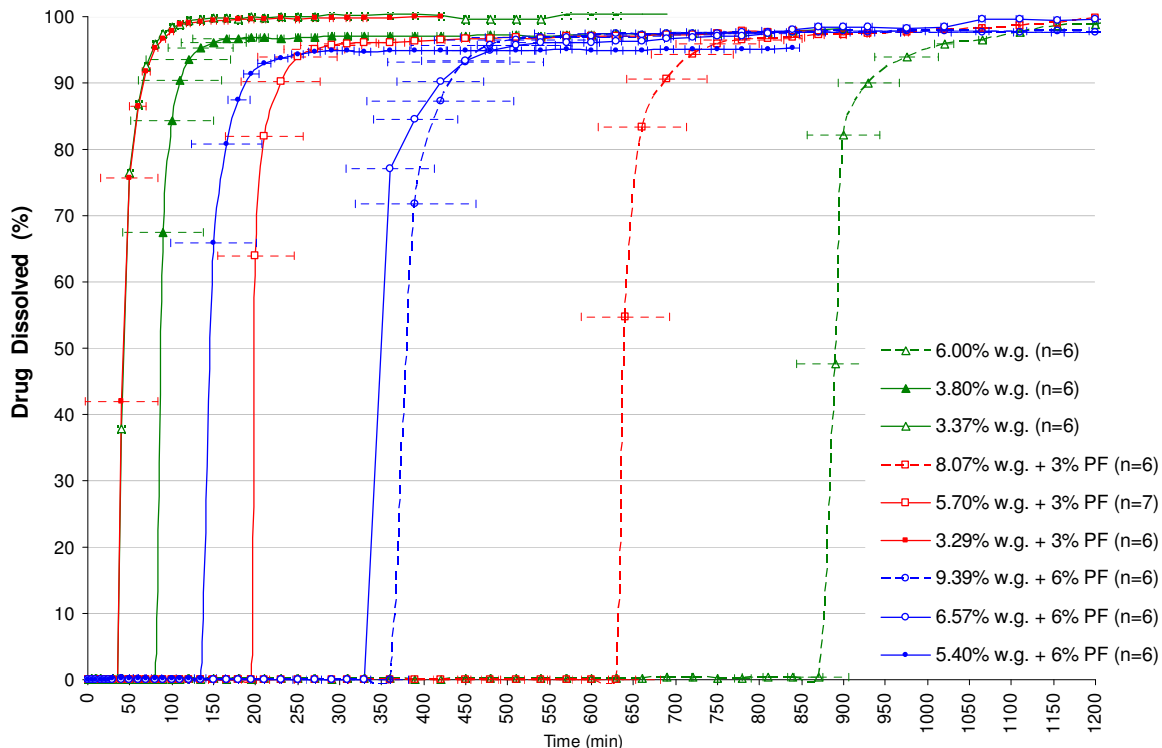


**Figure 4.5.4.a)** Summary of drug release profiles from tablets containing the ratio 10:88 (w/w) of drug:cellulose II. Coated with different rates of Aquacoat<sup>®</sup> ECD, expressed in percentage of weight gain (w.g.); and in the presence, or absence, of pore former (PF). (Mean, +/- SD).

The rupture of the coating membrane strongly depended on the mechanical properties of the coating layer: highly flexible films, such as Eudragit<sup>®</sup> RS and RL, with high elongation were not ruptured in this study (Figure 4.5.3), and as consequence the drug release was prolonged without a lag time. Using the mechanically weaker and nonflexible film, such as ethylcellulose, the drug release profile was sigmoid and reproducible (Figures 4.5.4.a and b).

A deeper study about the mechanical properties of ethylcellulose and Eudragit<sup>®</sup> was done by Bussemer et al. (2003).

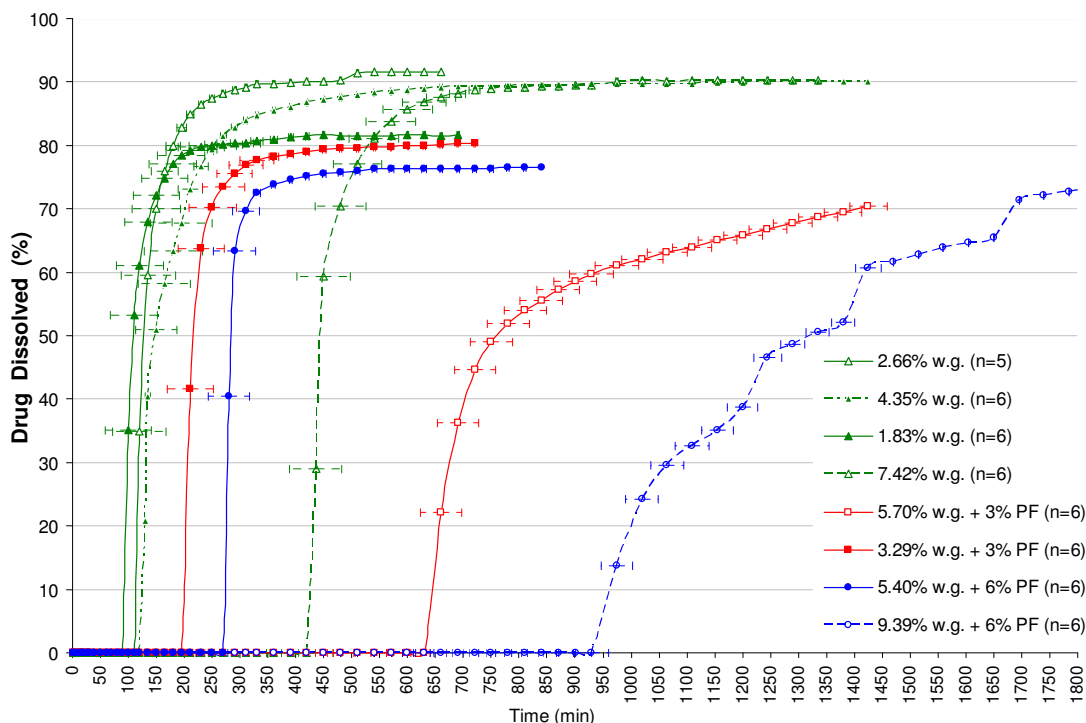


**Figure 4.5.4.b)** Summary of drug release profiles from tablet containing the ratio 50:48 (w/w) of drug:cellulose II. Coated with different rates of Aquacoat<sup>®</sup> ECD, expressed in percentage of weight gain (w.g.); and in the presence, or absence, of a pore former (PF). (Mean, +/- SD).

In the figure 4.5.4.c can be noticed that the drug release profile from formulations containing 08%-wt of cellulose type II showed to be less sigmoidal. In these formulations the decrease in the drug release rate can be attributed to a decreased internal osmotic pressure, probably a consequence of the small amount of osmotic agent in the tablet core. This suggests that the level of cellulose type II used in this formulation (08%-wt, i.e. 6.5% in volume) may not be adequate to, alone, promote the fast water uptake that drives to the coating rupture (and improve the release and dissolution of the proquazone drug); especially after had passed through a wet granulation process and aqueous coating. The influence of granulation process on super disintegrants performance had been studied (Zhao and Augsburger, 2006) and it was demonstrated a negative impact on the functionality of the disintegrants tested, probably caused by the particle size enlargement.

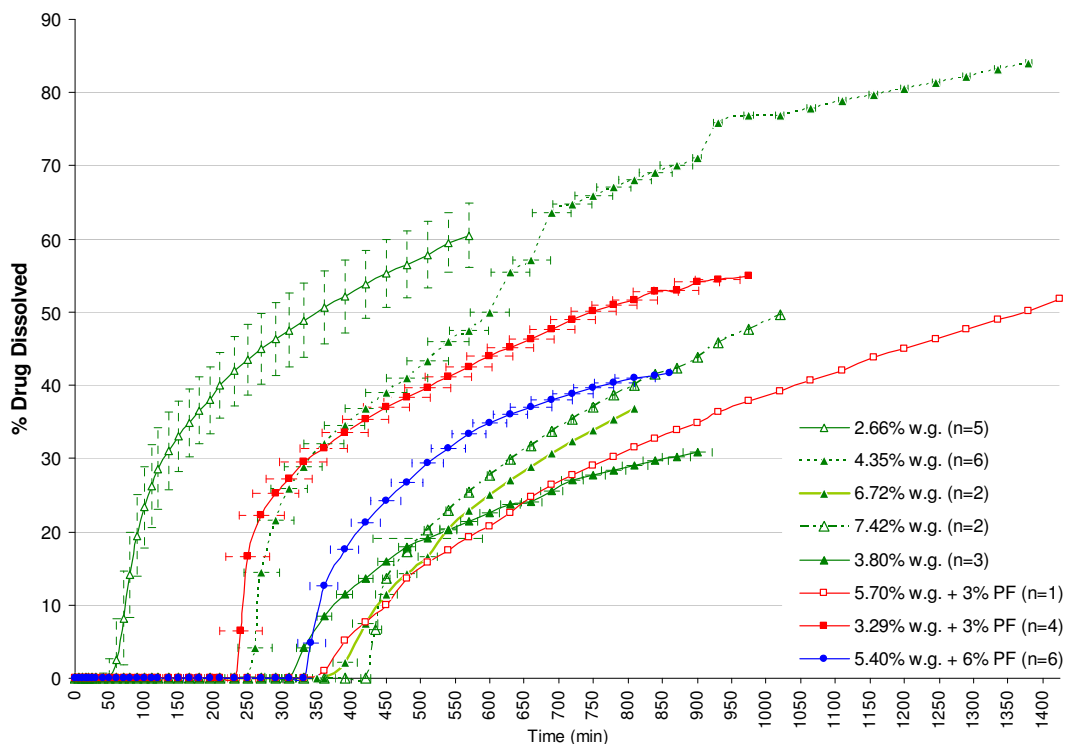


**Figure 4.5.4.c)** Summary of drug release profiles from tablets containing the ratio 90:08 (w/w) of drug:cellulose II. Coated with different rates of Aquacoat<sup>®</sup> ECD, expressed in percentage of weight gain (w.g.); and in the presence, or absence, of a pore former (PF). (Mean, +/- SD).

It could be also interesting to question the possibility of chemical interaction between drug and excipient that may occur and consequently affect drug dissolution. Interesting work had been published by Chien et al. (1981), Gary Hollenbeck et al. (1983) and Balasubramaniam et al. (2008) regarding the effect of drug-excipient or drug-disintegrant interactions. In this study, the formulation 55.5:42.5 (% v/v) proquazone:cellulose type II did not reach 100% of drug dissolution in most of tests. Considering the test was under sink conditions, it could be due to a lack of uniformity in the drug content causing variation among samples and/or batches, or a drug-excipient interaction favored at these proportions of the two compounds.

Lag time was plotted as a function of the coating thickness in the Figures 4.5.5.a and b. The results show that the lag time was direct proportional to the coating thickness; it was increased with the increasing of coating level.



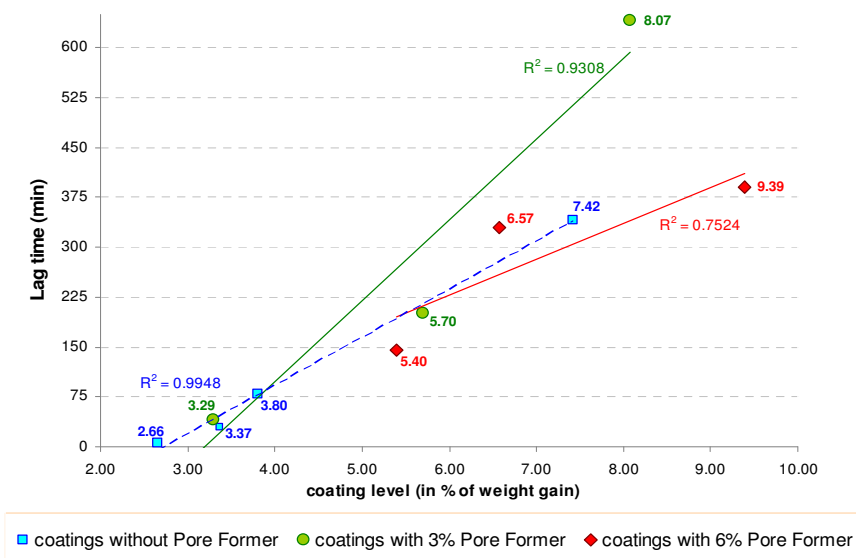


**Figure 4.5.5.a:** Effect of coating level on the lag time (min) of tablets made of 10%-wt. drug. Coating levels (in % of tablet weight gain) are shown in the data label values. Each point represents the mean  $\pm$  SE ( $n \geq 4$ ).

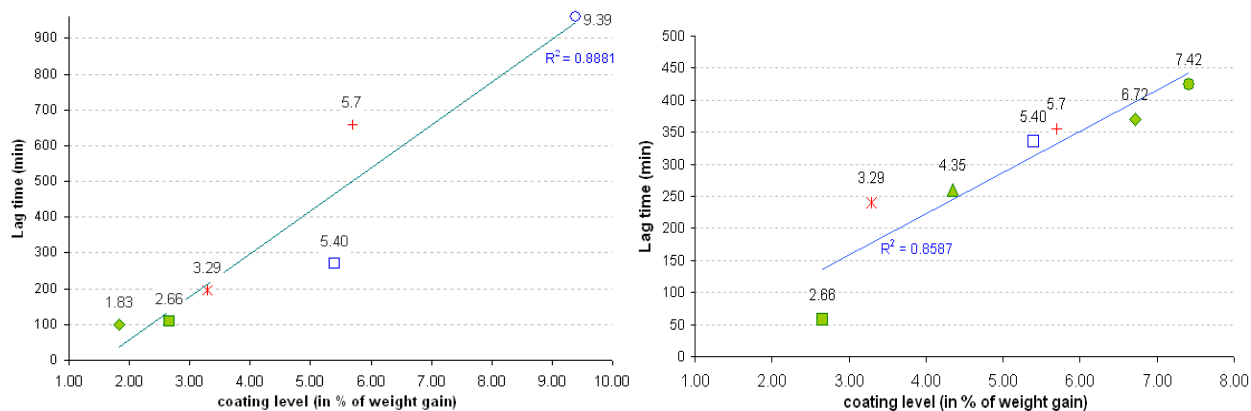


**Figure 4.5.5.b:** Effect of coating level on the lag time (min) of tablets made of 50%-wt drug (at left) and tablets of 90%-wt drug (at right). Coating levels (in % of tablet weight gain) are shown in the data labels. Full background markers represent coatings without pore former (PF). Star and + are 3% PF and empty markers 6% PF. Each point represents the mean  $\pm$  SE ( $n \geq 3$ ).

The influence of the amount of cellulose type II present in the core over the release lag time is shown in the figure 4.5.6.

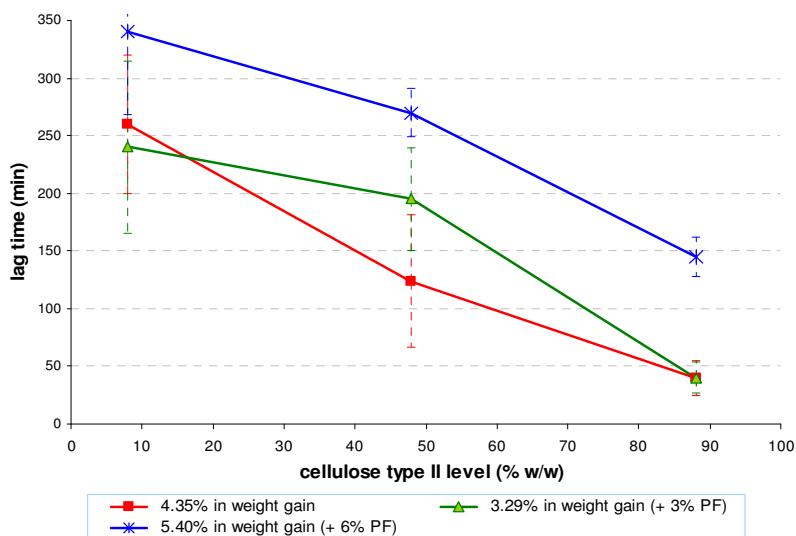


**Figure 4.5.6:** Effect of core composition (% w/w of cellulose type II) on the lag time of tablets with different coating levels (in % of weight gain). Each point represents the mean  $\pm$  SE ( $n \geq 3$ ).

Cores containing three ratios of cellulose II were tested: 6.5, 42.5 and 85.5% in volume of the total formulation. As expected, increased amounts of cellulose type II in the tablets core reduced the lag time. The high affinity of cellulose II for water molecules promoted a fast hydration of the core, which with the generated high pressure burst the coating layer. That process showed to be dependent of the cellulose II level present in the core.

The water-soluble polymer (HPMC) served as a channel-former controlling the water penetration and its presence increased the permeability and therefore reduced the lag time, see Figure 4.5.7.

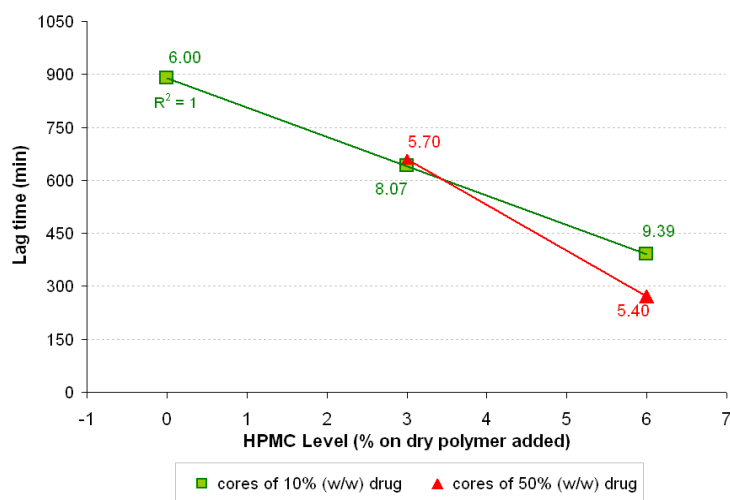


**Figure 4.5.7:** Effect of the pore former level, incorporated in the coating layer, on the lag time of tablets with similar coating levels (shown in % of weight gain in the data label values). Each point represents the mean  $\pm$  SE ( $n \geq 5$ ).

The water penetration into the system could also be affected by the type of pore former. According to Dürig et al. (2006), decreasing the molecular weight grade of pore forming has a markedly reductive effect in drug release. Increased swelling of high molecular weight polymers allows faster diffusion through hydrophilic domains of the film. Also for poor soluble drugs an addition in the pore former levels should be adequate. This could be an important aspect affecting the drug release profile, especially for the tablets comprised of higher proquazone content, once that the HPMC used in this study was of low molecular weight. Also in some experiments the amount of pore former applied showed to be insufficient to generate significant lag time differences.

Except for the time-lag, the release kinetics of the drug retained in the tablet core was not significantly influenced by the presence of the rupturable barrier (but could be widely modulated using an elastic polymeric shell, e.g. Eudragit polymers). Extracted from the release profiles, the  $T_{50\%}$  and  $T_{85\%}$  values are plotted on the Figure 4.5.8.a and b.

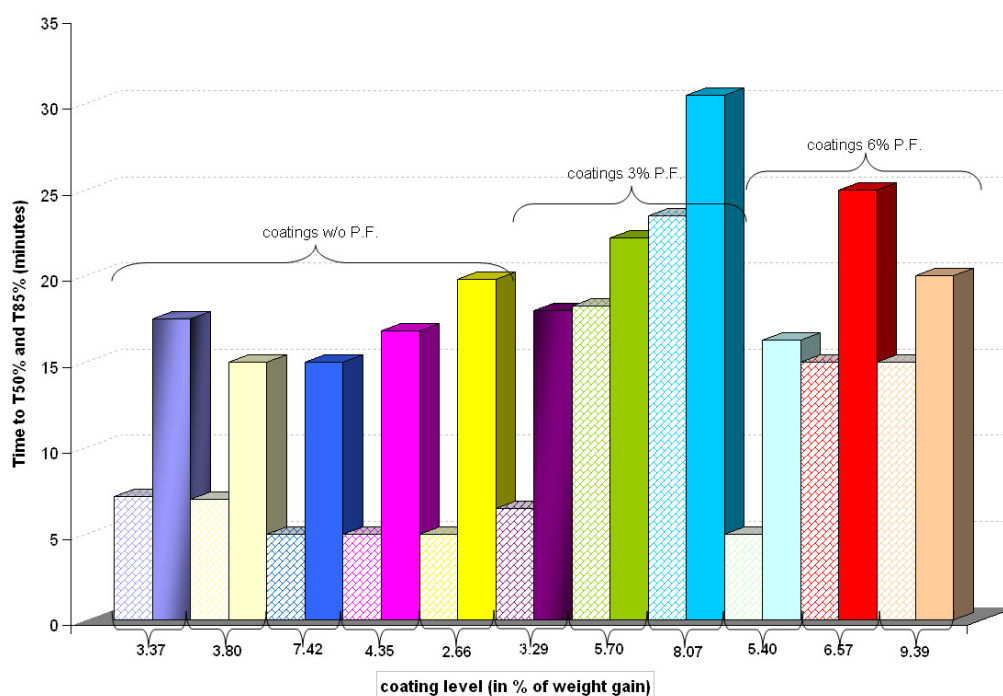


**Figure 4.5.8.a)** Time spent on the release of 50 and 85 percent of PQZ, after coating rupture, from the tablets composed of 85.5% (in volume) of cellulose type II. The brick columns represent the  $T_{50\%}$  and the full coloured ones  $T_{85\%}$ . The different coating levels are shown in the x-axis.

For delayed release products the FDA advocates that at least 80% of the drug should be released to guarantee a robust formulation (FDA, 1997). Also by FDA a drug product is considered *rapidly dissolving* when no less than 85% of the labelled amount of drug dissolves within 30 minutes, using USP dissolution tests (FDA, 2000). For the tablets

containing 85.5% (v/v) cellulose II in the core, the time necessary to the release of 50% and 85% of proquazone ( $T_{50\%}$  and  $T_{85\%}$ ) was < 15 minutes (in most cases) and < 30 minutes, respectively. These values confirm that the release of the drug from the system, after the lag time, was done fast in a single pulse. Once that no drug was released before coating rupture, it can be concluded that what control the drug release was the rate of de-aggregation of the system, i.e. bulk erosion of the core followed by de-aggregation of the granules. And both can happen simultaneously. Nevertheless, the coating rupture was controlled by the coating thickness and the amount of osmotic agent present in the core.

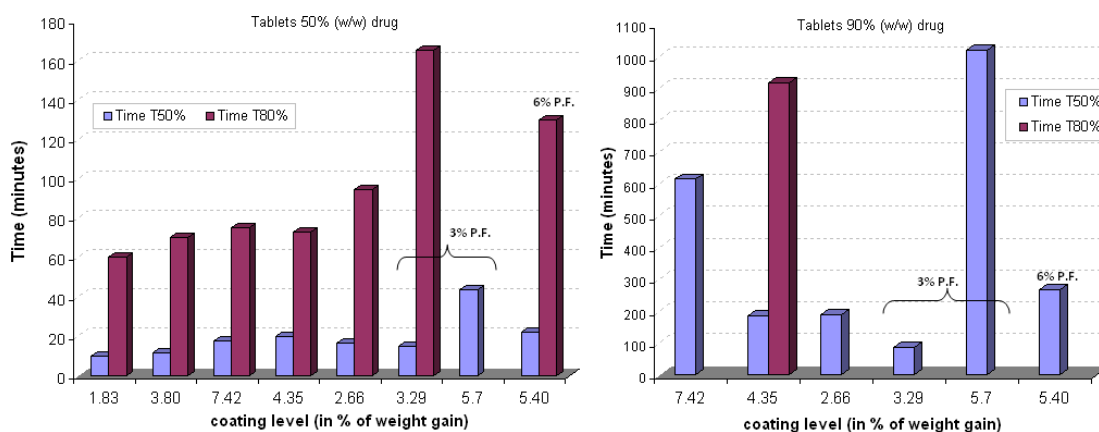


**Figure 4.5.8.b)** Time spent on the release of 50 and 80 percent of PQZ, after coating rupture, from the tablets composed of 42.5% (left) and 6.5% (right) of cellulose type II (v/v). The different coating levels are shown in the x-axis.

Distinctly, for tablets containing 42.5% (v/v) cellulose II in the core (Figure 1.5.8.b) the time to reach 50% of PQZ dissolved was smaller than 20 minutes, in most cases. But 80% of drug release was reached after 1 or 2h.

For cores containing only 6.5% (v/v) of cellulose II, the time necessary to release 50% of drug was more divergent among the experiments (with shorter times for thinner coatings, which coincidentally had the shorter lag times too). In many experiments it was not possible to determine  $T_{80\%}$  for that formulation. These results are in disagreement with the drug release from the uncoated cores, where 80% of drug was released before 50 minutes. This can be an indication of some modification(s) on the core properties after the coating process and/or during the long exposition to the dissolution medium.

The release medium permeated through the coating, penetrated into the tablet through the hydrophilic pores and the continuous cellulosic network, which conveyed water from one particle to the next, imparting a significant hydrostatic pressure, thereby breaking the forces that held the tablet together, and resulting in the disintegration of the tablet. Below  $p_{ca}$  (pore percolation threshold) the rate of fluid penetration into a tablet would be drastically reduced, since the pore clusters are isolated.

In addition, as the amount of cellulose type II was increased, the size and number of clusters increased. This happened until a level of cellulose II was reached, at which the finite clusters became connected and start to percolate the entire system. The proquazone finite clusters become more and more insulated and this continues until the percolation threshold where the cellulose II predominates in the system by completely surrounding the drug, what enables dissolution of the poorly water-soluble drug within the clusters very fast.

At 6.5% (v/v) level of cellulose II, it formed only disconnected finite clusters which are surrounded by the infinite proquazone clusters (91.6% v/v). The drug clusters, being hydrophobic, limit the water penetration and thus core disintegration. At this low level the cellulose II was enough to help in the rupture of the coating layer but not enough for keeping fast and complete self-erosion of the matrix core, what could be seen by the partial drug release during dissolution tests. However, is important to highlight that before coating the drug release from this formulation tablets was complete.

Considering both the porosity of the core before the coating process (approx. 10%, for the formulation of 90%-wt. drug) and the true density of compounds, that tablets had 83.26% (in volume) of PQZ and 17.62% (in volume) of other: cellulose II, HPMC and porous. Except for the drug, all the other components are facilitators in the water permeation and thus core disintegration. Analyzing the tablet product as a two-component, i.e. drug/matrix-carrier-system, the percentage of matrix was probably sufficient to span through the system, surrounding the big PQZ clusters and promoting the fast erosion of the core for the uncoated tablets. However, after aqueous coating process a change in the matrix-carrier-system probably happened; that could be a reduction of porosity, caused by HPMC gel formation in contact with the aqueous coating solution (and hence blocking/reducing the pores), as well as a loss in water uptake capacity by the disintegrant.

Three critical percolation thresholds should be considered: the cellulose type II, the drug and the pore percolation. For a precise determination of them further experiments with more ratios of compounds should be necessary.

## 4.6 Conclusion

As discussed above, the tablets must have the proper porosity, surface roughness, hardness, and moisture content. One can not have consistent coating without consistent tablet quality. Good adhesion between a polymeric film and a surface of the core is a fundamental requirement to guarantee a good result. For that, the atomized droplets, to a certain degree, have to penetrate into the substrate. The presence of cellulose type II showed to be beneficial for that and to surpass all the difficulties in the process steps, also adding good mechanical and functional properties to the final product.

Rupturable pulsatile systems can release the drug after rupture of the outer polymeric coating. Rupture is generally induced by the development of high pressure within the system. The mechanical properties of the coating polymer are therefore very important for the performance of rupturable pulsatile drug delivery systems. Eudragit® films were very flexible, an advantage for conventional extended release systems. In contrast, ethylcellulose films were more brittle and showed complete film rupture.

The lag time prior to drug release, for ethylcellulose coatings, was controlled by coating layer thickness and its HPMC content. The time of drug release was inversely proportional to the membrane thickness, however, directly related to the level of pore former present in the membrane.

The system probably works better for poorly water-soluble drugs, particularly the ones that cannot be released by diffusion through a porous membrane. Highly water-soluble drugs could possibly diffuse through the open pores prior to complete coating rupture and core erosion.

Following Bussemer and Bodmeier (2003) definitions, the drug delivery system presented in this study can be classified as a rupturable system (a class of reservoir-type pulsatile system based on rupturable coating) with a sigmoidal drug release. The main advantage of the system presented in this work is its simple and inexpensive manufacturing process and using well-known and approved excipient, which not only supports very well the coating rupture but also provides good compressibility and core mechanical properties. Being a good pharmaceutical aid to all manufacturing steps and process, the cellulose type II acts as a real multi-functional excipient.

In addition, experts forecast a continuously rising demand for dosage forms with pulsatile drug release, since circadian rhythms have been extensively described for many diseases. In such a way, delayed release systems offer “convenience functionality” for the patient.

## 4.7 Appendix

### Calculation of the Tablet Geometric Volume

The geometric volume ( $\text{mm}^3$ ) of the tablets was computed according to the following formula:

$$V_{\text{tablet}} = \frac{2}{6} \pi h (3a^2 + h^2) + \pi a^2 b$$

For a biconvex tablet the variables  $h$ ,  $a$  and  $b$  stands for height of the spherical caps (mm), radius of the tablet (mm) and height of the central cylinder (mm) respectively (Råde and Westergren, 1992).

These variables can be clearly observed in Figure 4.7.1.

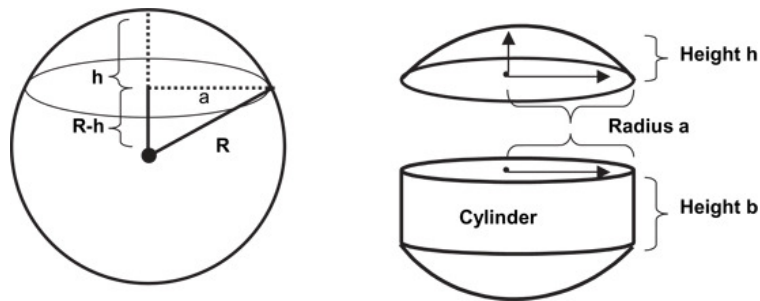


**Figure 4.7.1:** Biconvex tablet dimensions.

## 5 References of chapter I

Alderborn, G. (1996). Particle Dimensions. In: Alderborn, G. and Nyström, C. (ed.). *Pharmaceutical Powder Compaction Technology*. New York: Marcel Dekker, 245-282

Alderborn, G. (2007). Tablets and Compaction. In: Aulton, M.E. (ed.). *Aulton's Pharmaceutics: The design and manufacture of medicines*, third edition. Amsterdam: Churchill Livingstone, Elsevier, 441-482

Alderborn, G., Läng, P.O., Sägström, A., Kristensen, A. (1987). Compression characteristics of granulated materials. I. Fragmentation propensity and compactibility of some granulations of a high dosage drug. *International Journal of Pharmaceutics*, 31, 155-161

Amidon, G.L., Lennernas, H. Shah, V.P. Crison, J.R. (1995). A Theoretical Basis for a Biopharmaceutical Drug Classification: The Correlation of In Vitro Drug Product Dissolution and In Vivo Bioavailability. *Pharm. Res.*, 12, 413-420.

Aquacoat® Aqueous polymeric dispersion. Compilation of FMC guidelines and documents. FMC Corporation, USA.

Augsburger, L.L., Hahm, H.A., Brzezczko, A. , Shah, U. (2007). Super disintegrants: characterization and function. In: Swarbrick, J. (ed.). *Encyclopedia of Pharmaceutical Technology*, third edition. New York: Marcel Dekker, 3553 - 3567

Aulton, M.E. and Twitchell, A.M. (1995). Solution properties and atomization in film coating. In: Graham Cole (ed), *Pharmaceutical Coating Technology*. London, UK: Taylor & Francis, 65

Balasubramaniam, J., Bindu, K., Rao, V.U., Ray, D., Haldar, R., Brzezczko, A.W. (2008). Effect of superdisintegrants on dissolution of cationic drugs. *Dissolution technologies*, May, 18-25.

Baldrick, P. (2007). Pharmaceutical Excipient Testing - A Regulatory and Preclinical Perspective. In: Swarbrick, J. (ed.). *Encyclopedia of Pharmaceutical Technology*, third edition. New York: Marcel Dekker, 2771 - 2782

Balzano, V. (2009). Soft tableting of MCC 102 and UICEL-A/102 pellets into multiple unit pellet systems. PhD Thesis, Faculty of Natural Sciences, University of Basel, Switzerland.

Beckert, T.E.; Lehmann, K.; Schmidt, P.C. (1996). Compression of Enteric-Coated Pellets to Disintegrating Tablets. *Int. J. Pharm.*, 143, 13-23.

Benbow, J.J. (1983). *Enlargement and Compaction of Particulate Solids*. In: N.G. Stanley-Wood (ed.). London: Butterworths, 161

Bodmeier, R. and Paeratakul, O (1991). Process and formulation variables affecting the drug release from chlorpheniramine maleate-loaded beads coated with commercial and self-prepared aqueous ethyl cellulose pseudolatexes. *International Journal of Pharmaceutics*, 70 (1-2), 59-68.



- Bolhuis, G.K., Chowhan, Z.T. (1996). Materials for direct compaction. In: Alderborn, G. and Nyström, C. (ed.), *Pharmaceutical Powder Compaction Technology*. New York: Marcel Dekker, 428-429
- Brown, M.R. (1999). Cellulose structure and biosynthesis. *Pure Appl. Chem.*, 71 (5), 767-775
- Brown, M.R. (2004). Cellulose Structure and Biosynthesis: What is in Store for the 21st Century? *Journal of Polymer Science: Part A: Polymer Chemistry*, 42 (3), 487 - 495
- Bussemer, T., Bodmeier, R. A. (2007). Drug Delivery - Pulsatile Systems. In: Swarbrick, J. (ed.), *Encyclopedia of Pharmaceutical Technology*, third edition. New York: Marcel Dekker, 1287 - 1297
- Bussemer, T., Dashevsky, A., Bodmeier, R. (2003). A pulsatile drug delivery system based on rupturable coated hard gelatin capsules. *Journal of Controlled Release*, 93, 331– 339
- Bussemer, T., Peppas, N.A., Bodmeier, R. (2003). Time-Dependent Mechanical Properties of Polymeric Coatings Used in Rupturable Pulsatile Release Dosage Forms. *Drug Dev. and Ind. Pharm.*, 29 (6), 623-630.
- Caraballo, I., Fernández-Arévalo, M., Millán, M., Rabasco, A.M., Leuenberger, H. (1996). Study of percolation thresholds in ternary tablets. *International Journal of Pharmaceutics*, 139 (1-2), 177-186
- Cartensen, J.T. (2001). *Advanced Pharmaceutical Solids*. New York: Marcel Dekker, 7
- Chien, Y.W., Lin, S. (2007). Drug Delivery - Controlled Release. In: Swarbrick, J. (ed.), *Encyclopedia of Pharmaceutical Technology*, third edition. New York: Marcel Dekker, 1082 - 1103
- Chien, Y.W., Van Nostrand, P., Hurwitz, A.R., Shami, E.G. (1981). Drug-Disintegrant Integrations: Binding of Oxymorphone Derivatives. *Journal of Pharmaceutical Sciences*, 70, 709-710
- Citroflex, Data sheet. 2005. CBC (Europe) Ltd., Italy.
- Collett, J. H. (2007). Dosage Regimens. In: Aulton, M.E. (ed.), *Aulton's Pharmaceutics: The design and manufacture of medicines*, third edition. Amsterdam: Churchill Livingstone, Elsevier, 324 - 334
- Conte, U., Maggi, L., Torre, M.L., Giunchedi, P., and La Manna, A. (1993). Press-coated tablets for time-programmed release of drugs. *Biomaterias*, 14(13), 1017-1023
- Costa, P., Lobo, J.M.S. (2001). Modeling and comparison of dissolution profiles. *European Journal of Pharmaceutical Sciences*, 13(2), 123-133
- Dawoodbhai, S. and Rhodes, C.T. (1989). The Effect of Moisture on Powder Flow and on Compaction and Physical Stability of Tablets. *Drug Dev. Ind. Pharm.*, 15 (10), 1577-1600
- De Geest, B.G., De Koker, S., Demeester, J., De Smedt, S.C., Hennink, W.E. (2009). Pulsed in vitro release and in vivo behavior of exploding microcapsules. *Journal of Controlled Release*, 135 (3), 268-273
- Dürig, T., Harcum, W.W., Kinsey, B.R., Tewari, D., Habash, S., Magee, C.E. (2006). Water-soluble cellulose ethers as release modulators for ethylcellulose coatings on multiparticulates. Work

presented at the Annual Meeting of the American Association of Pharmaceutical Scientists, Nov. 2, San Antonio, Texas, USA.

Eudragit® Application Guidelines. 10th Edition, 06/2008. Evonik Industries AG. Germany.

FDA (1997). Guidance for SUPAC-MR: Modified Release Solid Oral Dosage Forms. Food and Drug Administration, Center for Drug Evaluation and Research (CDER), Rockville, MD, pp. 34

FDA (2000). Guidance for Industry: Waiver of In Vivo Bioequivalence Studies for Immediate Release Solid Oral Dosage Forms Based on a Biopharmaceutics Classification System. Food and Drug Administration, Center for Drug Evaluation and Research (CDER), Rockville, MD, pp. 2

Galichet, L.Y. (2006). Cellulose, Microcrystalline. *Handbook of pharmaceutical excipients*. 5<sup>th</sup> ed. London: Pharmaceutical Press, 132-135.

Ganderton, D. (1969). The effect of distribution of magnesium stearate on the penetration of a tablet by water. *J. Pharm. Pharmacol.*, 21(suppl.): 9S - 18S.

Ganderton, D. and Shotton, E. (1961). The strength of compressed tablet. III. The relation of particle size, bonding and capping of sodium chloride, aspirin and hexamine. *J. Pharm. Pharmacol.*, 12, 144T-152T.

Gari Hollenbeck, R., Mitrevej, K.T., Fan, A.C. (1983). Estimation of the extent of drug-excipient interactions involving croscarmellose sodium. *Journal of Pharmaceutical Sciences*, 72, 325-327

Gothoskar, A.V., Joshi, A.M., Joshi, N.H. (2004). Pulsatile drug delivery system: A Review. *Drug. Deliv. Technol.*, 4(2), 855-871

Hearn, G.L. (2002). *Static Electricity*, Guidance for Plant Engineers [online]. Available at: [http://www.wolfson-electrostatics.com/01\\_hazards/pdfs/guidanceforplantengineers-staticelectricity.pdf](http://www.wolfson-electrostatics.com/01_hazards/pdfs/guidanceforplantengineers-staticelectricity.pdf). Accessed on April 2010.

Howard, S.A. (2007). Solids: Flow properties. In: Swarbrick, J. (ed.), *Encyclopedia of Pharmaceutical Technology*, third edition. New York: Marcel Dekker, 3275 - 3296

Ishikawa, A., Okano, T., Sugiyama, J. (1997). Fine structure and tensile properties of ramie fibres in the crystalline form of cellulose I, II, III and IV. *Polymer*, 38 (2), 463-468

Jackson, K., Young, D., Pant, S. (2000). Drug–excipient interactions and their affect on absorption. *Pharmaceutical Science & Technology Today*, 3 (10), 336 - 345

Johns Hopkins Health Alert (2009). Chronotherapy: Taking Medications at the Right Time [online]. Available at: [www.johnshopkinshealthalerts.com](http://www.johnshopkinshealthalerts.com), Accessed on 4 May 2010

Khan, K. A., Musikabhumma P., Warr, J. P. (1981). The Effect of Moisture Content of Microcrystalline Cellulose on the Compressional Properties of Some Formulations. *Drug Dev. Ind. Pharm.*, 7(5), 525-538

- Khan, Z., Pillay, V., Choonara, Y.E. and Toit, L.C. (2009). Drug delivery technologies for chronotherapeutic applications. *Pharmaceutical Development and Technology*, 14(6), 602–612
- Kono, H., Numata, Y., Erata, T. and Takai, M. (2004).  $^{13}\text{C}$  and  $^1\text{H}$  Resonance Assignment of Mercerized Cellulose II by Two-Dimensional MAS NMR Spectroscopies. *Macromolecules*, 37, 5310-5316
- Kumar, V., Reus-Medina, M.L., Yang, D. (2002). Preparation, characterization, and tableting properties of a new cellulose-based pharmaceutical aid. *International Journal of Pharmaceutics*, 235 (1-2), 129-140
- Labella, G., McDougal, M. (2006). Multifunctional Excipients. *Pharma Magazine*, Sept/Oct, 26-28
- Lanz, M. (2006). Pharmaceutical Powder Technology: Towards a science based understanding of the behaviour of powder systems. PhD Thesis, Faculty of Natural Sciences, University of Basel, Switzerland.
- Lempiäinen, M. and Mäkelä, A. (1985). Determination of proquazone and its m-hydroxy metabolite by high-performance liquid chromatography. Clinical Application: pharmacokinetics of proquazone in children with juvenile rheumatoid arthritis. *Journal of Chromatography*, 341, 105-113.
- Lerner, I.E., Penhasi, A. (2003). Immediate release gastrointestinal drug delivery system. United States Patent 6531152, 03 Nov.
- Leuenberger, H. (1999). The application of percolation theory in powder technology. *Advanced Powder Technology*, 10, 323-352
- Leuenberger, H. (2006). From “Functional Excipients” towards “Drug Carrier Systems”. *Chemistry Today*, 24 (5), 64-66
- Leuenberger, H. and Lanz, M. (2005). Pharmaceutical powder technology - from art to science: the challenge of the FDA's Process Analytical Technology initiative. *Advanced Powder Technol.*, 16, 3-25
- Leuenberger, H., Bonny, J.D., Kolb, M. (1995). Percolation effects in matrix-type controlled drug release systems. *International Journal of Pharmaceutics*, 115 (2), 217-224
- Leuenberger, H., Leu, R., Bonny, J-D. (1996). Application of Percolation Theory and Fractal Geometry to Tablet Compaction. In: Alderborn, G. and Nyström, C. (ed.), *Pharmaceutical Powder Compaction Technology*. New York: Marcel Dekker, 133-164
- Levina, M. and Cunningham, C.R. (2005). The effect of core design and formulation on the quality of film coated tablets. *Pharm. Technol. Eur.*, 17(4), 29-37
- Li, B., Zhu, J., Zheng, C., Gong, W. (2008). A novel system for three-pulse drug release based on “tablets in capsule” device. *International Journal of Pharmaceutics*, 352 (1-2), 159-164

- Luginbühl, R., Leuenberger, H. (1994). Use of percolation theory to interpret water uptake, disintegration time and intrinsic dissolution rate of tablets consisting of binary mixtures. *Pharmaceutica Acta Helvetiae*, 69 (3), 127-134
- Medicines Order (1997). *The medicines (General Sale List) Order*. The stationary Office Ltd.: London.
- Monkhouse, D.C., Lach, J.L. (1972). Drug-exciipient interactions. *Can. J. Pharm. Sci.*, 7 (2), 29-46.
- Moreton, R.C. (2004). Exciipient functionality. *Pharmaceutical Technology*, May, 28 (5), 98-119
- Moreton, R.C. (2006). Functionality and Performance of Exciipients. *Pharmaceutical Technology*, Oct 1, 30 (Exciipient Supplement), ps4-s14
- Müller, F.S. (2008). Modified Celluloses as Multifunctional Exciipients in Rapidly Dissolving Immediate Release Tablets. PhD Thesis, Faculty of Natural Sciences, University of Basel, Switzerland.
- Narayan, P., Hancock, B.C. (2003). The relationship between the particle properties, mechanical behavior, and surface roughness of some pharmaceutical excipient compacts. *Materials Science and Engineering*, A355, 24-36
- National Center for Biotechnology Information – NCBI. PubChem. Compound database: Proquazone (CID: 31508) [online]. Available at: <http://pubchem.ncbi.nlm.nih.gov/>. Accessed on September 2008
- Nayak, U.Y., Shavi, G.V., Nayak, Y., Averinen, R.K., Mutalik, S., Reddy, S.M., Gupta, P.D., Udupa, N. (2009). Chronotherapeutic drug delivery for early morning surge in blood pressure: A programmable delivery system. *Journal of Controlled Release*, 136 (2), 125-131
- Nogami, H., Hagai, T., Fukuola, E. and Sonobe, T. (1969). Disintegration of aspirin tablets containing potato starch and microcrystalline cellulose in various concentrations. *Chem. Pharm. Bull.*, 17 (7), 1450-1455
- O'Donnell, P.B., McGinity, J.W. (1997). Mechanical properties of polymeric films prepared from aqueous polymeric dispersions. In: McGinity, J.W. (ed.), *Aqueous polymeric coatings for pharmaceutical dosage forms*, 2<sup>nd</sup> ed. New York: Marcel Dekker, 517-548
- O'Neil, M.J. (2006). *The Merck Index: An Encyclopedia of Chemicals, Drugs, and Biologicals*, 14th ed. USA: Merck Publishing: Merck & Co.
- Owens, D.K. and Wendt, R.C. (1969). Estimation of the surface free energy of polymers. *J. Appl. Polym. Sci.*, 13, 1741-1747.
- Patel, G.C., Patel, M.M. (2009). Developing a modified Pulsincap system. *Pharmaceutical Technology Europe*, 21(11), 45-51
- Peppas, N.A., Colombo, P., Conte, U., Gazzaniga, A., Caramella, C. and Ferrari, F. (1989). Energetics of tablet disintegration. *International Journal of Pharmaceutics*, 51, 77-83

- Percel, P.J., Vishnupad, K.S., Ventakatesh, G.M., Lee, D.Y. (2006). Timed pulsatile drug delivery system. United States Patent 7.048.945, 23 May.
- Pitt, K.G., Newton, J.M., Richardson, R., Stanley, P. (1989). The material tensile strength of convex-faced tablets, *J. Pharm. Pharmacol.*, 41, 289-292
- Quadir, A., Kolter, K. (2006). A comparative study of current superdisintegrants. *Pharmaceutical Technology*, Oct 1, 30 (Excipient Supplement), ps38-s42.
- Råde, L., Westergren, B. (1992). Spheres Segment (One base). *BETA Mathematics Handbook*. Sweden: Studentlitteratur-Lund, p 73
- Reus-Medina, M., Kumar, V. (2006). Evaluation of cellulose II powders as a potential multifunctional excipient in tablet formulations. *International Journal of Pharmaceutics*, 322, 31-35
- Reus-Medina, M., Kumar, V. (2007a). Modified Cellulose II powder: Preparation, characterization, and Tableting Properties. *J. Pharm. Sci.*, 96, 408-420.
- Reus-Medina, M., Kumar, V. (2007b). Comparative evaluation of powder and tableting properties of low and high degree of polymerization cellulose I and cellulose II excipients. *Int. J. of Pharmaceutics*, 337, 202-209
- Reus-Medina, M., Lanz, M., Kumar, V. and Leuenberger, H. (2004). Comparative evaluation of the powder properties and compression behaviour of a new cellulose-based direct compression excipient and Avicel PH-102. *J.P.P.*, 56, 951–956
- Rios, M. (2006). Debating excipient functionality. *Pharmaceutical Technology*, Sep 2, 30 (9), 50-60
- Roberts, R. J. and Rowe, R.C. (1989). Brittle-ductile transitions in die compaction of sodium chloride. *Chemical Engineering Science*, 44 (8), 1647-1651
- Rowe, R.C. and Roberts, R.J. (1996). Mechanical properties. In: Nystrom, C. and Alderborn, G. (ed.). *Pharmaceutical Powder Compaction Technology*. New York: Marcel Dekker, 283–322
- Rowe, R.C., Sheskey, P.J., Owen, S.C. (2006). *Handbook of pharmaceutical excipients*. 5<sup>th</sup> ed., London: Pharmaceutical Press
- Roy, P., Shahiwala, A. (2009). Multiparticulate formulation approach to pulsatile drug delivery: Current perspectives. *Journal of Controlled Release*, 134, 74–80
- Rumman, M. (2009). Understanding the functionality of MCC Rapid as an excipient for CD – Moving towards QbD. PhD Thesis, Faculty of Natural Sciences, University of Basel, Switzerland.
- Sajan, J., Cinu, T.A., Chacko, A.J., Litty, J. and Jaseeda, T (2009). Chronotherapeutics and Chronotherapeutic Drug Delivery Systems. *Trop. J. Pharm. Res.*, 8 (5), 467-475
- Satarkar, N.S., Hilt, J.Z. (2008). Magnetic hydrogel nanocomposites for remote controlled pulsatile drug release. *Journal of Controlled Release*, 130(3), 246-251

- Schellekens, R.C.A., Stellaard, F., Mitrovic, D., Stuurman, F.E., Kosterink, J.G.W., Frijlink, H.W. (2008). Pulsatile drug delivery to ileo-colonic segments by structured incorporation of disintegrants in pH-responsive polymer coatings. *Journal of Controlled Release*, 132 (2), 91-98
- Shangraw, R.F., Mitrvej, A., Shah, M.N. (1980). A new era of tablet disintegrants. *Pharm. Tech.*, 4, 49-57
- Singh, P., Desai, S. J., Simonelli, A. P. and Higuchi, W. I. (1968). Role of wetting on the rate of drug release from inert matrices. *J. Pharm. Sci.*, 57, 217-226.
- Smolensky, M.H., Peppas, N.A. (2007). Chronobiology, drug delivery, and chronotherapeutics. *Advanced Drug Delivery Reviews*, 59, 828–851
- Stauffer, D. (1994). *Introduction to Percolation Theory*, 2<sup>nd</sup> ed. London: Taylor and Francis
- Stevens, H.N.E. (2003). Pulsincap and Hydrophilic Sandwich (HS) Capsules: Innovative Time-Delayed Oral Drug Delivery Technologies. In: Rathbone, M.J., Hadgraft, J., Roberts, M.S. (ed.), *Modified-Release Drug Delivery Technology*. New York: Marcel Dekker, 257 - 262
- Sweetman, S.C., Blake, P.S., McGlashan, J.M., Neatherco, G.C., Parsons, A.V. (2007). *Martindale: The Complete Drug Reference*, 35th Edition. London, UK: Pharmaceutical Press
- Tousey, M. D. (2005). Tablet coating basics. *Tablets & Capsules*, 3 (3), 20-24 [online]. Available at: <http://www.techceuticals.com/>. Accessed on 23 May 2008
- U.S. National Library of Medicine, Division of Specialized Information Services. ChemIDplus Advanced: Proquazone (RN: 22760-18-5) [online]. Available at: <http://chem.sis.nlm.nih.gov/chemidplus/>. Accessed on September 2008.
- U.S. Pharmacopeia (2007). Excipients. *USP Guideline for submitting requests for revision to USP-NF*. V3.1, pp. 1 [online]. Available at: <http://www.usp.org/pdf/EN/USPNF/chapter3.pdf>. Accessed on 3 May 2010
- US Pharmacopeia XXXI (2009). US Pharmacopeial Convention, Rockville, MD, pp. 2379-2380
- Van Kamp, H.V., Bolhuis, G.K., Lerk, C.F. (1983). Improvement by super disintegrants of the properties of tablets containing lactose prepared by wet granulation. *Pharm. Weekbl ad.*, 5 (4), 165–171.
- Von Orelli, J., Leuenberger, H. (2004). Search for technological reasons to develop a capsule or a tablet formulation with respect to wettability and dissolution. *International Journal of Pharmaceutics*, 287, 135-145.
- Wikberg, M., Alderborn, G. (1991). Compression characteristics of granulated materials. IV. The effect of granule porosity on the fragmentation propensity and compactibility of some granulations. *Int J Pharm.*, 69, 239-253.
- Zhang, Y., Zhang, Z., Wu, F. (2003). A novel pulsed-release system based on swelling and osmotic pumping mechanism. *Journal of Controlled Release*, 89, 47–55

Zhao, N., Augsburger, L.L. (2005). Functionality Comparison of 3 classes of superdisintegrants in promoting aspirin tablet disintegration and dissolution. *AAPS PharmSciTech*, 6 (4), E624-E640.

Zhao, N., Augsburger, L.L. (2006). The influence of granulation on super disintegrant performance. *Pharmaceutical Development and Technology*, 11, 47-53.

Zugenmaier, P. (2001). Conformation and packing of various crystalline cellulose fibers. *Progress in Polymer Science*, 26 (9), 1341-1417

## Second Chapter

**Influence of the drug load, liquid addition rate and batch size on the power consumption profile during wet granulation process.****Abstract**

Granulation is one of the fundamental operations in particulate processing and has a very ancient history and widespread use. In the pharmaceutical industry the moist agglomeration process by high-shear mixing is a critical unit operation that remains more of ‘an art’ than a science-based approach. This study was performed to investigate the influence of drug load, liquid addition rate and batch size over the power consumption profile recorded during a high shear mixer granulation. The powder liquid saturation and particles agglomeration behaviour was compared between three formulations, containing 10%, 50% and 90% (w/w) drug. In all formulations the binder was added dry to the mixture, with the granulation liquid being distilled water. The experiments were carried out in a lab scale high shear mixer with batches sizes of approximately 30%, 50% and 70% of filling capacity of the working vessel, and two main liquid addition rates were set constants at 38 and 50g.min<sup>-1</sup>. The load of a drug with poor water solubility showed to be the most influential factor in both, the kinetics of granule growth and hence the power consumption profile. The maximum power consumption values were directly proportional to the batch size but inversely proportional to the amount of drug in the formulation. The amount of liquid needed to reach the MAX in the power consumption, as well as the particles liquid saturation, was found to be dependent of drug concentration, mainly due to the poor water solubility of the drug chemical and physical properties. The agglomeration of high load drug formulations began at very low liquid saturations ( $\pi < 25\%$ ) in contrast to the agglomeration of high MCC content mixtures ( $\pi$  about 59%). For formulations containing 90% (w/w) of drug the targeted/desired granules size were found at 42.37% of system saturation, in average; and the value was 50.64% and 62.24% for 50% and 10% drug formulations, respectively. Phase I of a typical PC profile could briefly be seen in high drug load formulations, followed by a long plateau phase. In the mixtures with similar volume between drug and excipients, the second showed to predominate in the growth kinetics and agglomeration behaviour. The batch size did slightly deviate in the relevant points of the PC profile (more noticeable in the power values), as well did the liquid addition rate. The “in process” measurement of power consumption showed to be a reliable analytical tool for monitoring the moisture content and particle agglomeration. Understanding and controlling the granulation process is a key factor in robust dosage form design. The latter is the goal of the PAT (Process Analytical Technology) Initiative emphasizing “Quality by Design”.

**Keywords**

Wet granulation; high-shear mixer; power consumption; in process control; process and formulation design.



## 6 Introduction

Control and optimization of the granulation process by the pharmaceutical industry is a fundamental requirement to guarantee a constant product quality. Nevertheless, this process still is very unsettled and troublesome, mostly employing operator practice rather than a science-based approach. More accurate methods need to be developed in order to better control granulation and stop the process when higher percentages of the desired granules size is reached, since the particle size distribution is usually wider than the one specified.

Cameron et al. (2005) pointed out that one of the most important issues for the effective control of granulation processes is the development of fast and reliable measurement techniques for the characterization of particulate systems. Because of the difficulties associated with the direct measurement of particle characteristics, such as particle size distribution, moisture contents and deformability, some indirect monitoring parameters have been adopted. A commonly accepted monitoring parameter in the pharmaceutical industry is the power consumption.

A series of investigations carried out by Leuenberger et al. (1979, 1982, 1986) demonstrated that granulation power consumption, liquid saturation level and granule particle size are inter-related, providing a technical basis for the use of power consumption as a monitoring tool for the characterization of particles within a high-shear mixer. A more detailed description of this control strategy is also provided in Leuenberger (1994).

Betz et al. (2003) made a correlation between power consumption and tensile strength, showing that power consumption measurements are capable of determining the cohesiveness of powder particles, expressed by the resistance to flow of the powder mixture inside the mixer vessel. Holm et al. (1985b) has also correlated granule growth and power consumption measurement.

The uptake of granulation liquid by the powder mixture is also an important factor, either driving particle interactions to agglomerate growth or to the formation of a slurry mass. The liquid saturation is claimed to be the major controlling factor for the granule growth process. High loads of less hydrophilic compounds, what today corresponds to approximately 40% of new active entities, can strongly affect the agglomeration process and therefore the power consumption profile.

Although many parameters can be set constant during process design, variations during production occur due to the variable nature of the powder feed. The power consumption profile depends on the nature of the mixture constituents and its proportions, since components differ tremendously in their physical-chemical properties and, as a result, in their processing and output features.

The use of power consumption measurement to monitor the granulation process is a relatively simple and inexpensive method because of the absence of specialized or expensive equipment. It gives the operator accurate data about the moisture content and kinetic of agglomerate growth, making it possible to reduce batch-to-batch variability and to improve the production of desirable and usable granulates (Betz et al., 2004).

## **6.1 Agglomeration process and control: background**

As Pietsch (2002) described in his book, humans most probably first used agglomeration during the making of bread by taking flour (= particulate solids including an inherent binder, starch) and liquid additives (= additional binder for plasticity and "green" bonding), mixing and forming the mass, and, finally, "curing" the product; i.e., removing of the moisture excess that was added during the mixing and agglomeration steps, to obtain structure and permanent bonding during baking. The technology of bread making combines all components of a complex agglomeration process including preparation of solid feed particles by milling (= adjustment of particle size and activation of the inherent binder, starch), mixing of particulate solids with additional binder(s), forming the mass into a "green" agglomerate, and a "post-treatment" (curing=baking=heating and cooling) to provide strength and texture. As a "tool" to improve powder characteristics, agglomeration was used by ancient "doctors" in the production of pills from medicinal powders and a binder (e.g., honey) or by food preparers during the making of bread from flour, with its inherent starchy components acting as binder (Pietsch, 2002).

The cohesive forces that operate during the moist agglomeration process result from liquid bridges that form between solid particles, holding them together by capillary and viscous forces (Tardos et al., 2007).

One of the primary factors controlling agglomerate growth is the degree of saturation in the granule structure, see figure 6.1.1. The filling of the binder in the granule pores is expressed as the saturation ratio, correlating the binder bridging volume between particles within the agglomerate to the total available pore and void space between particles. Considering the moisture of a bulk material independently of its origin, it can be generally said that a small

quantity of liquid saturation causes the formation of bridges between the individual particles (pendular state). By increasing the amount of liquid, we first get the funicular state, where both liquid bridges and pores filled with liquid are present, and then the capillary state where the pores are completely filled (Schubert, 1984). More growth occurs with increasing binder saturation, especially as the saturation approaches 100%. In the (fully-saturated) capillary state, rapid growth occurs by coalescence. Beyond 100% saturation, the particles are suspended in a continuous liquid phase (droplet) and a paste or over-wet mass results (Mort, 2007).

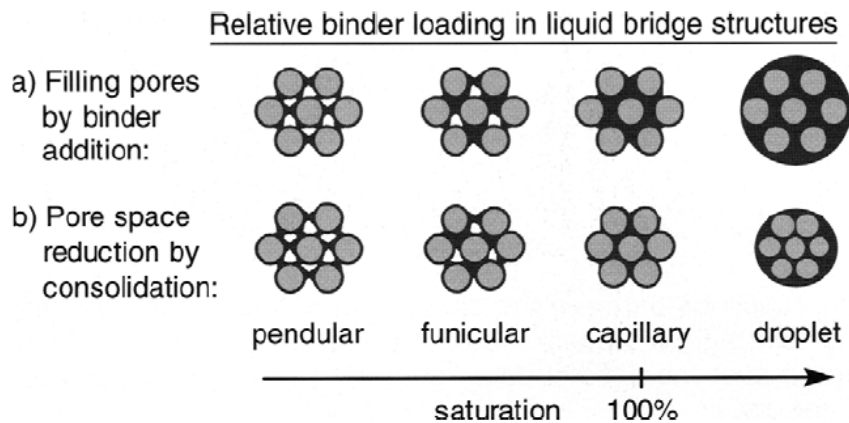


**Figure 6.1.1:** the structure of granules evolves with the increasing binder saturation. Saturation increases by: (a) additional binder loading and/or (b) granular consolidation. (Extracted from Mort, 2007)

Granulation mechanisms or *rate processes* have traditionally been described in terms of a number of different mechanisms (Iveson et al., 2001; Ennis, 2005). However, it is becoming more common to view granulation, in a modern approach, as a combination of only three sets of mechanisms:

1. *Wetting and nucleation*, where the liquid binder is brought into contact with a dry powder bed, and is distributed through the bed to give a distribution of nuclei granules;
2. *Consolidation or coalescence and growth*, where collisions between two granules, granules and feed powder, or a granule and the equipment lead to granule compaction and growth;
3. *Attrition and breakage*, where wet or dried granules break due to impact, wear or compaction in the granulator or during subsequent product handling.

Since the statement “granulation is still rather an art than a science”, in the 70’s, many works have been published about granulation process control; for example by Leuenberger,

Kristensen, Rowe, Knight, Faure, Holm and others. But unfortunately most of them still bring that affirmation.

The aim of using instrumental methods in the control of granulation processes is to detect changes of the resistance of the mass against agitation, i.e., the changes of the rheological properties (Holm et al., 1985a).

Several approaches for controlling the granulation process at one scale are available according to Faure et al. (2001). Those strategies can be grouped as follows:

- methods based on the monitoring of one representative parameter: the representative parameter relates back to one or more properties of the wet mass or of the dry granules, e.g., power consumption of the high-shear mixing, moisture and vibration sensor outputs;
- modeling the process using experimental design: once established, the models can estimate the quality of the granules produced when the process conditions are changed within the domain studied;
- modeling the granule population balance: contrary to the previous models, some assumptions on the granulation regime are needed.

Methods such as imaging processing by video camera (Watano and Miyanami, 1995; Watano et al., 2001), Acoustic Emission Signal Monitoring (Whitaker et al., 2000), Raman spectroscopy (Walker et al., 2009) and measurement of the stress fluctuations (Talu et al., 2001) are also adapted for direct monitoring of granular flows and agglomerate growth. Acoustic chemometric monitoring is also used in fluidized beds (Halstensen et al., 2006).

Nowadays, most of the mixer/granulator types offered on the market are or can be equipped with the option to measure the power consumption or torque profile during the moist agglomeration process. The relationship between power consumption, conditions of granulation and resulting agglomerate characteristics also have been studied (Bier et al., 1979; Leuenberger, 1982; Leuenberger and Imanidis, 1986; Betz et al., 2003, 2004).

The power consumption curve obtained by adding the binding liquid continuously to the powder is made up of five phases, as already described (Leuenberger and Usteri, 1989; Leuenberger and Betz, 2007) (Figure 6.1.2).

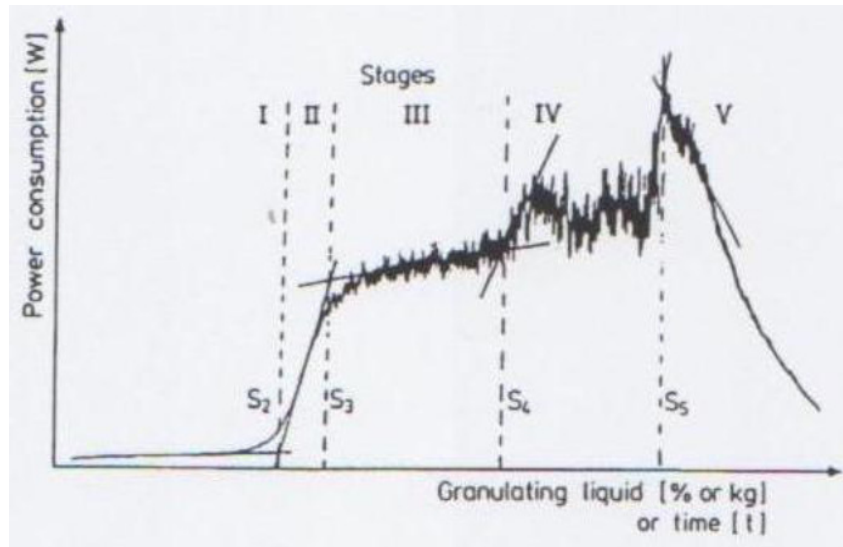


**Figure 6.1.2:** Division of a power consumption curve according to Leuenberger (1989).

- Phase I (S1-S2): the moisture is adsorbed by powder particles to saturate the moisture content without any formation of liquid bridges (equilibrium moisture content at 100% relative humidity of the air).
- Phase II (S2-S3): a sharp increase in power is observed due to the build-up of liquid bridges between the primary particles (pendular state).
- Phase III (S3-S4): characterized by a constant power level (plateau phase), i.e., filling up the interparticulate void space with the granulation liquid (transition from the pendular to the funicular state). The liquid bridges are mobile.
- Phase IV (S4-S5): where the funicular state is found with isolated three-dimensional clusters having already reached the capillary state.
- Phase V (>S5): further addition of liquid leads to a phase transition point, S5. After that the whole interparticulate void space is completely filled with liquid and the overwetted, damp mass becomes slurry. It represents the transition from the capillary state to a suspension.

Betz et al. (2003), in order to facilitate the comparison between measurements, introduces the characteristic point MAX (maximum power consumption) which equals to 100% saturation of the particulate system and is defined as the point at which maximum power is taken by the motor of the mixer. After the MAX point the mixture becomes a suspension. At the overwetting point, the power consumption does not result from individual agglomerates collisions, but is a direct function of the wet mass rheology.

It is important to note that the power consumption profile is different if the moisture equilibration (water absorption) does not take place due to the use of an organic solvent as

granulation liquid. If water or alcohol is used as the granulating liquid, it is important to check whether some of the components of the powder mix may form a hydrate or alcoholate, i.e., that certain molecules uptake some water or alcohol molecules in their crystalline structure. In such a case, the power consumption profile is different from the one plotted in Figure 6.1.2 (Leuenberger and Betz, 2007). The change of the type of the mixer also changes the profile and the absolute power consumption values (Leuenberger, 2001). Important rules for a successful application of the power consumption method are highlighted in Leuenberger et al. (2009).

From the power consumption profile a distinction was made between peak and level detection (Leuenberger, 1982) that could be used as control signals. Also, a modified signal analysis system was proposed by Laicher et al. (1997) in case of active ingredients which react sensitive to the granulation process.

In his study about different methods of monitoring the granulation process by electrical measurements of the drive motor, Kopcha and co-workers (1992) found that power consumption, direct torque and reactive torque measurements give the same general profile for the operation; however, direct torque is more descriptive. It has also been reported (Knight et al., 2001) that the torque, or power consumption, required to turn the impeller varies with impeller blade design, rotational speed, fill and bowl size.

Ascanio et al. (2004) in his review about methods for measuring power consumption in stirred vessels concluded that although electrical measurements are the simplest and most widely used method on large scale processes, care must be taken at laboratory and bench scale to discount external power losses.

Many are the research challenges in granulation technology, focusing on mechanical impeller-type mixers, also termed high shear mixers. Improvements in the quality of data and in data analysis have been achieved in the last 20 years. However, in order to reach better process control improvements in the design and operation of granulators are also necessary (Knight, 2004).

The aim of the present study was to investigate the influence of drug load, liquid addition rate and batch size on the power consumption profile during moist agglomeration process in a high shear mixer granulator. Finally, the comparison will lead to a conclusion on how the formulation properties, process design parameters and the scale-up can affect the power consumption profile.

## 7 Experimental details

### 7.1 Materials

Microcrystalline Cellulose (MCC101, Pharmatrans Sanaq AG), Paracetamol (Mallinckrodt Pharmaceuticals) and Hydroxypropylmethylcellulose (Methocel K100, Dow Chemical) were used to prepare three different mixtures in different batch sizes.

### 7.2 Methods

#### 7.2.1 Characterization of starting material

The particle size distribution of the starting materials was analyzed by laser diffraction (MasterSizer X Long Bed, Malvern Instruments, UK). The measurement was performed using the Manual Dry Powder Feeder, and the obscuration was set around 20%. For the moisture content, 'loss on drying' was determined thermogravimetrically (Mettler-Toledo LP16M, Mettler Instruments, Switzerland). Before and after granulation, specimens of 1 to 2 g were heated up at 105°C for 20 minutes. The loss of moisture was calculated in weight percent. True density  $\rho_t$  was determined using a Helium Pycnometer (AccuPyc 1330, Micromeritics Instruments Corporation, USA). Bulk and Tapped Densities ( $\rho_{\text{bulk}}$  and  $\rho_{\text{tap}}$ , respectively) were determined according to U.S. Pharmacopeia 31, using the apparatus Type STAV 2003, Engelsmann AG, Germany. Powder porosity ( $\epsilon$ ) was calculated using the true and bulk densities, according to the formula  $\epsilon = 1 - \rho_{\text{bulk}}/\rho_t$ . The *Compressibility Index* of the three powder mixtures was calculated by the bulk and tapped volumes, according to U.S. Pharmacopeia 31. Scanning Electron Microscopy (SEM) pictures were taken at the Microscopy Center of the University of Basel, ZMB-UniBasel (Scanning Electron Microscopy, Philips XL 30 FEG ESEM, Philips, Eindhoven, Netherlands). Sample preparation consisted of fixing the samples over aluminum holders and sputtering them with gold to achieve conductivity.

#### 7.2.2 Granulation design and procedure

Three main formulations containing Microcrystalline Cellulose (MCC) and Paracetamol (PCM) in different proportions were produced. The percentage of drug in the total formulation was zero, 10%, 50% and 90% (w/w). In all formulations 2% of Hydroxypropylmethylcellulose (HPMC) was added as a dry binder into the mixture, and the granulation liquid was distilled water. A lab scale Diosna® P10 high-shear mixer (Dierks &

Söhne, Osnabrück, Germany) with a volume of 10L was used. Three batch sizes were chosen: approximately 30, 50 and 70% in volume of the filling capacity of the mixer working vessel. The granulation liquid was added using a peristaltic pump under constant addition speeds, two main ones set at 38 and 50 g.min<sup>-1</sup>. The total amount of blend was mixed for 5 minutes inside the mixer with an impeller speed of 452 rpm. After the mixing time, the liquid addition and the power consumption measurement were started simultaneously. During the whole process the main impeller and chopper speeds were kept constant at 430 and 3000 rpm, respectively. The temperature inside the mixing vessel in the moment of sampling was also measured.

### **7.2.3 Power consumption profile recording**

An “in process” computer calculation program was used to record the power consumption (P.C.) profile during all granulation experiments. The power consumption of the mixer motor (*i.e.* main impeller) was determined by the electric current consumption of the motor according to the equation  $P = U \times I$ , where  $P$  is the power (W),  $U$  the electric potential (V), and  $I$  is the electric current (A). The product of electric potential (V) times electric current (A) is measured by a measuring transducer (Sineax Type PQ 502, 0–2kW, Camille Bauer AG, Switzerland). The power consumption is converted into an electric potential signal between 0 and 10V, 10V corresponding to 2 kW and sampled by an I/O Multifunction DAQ-Card connected to a laptop computer and displayed graphically by the Recorder Software (produced in co-operation with Pharmatronic Ltd, Switzerland) (Betz et al., 2003).

### **7.2.4 Granules characterization**

Samples were taken at predetermined time intervals and its residual moisture was immediately determined thermogravimetrically (Mettler-Toledo LP16M balance, Mettler Instruments). The loss of moisture was calculated in percent by weight. The drawn samples were dried in a dish dryer at 40°C for around 10 hours before sieve analysis, which was carried out in ISO-norm sieve oscillator type equipment (Rietsch, Germany). The eight selected sieves ranged from 1000 µm to 90 µm mesh. The particle-size distribution percentage was calculated by the ratio of cumulative sieves and total sample weight. In this study, the desired granules particle size, also called target granules (T.G.), was set between 125µm and 710µm, *i.e.*, cumulative weight from sieves 125µm to 500µm.



### 7.2.5 Calculations of Liquid Saturation and Power Number

The formulations studied differ in composition and batch size and as a consequence also vary in the amount of granulating liquid required. In order to facilitate the comparison between measurements, three ways to calculate the liquid saturation were investigated and compared.

A dimensionless amount of granulating liquid  $\pi$ , which can be defined as the degree of saturation of the interparticulate void space between the solid materials (Leuenberger and Imanidis, 1986):

$$\pi = (S - S_2) / (S_5 - S_2) \quad (\text{Equation 1})$$

where  $S$  is the amount of granulating liquid (in liters) to a desired point,  $S_2$  the amount of granulating liquid (in liters) necessary, which corresponds to a moisture equilibrium at approximately 100% relative humidity (the end of phase I in power consumption profile), and  $S_5$  is the complete saturation of interparticulate void space before a slurry is formed, corresponding to MAX in the profile (amount of liters). Power consumption measurements are used as an analytical tool to define  $S$  values for different compositions. Thus, the granule formation and granule size distribution can be analyzed as a function of the dimensionless amount of granulation liquid  $\pi$ .

The moist agglomerates can exist in the following three states, based on the amount of the liquid they contain: the pendular state, the funicular state, and the capillary state, as described before (see item 6.1). The three states can be distinguished by the *relative liquid saturation of the pores*  $S$ , which is the ratio of pore volume occupied by the liquid to the total volume of the pores available in the agglomerate. Agglomerates are in the pendular state when the liquid saturation of the pores  $S < 25\%$ ; in the funicular state when  $S$  is between 25% and 80%; and in the capillary state when  $S > 80\%$  (Gokhale, 2005). Following this thought, the liquid saturation  $S$  is determined by the amount of binder solution and the intragranular porosity, which can be calculated based on the following equation (Kristensen et al., 1984):

$$S = \frac{H(1 - \varepsilon)}{\varepsilon} \rho \quad (\text{Equation 2})$$

where  $H$  is the ratio of the mass of liquid binder to the mass of solid particles,  $\varepsilon$  is the intragranular porosity, and  $\rho$  is the particle density of the feed material.

Also the dimensionless group  $\pi_2$ , specific amount of granulation liquid, according to Buckingham's theorem (Buckingham, 1914), was calculated:

$$\pi_2 = q \cdot t / V \cdot \rho \quad (\text{Equation 3})$$

Where  $\rho$  is specific density of the particles,  $q$  is the mass (kg) of granulating liquid added per unit time,  $t$  is the process time, and  $V$  the volume loaded with particles (Leuenberger, 2001).

For better understanding of the process the dimensionless Power Number ( $\pi_1$ ), that is applied to analyze process similarities between different scales and represents a measure of power requirement to overcome friction in fluid flow in a stirred reactor, was calculated according to the following equation (Leuenberger, 1979):

$$\pi_1 = P / r^5 \cdot \omega^3 \cdot \rho \quad (\text{Equation 4})$$

where  $P$  is the power consumption ( $\text{kg m}^2/\text{s}^3$ ),  $r$  is the radius of the impeller blade (m),  $\omega$  is the angular velocity ( $\text{rad/s}$ )\* and  $\rho$  is the specific density of the particles ( $\text{kg/m}^3$ ). In a first approximation, it was neglected the effect of the addition of granulating liquid on the bulk density of the powder mixture. Thus the bulk density of the dry mixture was used in the calculation.

\*( $\omega = 2 \cdot \pi \cdot f$  where  $f$  is the frequency in revolutions/s)

## 8 Results and discussion

### 8.1 Characterization of starting material

The physical properties of the compounds are compiled in Table 8.1.1. The mean particle size of PCM was smaller than other compounds. The hydrophobic property of PCM was confirmed by the very low residual moisture, 0.08% by loss on drying. The residual moisture content of MCC was 4.23%. The true density of PCM was much smaller than MCC, but the bulk and tapped densities were bigger. The porosity of PCM was also smaller compared to MCC, 64% and 78%, respectively.

The *Compressibility Index* showed that the mixture of 90%-wt. PCM had a very poor ability to flow. The 50%-wt. PCM formulation presented a poor flowability and the 10%-wt. drug a passable one. For poorer flowing materials, there are frequently greater interparticle interactions, that is calculated when a greater difference between the bulk and tapped densities is observed (USP 31, 2009).

**Table 8.1.1:** Characterization of MCC, PCM, HPMC and the three dry mixtures in % w/w (drug/excipients).

	Mean particle size ( $\mu\text{m}$ )	Residual Moisture (%)	True Density ( $\text{g}/\text{cm}^3$ )	Bulk Density ( $\text{g}/\text{cm}^3$ )	Tapped Density ( $\text{g}/\text{cm}^3$ )	Powder Porosity (%)	Other Properties (Rowe et al., 2006; WHO, 2005)
<b>MCC 101</b>	81.88	4.23	1.5385	0.344	0.417	78	hygroscopic
<b>Paracetamol</b>	79.66	0.08	1.2769	0.463	0.560	64	hydrophobic (1:70)
<b>HPMC</b>	113.33	5.9	1.3217	0.341	0.557	74	hygroscopic
							<b>Compressibility Index</b>
<b>Mix 1</b> (10% drug)	-	4.09	1.5028	0.340	0.439	77	22.62
<b>Mix 2</b> (50% drug)	-	2.17	1.3914	0.354	0.485	75	27.06
<b>Mix 3</b> (90% drug)	-	0.62	1.2954	0.367	0.568	72	35.37

The percentage by volume of each compound in each formulation is shown in table 8.1.2.

**Table 8.1.2:** Percentage by volume of each compound.

	MCC (% v/v)	PCM (% v/v)	HPMC (% v/v)
<b>Mix 1</b> (10% drug w/w)	85.95	11.76	2.27
<b>Mix 2</b> (50% drug w/w)	43.41	54.47	2.10
<b>Mix 3</b> (90% drug w/w)	6.73	91.30	1.96

From the Scanning Electron Microscopy images (see Figures 8.1a e 8.1.b) could be more clearly seen the morphology difference between PCM and MCC particles; the long porous fibres that awards a high superficial area to MCC particles in contrast with the very smooth surface of the more regular shaped particles of paracetamol.

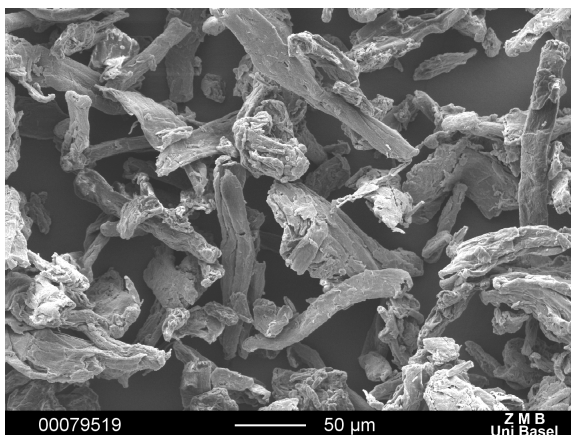


**Figure 8.1.a:** SEM of MCC 101

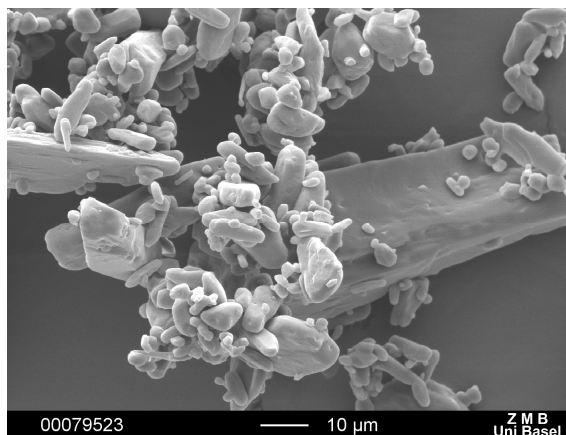


**Figure 8.1.b:** SEM of Paracetamol

## 8.2 Liquid Saturation

As demonstrated by Gokhale (2005), the relative liquid saturation of the pores  $S$  shows that only the target granules from mixtures of zero and 10% (w/w) drug content were in the funicular state when sampled. For the other mixtures, the desired granules were found at pendular state (i.e.,  $S < 25\%$ ). The intragranular porosity varies during granulation; and the porosity of the dry mixture was used for the calculation of  $S$ , what can lead to an imprecise calculation. When the powder dissolves partly or totally in the liquid, the relation becomes invalid because the porosity of the particles, the intra granular void space and hence its density, change. However, it is valid to conclude that the agglomeration of high load paracetamol formulations began at very low liquid saturations in contrast to the agglomeration of high MCC content mixtures (See table 8.2).

The physical properties of the powder strongly affect the liquid saturation, influencing the amount of liquid penetration and the free surface liquid which is necessary for the coalescence of primary particles and/or agglomerates. The relation between the median diameter of the agglomerates of the four formulations and the amount of granulating liquid  $\pi$  is plotted in Figure 8.2. Evidently the regression lines shift to smaller  $\pi$  values with increasing percentage of paracetamol. While formulations with 10% (w/w) drug requires a dimensionless amount of granulating liquid  $\pi$  of about 59% for significant granule growth, for 90% (w/w) drug content it proceeds at less than 25% liquid saturations.

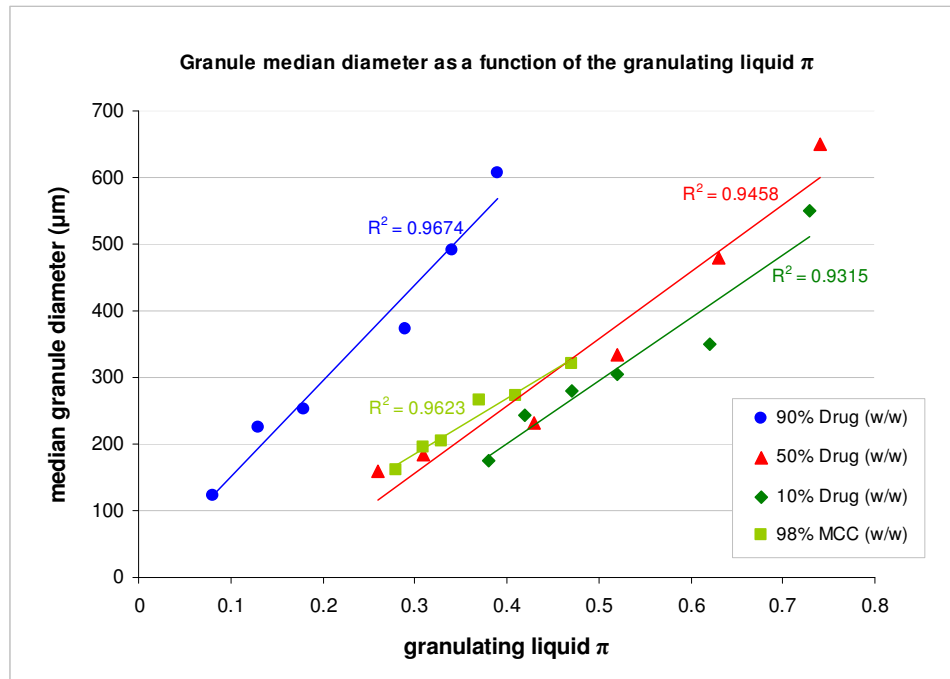


**Figure 8.2:** Granule median diameter as a function of the granulating liquid  $\pi$ .

Looking at Table 8.2, the ratio Liquid/Solid ( $H$ ) in the moment of maximum power consumption (MAX) was found in the range of 1.21 - 1.35 for the formulations containing 10% drug, 0.78 - 0.85 for 50% drug and 0.26 - 0.38 for 90% drug formulations, revealing a big difference in the total amount of water used to fully saturate the three systems. The liquid saturation  $S$  at MAX was in the range of 0.53 - 0.59, 0.37 - 0.40 and 0.14 - 0.19 for formulations of 10, 50 and 90% (w/w) drug, respectively. For the specific amount of granulation liquid,  $\pi_2$ , the values at MAX ranged from 0.28-0.32, 0.21-0.25 and 0.06-0.11 for the formulations of 10, 50 and 90% (w/w) drug, respectively.

Interestingly, the ratio  $H/S$  at was found to be constant for all experiments with same formulation; being 2.3 for 10% drug, 2.1 for 50% drug and 2.0 for 90% drug formulations. The ratio was independent of the batch size or liquid addition rate.

At the moment of the target granules (T.G.) the relative liquid saturation of the pores  $S$  drew small values ranging from 0.33-0.41, 0.18-0.25 and 0.05-0.09;  $\pi$  and  $\pi_2$  were 0.50-0.63 and 0.16-0.21, 0.43-0.51 and 0.10-0.14, 0.13-0.36 and 0.03-0.05, respectively for the formulations with 10, 50 and 90%-wt. drug.

**Table 8.2:** Summary of experiments and its liquid saturation calculations at the relevant points: Target Granules (T.G.) and maximum power consumption (MAX).

% drug in the formulation (w/w)	batch size [kg]	liquid addition rate [g/min]	water at moisture equilibrium $S_2$ [liters]	$H$ (mass Liq/Solid) at T.G.	$S$ (Liquid Saturation) at T.G.	$\pi$ (at T.G.)	$\pi_2$ (at T. G.)	$H$ (mass Liq/Solid) at MAX	$S$ (Liq Saturation) at MAX.	$\pi_2$ (at MAX)
0	0.50	25	0.18	1.00	0.53	0.43	0.29	2.20	1.03	0.54
0	1.20	38	0.34	0.65	0.30	0.30	0.16	1.48	0.69	0.39
0	2.00	38	0.49	0.97	0.45	0.47	0.24	1.79	0.83	0.47
10	1.20	38	0.38	0.80	0.35	0.50	0.18	1.30	0.57	0.32
10	2.00	38	0.46	0.93	0.41	0.63	0.21	1.35	0.59	0.32
10	2.40	38	0.46	0.86	0.38	0.59	0.19	1.31	0.58	0.30
10	2.00	50	0.35	0.84	0.37	0.59	0.18	1.30	0.57	0.31
10	2.40	50	0.50	0.76	0.33	0.55	0.16	1.21	0.53	0.28
50	1.20	38	0.23	0.52	0.25	0.51	0.14	0.84	0.40	0.25
50	2.00	38	0.23	0.43	0.20	0.43	0.11	0.84	0.40	0.21
50	2.40	38	0.15	0.38	0.18	0.44	0.10	0.78	0.37	0.22
50	2.40	50	0.20	0.46	0.22	0.49	0.11	0.85	0.40	0.22
90	1.20	25	0.11	0.17	0.09	0.32	0.05	0.36	0.18	0.11
90	1.20	12.5	0.10	0.15	0.08	0.21	0.04	0.38	0.19	0.11
90	2.00	16	0.11	0.10	0.05	0.13	0.03	0.38	0.19	0.10
90	2.40	16	0.11	0.15	0.08	0.36	0.04	0.34	0.18	0.08
90	1.20	38	0.11	0.13	0.06	0.13	0.04	0.34	0.17	0.09
90	2.00	38	0.15	0.13	0.07	0.23	0.04	0.30	0.15	0.09
90	2.40	38	0.15	0.12	0.06	0.23	0.04	0.32	0.16	0.09
90	2.40	50	0.15	0.13	0.06	0.31	0.04	0.26	0.14	0.06

Considering MAX as 100% saturation of the entire particulate system (and also considering that the addition of the liquid was at constant rate) for the formulations containing 90% drug, the moisture equilibrium at 100% relative humidity ( $S_2$ ) was reached at 22.40% of system saturation and the target granules at 42.37%, in average. For the formulations with 50% drug the values were 12.54% and 50.64% for  $S_2$  and at the target granules point, respectively. As well as the system saturation value was 16.59% at  $S_2$  and 62.24% at target granules for 10% drug formulations.

The rate of granule breakage is a consequence of the freshly formed granules strength, what is related to the liquid penetration, as showed by Dries and Vromans (2009). All values

calculated of liquid saturation confirm a smaller liquid penetration when increasing the amount of paracetamol; what was also shown by the values of residual moisture of the agglomerates when they were sampled. These values were in average 45.76%, 30.36% and 11.35%, in the moment of T.G., for the 10, 50 and 90 percent drug content mixture, respectively.

### **8.3 Comparison of the power consumption profiles of three different formulation mixtures: the effect of a poor water soluble drug load**

The amount of drug in the formulation had a strong influence on how the power consumption profile looked like (Figures 8.3.1 and 8.3.2). In a concentration of 90% weight of the total formulation, the physicochemical properties of paracetamol were predominant in the mixture environment and in granules formation. The phase I of a typical profile could briefly be seen in these formulations, indicating a very fast saturation in the moisture content of the components, followed by a more accentuated and well-defined s-shaped ascent in phase II, compared with other formulations. The ascent slope represents the powder agglomeration and granule growth.

The hydrophobic behaviour of paracetamol molecule ( $\text{Log } P_{ow}: 0.49$ ) probably permitted that the water molecules entering the system become more available for inter-particulate interactions (Omar et al., 2006). Another factor was that there aren't significant internal pores in the primary particles to fill (attested by the low values of liquid used to reach the powder moisture equilibrium ( $S_2$ ): 0.10-0.15 liters). Therefore, agglomeration took place faster compared with low drug load formulations, even for bigger batches. The time for the entire system to change from a powder bed to an overwetted mass was shorter for formulations containing higher amounts of drug.

Due to the PCM hydrophobicity, hence the elevated water available, both the total amount of water used in the granulation (look at the values of  $H$ ,  $S$  and  $\pi_2$  for MAX) and the granules residual moisture presented much smaller values compared with the others systems. It was overwetted at reduced liquid concentration (see section 8.2 and table 8.2).

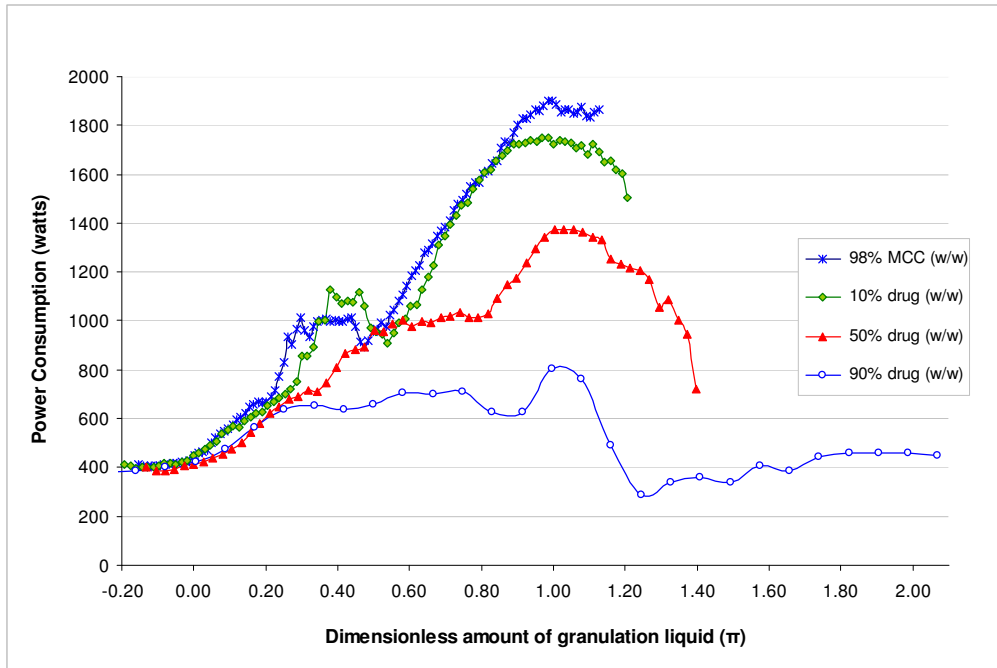


**Figure 8.3.1:** Power Consumption measurement of four different mixture proportions at same batch size (2kg) and constant liquid addition rate (38 grams per minute).

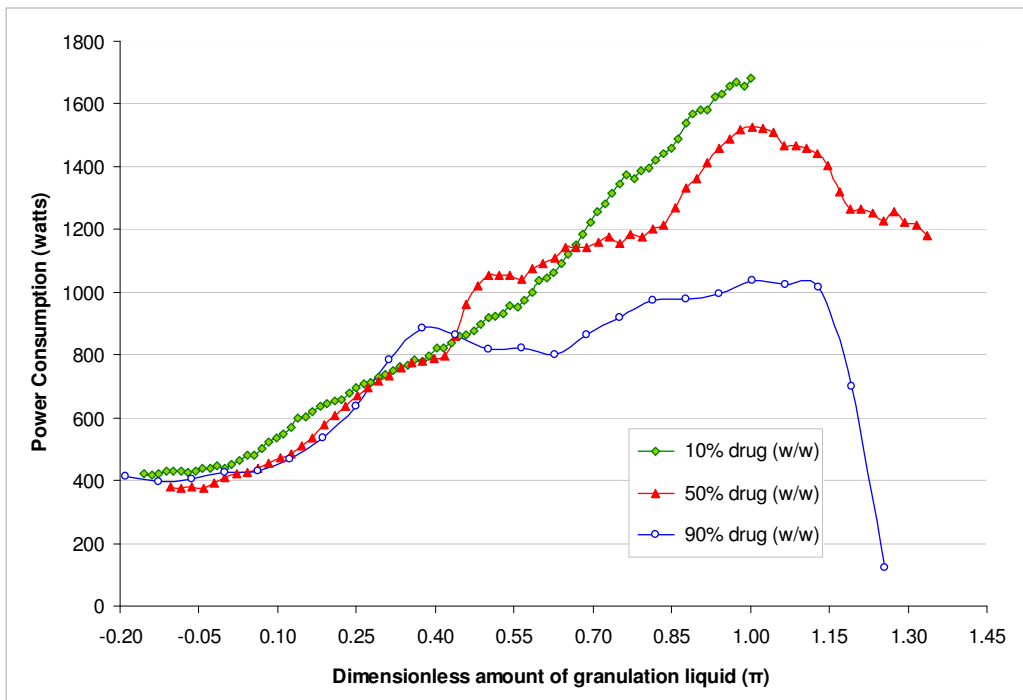


**Figure 8.3.2:** Power Consumption measurement of tree different mixture proportions at same batch size (2.4kg) and constant liquid addition rate (38g per minute).



Reduced values were also found for the power consumption for formulations containing increased amounts of paracetamol. Considering that power consumption values are correlated with the cohesion of the powders inside the mixer vessel and also its contact with the vessel walls and impeller blade, the results showed that the higher drug load formulation presented weaker interparticle interactions, smaller cohesiveness and resistance to impeller movement. The plateau found in the phase III of the P.C. profile indicates that this formulation presented equilibrium between granule growth and breakage, maybe due to crumb behaviour (Iveson et al., 2001). Consequently, the power consumption did not increase but showed an almost constant level until overwetting was reached.

In a granulation experiment using the high hydrophobic lubricant magnesium stearate, Pepin et al. (2001) observed in the P.C. profile only a very long phase I, until a very clear overwetting point was reached and the powder mass became a paste.

On the other hand, by decreasing the amount of the poor water soluble drug and increasing the amount of the hygroscopic microcrystalline cellulose the total amount of water necessary to reach the desired granules size and for overwetting the system increased dramatically (values of  $H$ ,  $S$ ,  $\pi$  and  $\pi_2$  at table 2), as well as the granules residual moisture.

MCC has the capacity of adsorbing water on its large and very porous surface area, making necessary the addition of more water to create the liquid bridges between particles that promote granules formation. What was confirmed by the higher values of liquid used to reach the powder moisture equilibrium (0.35-0.50 liters for mixtures with 10%-wt drug); and visualized by the more extended phase I in the PC profile.

The constant increase in power consumption for formulations with high content of MCC is probably caused by a further coalescence of particles. The high liquid saturation generated by the continuous addition of liquid brings MCC into a degree of plasticity that facilitates successful collisions, then keeping the granule growth. The time to reach MAX was longer and the temperature inside the mixer also higher compared with other mixtures.

For the formulations with a mixture of PCM/MCC 54.40/43.41 (% v/v) the power consumption profiles were more similar to formulations with 90%-wt excipients than for formulations of 90%-wt drug, showing the likely predominance of the MCC growth kinetics on the mixture agglomeration behaviour. Leuenberger and Usteri (1989) explained in a previous work the kinetics of binary mixtures agglomerate growth. Even that the MCC particles are surrounded by the PCM ones, it still dominating the granulation process at this concentration.

#### **8.4 Influence of the mixer bowl filling (mixer load) in the power consumption profile: scale-up invariants.**

The mixer bowl filling strongly affects the particles' flow pattern and how they collide and interact. In this study the possible interferences of wall adhesion and wall, lid or blade build-up were neglected, although the application of an anti-adherent material over the surfaces is recommended.

The absolute power consumption values (watts) were directly proportional to the batch size, for all formulations. As the load increases, so does the current draw of the motor.

Differences in the absolute MAX value could be noticed from batch to batch (Figure 8.4.1 and 8.4.2). The reason probably lies on the differences in total wet mass volume and faster saturation of the powders for small batches, once that the liquid addition rate was kept constant. Nevertheless, the values found were very proportional to the scale up of the batches; and their profile phases are presented similarly. Also the granulation liquid requirement was linearly dependent of the mass loaded. In previous works of the research group in Basel, it was reported that the P.C. profile, as defined by the parameters S3, S4, S5 (Leuenberguer, 1983, 2001) or MAX (Betz et al., 2003, 2004), is independent of the batch size.

When the batch size was changed but the liquid addition was kept constant for each formulation, similar profile phases could be found, but with a shift in time and absolute MAX value (Figures 8.4.1 and 8.4.2). However, when the rate of liquid addition was enhanced in proportion to the batch size, the characteristic phases I, II and III of the power profile appeared within the same range of time (Figure 8.4.3). That was an evidence of an invariant moment of the scale-up and could serve as an in-process control.

For batches of 2000 grams, corresponding to approximately 60% of the equipment filling capacity, the typical Leuenberger phases of power consumption curves were easily visualized.

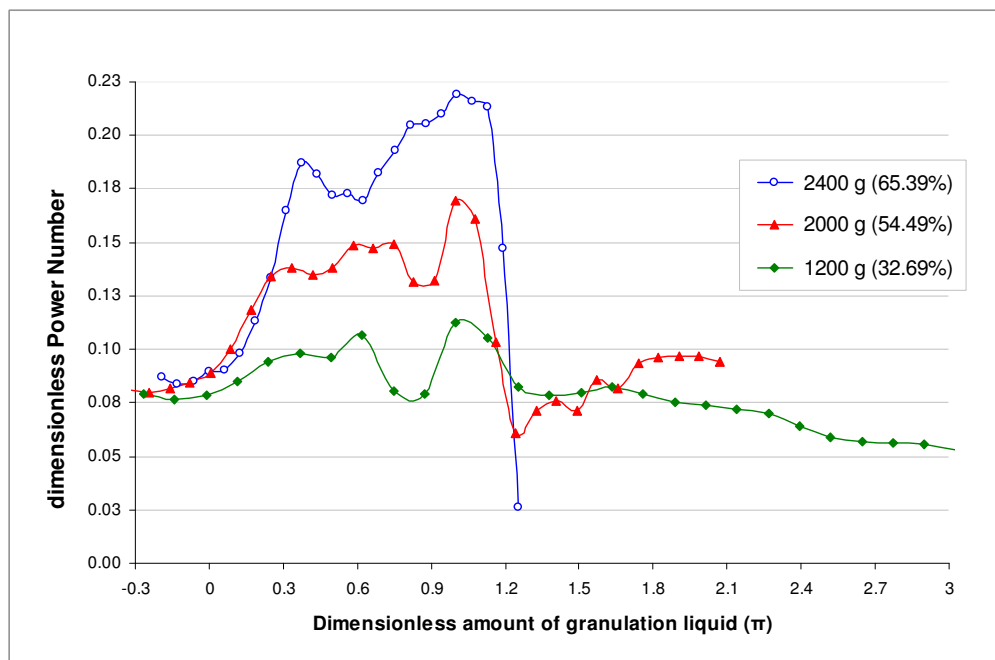


**Figure 8.4.1:** Power Consumption measurement of three batch sizes of the mixture containing 90% (w/w) drug and constant liquid addition rate (38 grams per minute). The percentual volume that the batch represents in the total filling of the working vessel is shown in brackets.

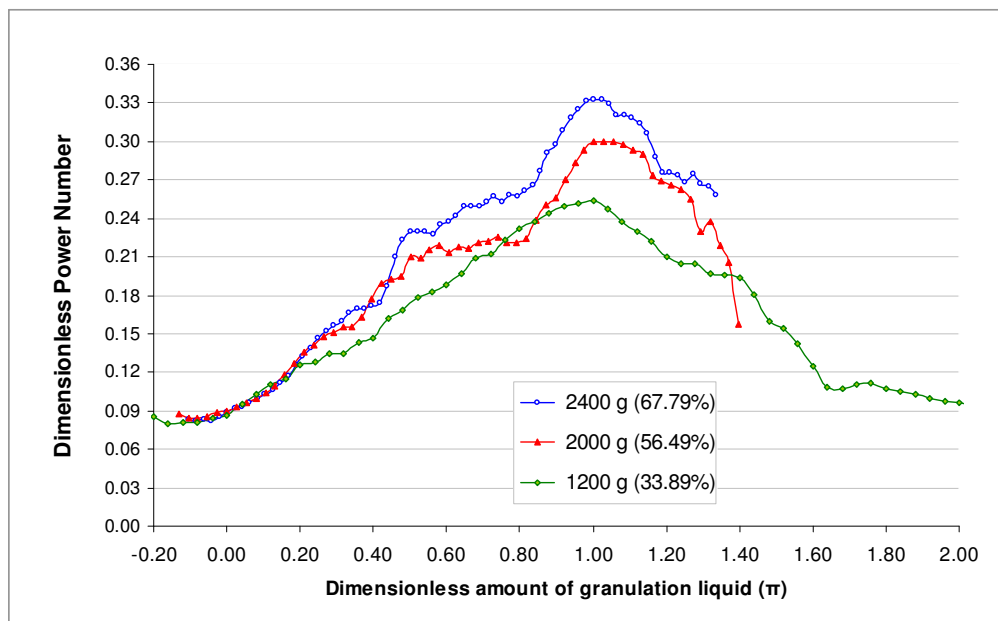


**Figure 8.4.2:** Power Consumption measurement of three batch sizes of the mixture containing 50% (w/w) drug and constant liquid addition rate (38 grams per minute). The percentual volume that the batch represents in the total filling of the working vessel is shown in brackets.

The batch size should not be too big in relation to the capacity of the mixer, so that powder particles can be properly fluidized by the impeller blades and an optimal mixing of the ingredients with binder can be achieved, neither so small that it can lead to high loss due to wall deposition, powder segregation during mixing, or the changes in powder cohesiveness, which are not easily measurable or reflected by the impeller movement.

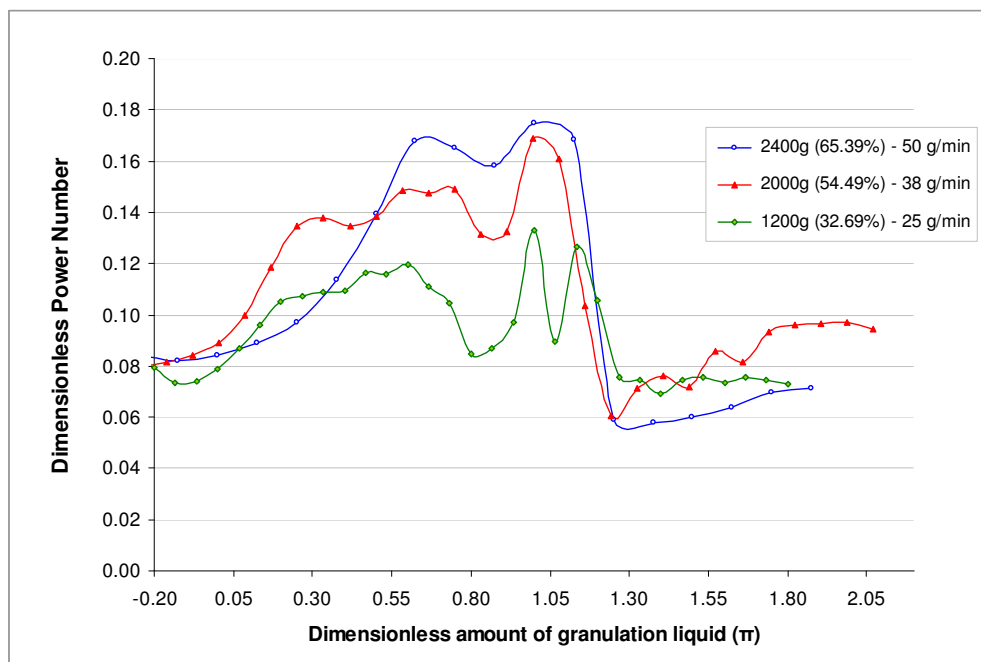


**Figure 8.4.3:** Power Consumption measurement of three batch sizes of the mixture containing 90% (w/w) drug and liquid addition rate (25, 38, 50 grams per minute) enhanced proportionally to batch size. The percental volume that the batch represents in the total filling of the working vessel is in brackets.

As presented by Faure et al. (1999), there is a limit to scale-down that corresponds to the point where the wall adhesion and friction effects start to dominate. It is indeed impossible to scale-down while conserving both geometric similitude and a constant ratio of wall surface to bowl volume. Dynamic similitude did not occur since wall adhesion seriously affects the flow pattern of the wet mass (Faure et al., 1999).

## 8.5 Effect of the liquid addition rate on the power consumption profile

The liquid addition rate slightly influenced the total amount of water used in the process. As remarked by Holm et al. (1985b), it is necessary to keep in mind that liquid flow rate and process time are interrelated and that low liquid flow rate favours compaction and, hence, an increasing liquid saturation.

In most of the experiments, the amount of liquid necessary to reach the desired granules size and the maximum in power consumption was slightly higher with decreased rate addition. This was confirmed by the values of  $H$  shown in table 8.2. It could be due to more liquid binder droplets penetrating into the material structure by capillary flow and/or some water evaporation happening during longer processes.

Liquid addition rate, as well as the impeller speed, influence linearly the granulate growth rate (Leuenberger, 1982; Leuenberger and Imanidis, 1986; Vonk et al., 1997). In the formulations containing 10 and 50 percent of drug with the increase in the liquid addition rate the plateau phase became less visible, sometimes disappearing for the higher addition rate. In the higher liquid addition rates the entire profile appears as a single ascent slope (Figure 8.5.1). In contrast, for the 90 percent drug formulations the ascent curve (in phase II) and the plateau (phase III) are very evident. In some experiments, specially the ones with bigger batch sizes, a non clear delimitation among the phases III, IV and V was present (Figure 8.5.2). *Vide* comments at section 8.3.

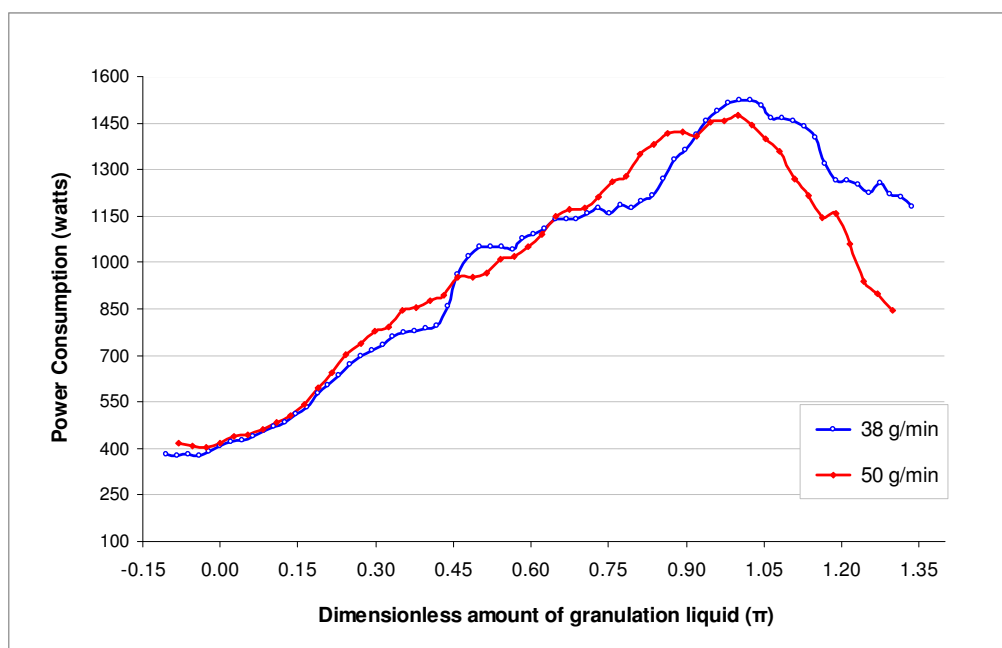


**Figure 8.5.1:** Power Consumption measurement of the mixture containing 50% (w/w) drug, batch size of 2.4 kg (67.79% in volume of the equipment filling capacity) and liquid addition rates of 38 and 50 grams per minute.

In general, the more notable influence of the liquid addition rate on the P.C. profile was a shift in the process time, which became shorter for all formulations and batches with the increase in liquid addition rate. This is a relevant point to consider when taking the decision of using 'time' as a granulation end-point control.

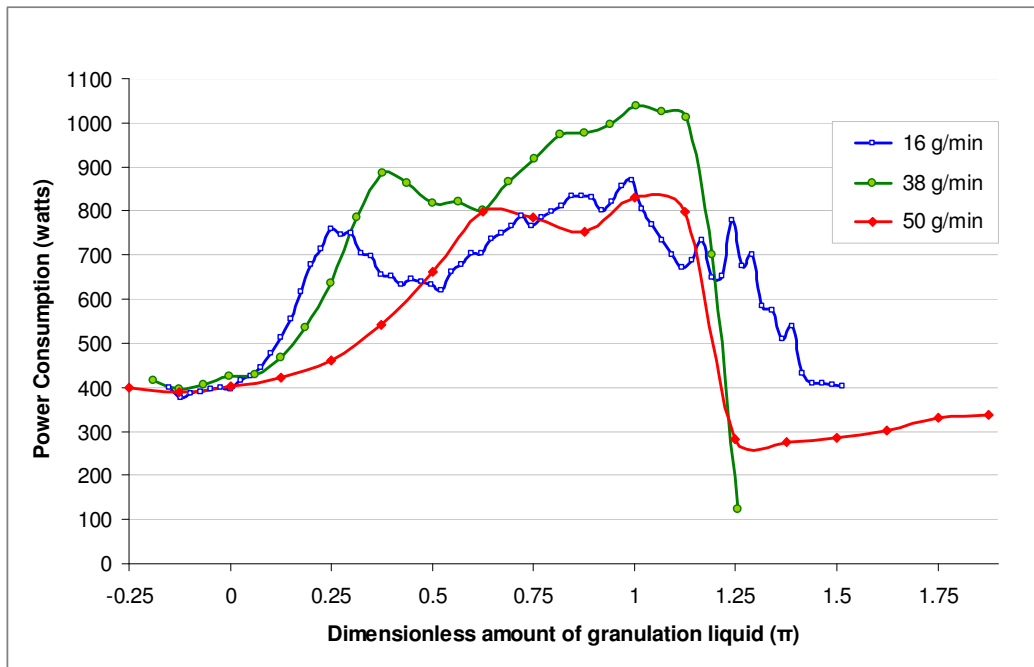


**Figure 8.5.2:** Power Consumption measurement of the mixture containing 90% (w/w) drug, batch size of 2.4 kg (65.39% in volume of the equipment filling capacity), and liquid addition rates of 16, 38 and 50 grams per minute.

The time necessary to reach the maximum power consumption, i.e., 100% saturation of the system was shorter for faster addition rates, as well as the absolute power value for some experiments. The maximum consumption of energy showed to be slightly smaller with the increase in liquid addition rate, probably because of a faster formation of liquid bridges between the particles and faster changes in the powder cohesiveness. This finding was similar to the one presented by Carius (1992), where he described that already during the significant longer spraying phase, agglomeration takes place besides distribution of the granulation liquid, and consequently the power consumption increases.

However, when power (watts) is plotted as a function of the degree of saturation ( $\pi$ ) it can be seen that at the start of phase III the saturation was smaller for the slower rates of liquid addition (Figure 8.5.2). The particles moving inside the high shear mixer are suffering consolidation and compaction along the time, reducing the interparticles space to be filled up with liquid.

## 8.6 Granule size analysis

The particle-size distribution analysis from specimens collected at different time points of the process made it possible to define in which moment of granulation and power consumption measurement a higher percentage of the desired particles was produced. The desired granules particle size was set between 125 $\mu\text{m}$  and 710 $\mu\text{m}$ , i.e., cumulative weight from sieves 125 $\mu\text{m}$  to 500 $\mu\text{m}$ , as described in the methods section. Most results are discussed but are not shown because of the higher number of experiments and samples analyzed.

Microscopic examinations of the granules (Figure 8.6.1) showed that granules sampled from a 10% drug formulation had a more uniform texture, with a melted and merged appearance, while the 90% drug granules were composed of a number of minor particles bound together or immersed in a mass.

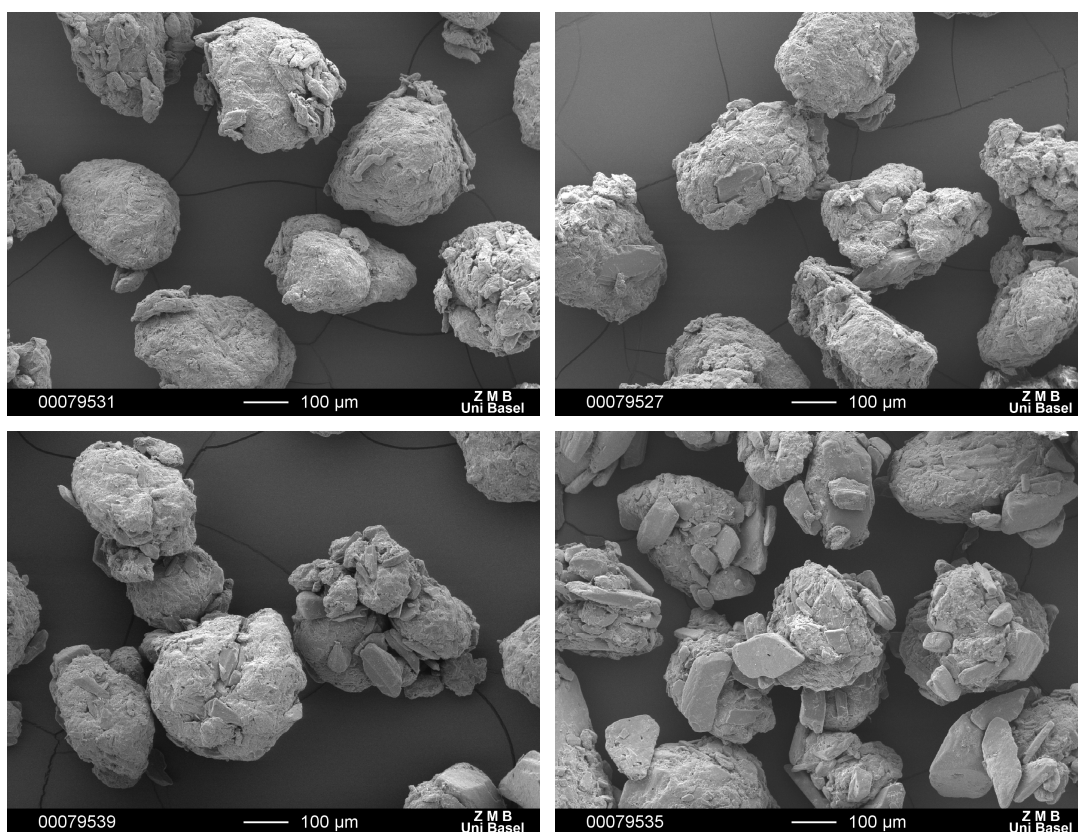


**Figure 8.6.1:** SEM of granules composed of 98% MCC (top left), 10% PCM (top right), 50% PCM (bottom left) and 90% PCM (bottom right).

In almost all situations, the median size of the agglomerates could be linearly related to the PC value. With increased amounts of PCM, however, the linearity was being lost (Figure

8.6.2). To produce similar particle size distribution among the formulations the amount of energy used was decreased with increasing drug content.

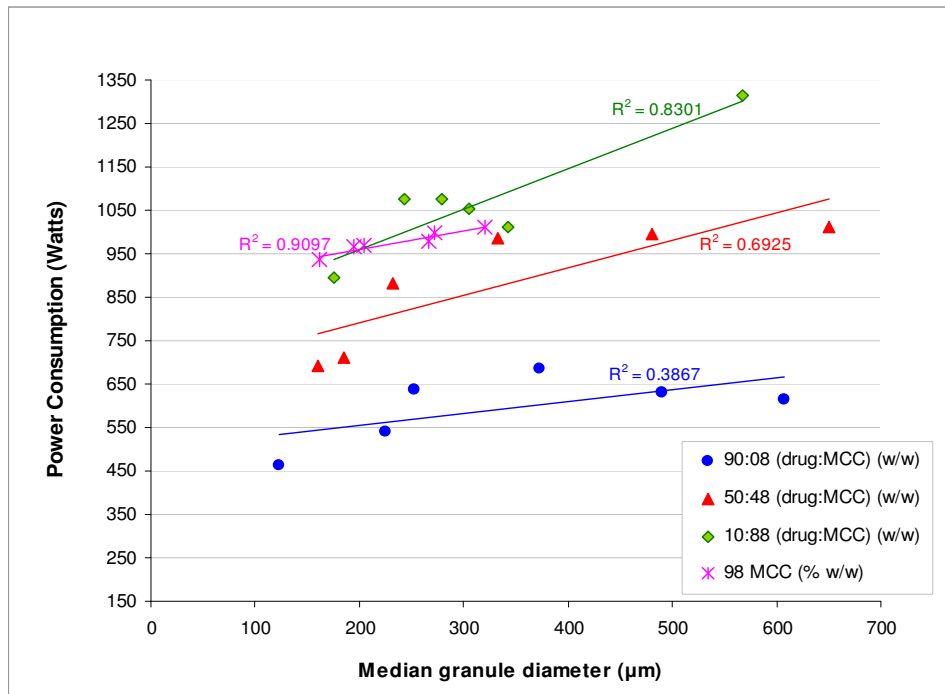


**Figure 8.6.2:** Absolute power consumption value as a function of the median granule diameter

In the case of a fixed amount  $\pi$  of granulating liquid (see Figure 8.6.3), it is interesting to note that the granules obtained from 50%-wt. PCM (equivalent to 54.48% of the formulation volume) lead to granule size distributions equivalent either to 10% or 0% PCM formulations. This can be interpreted based on the predominance of the MCC growth kinetics on the mixture agglomeration behaviour (Leuenberger and Usteri, 1989) and percolation theory (Leuenberger et al., 1989); i.e., the properties differ for compositions below or above a critical ratio  $p_c$  (percolation threshold) of components between the MCC and PCM. The cumulative weight fractions of the binary mixtures at a fixed  $\pi$ -value presented similarity, but it was dependent of the proportion of the compounds. In order to develop robust formulations, the theory of percolation should be taken into account and the critical ratios must be avoided (Leuenberger, 1999).



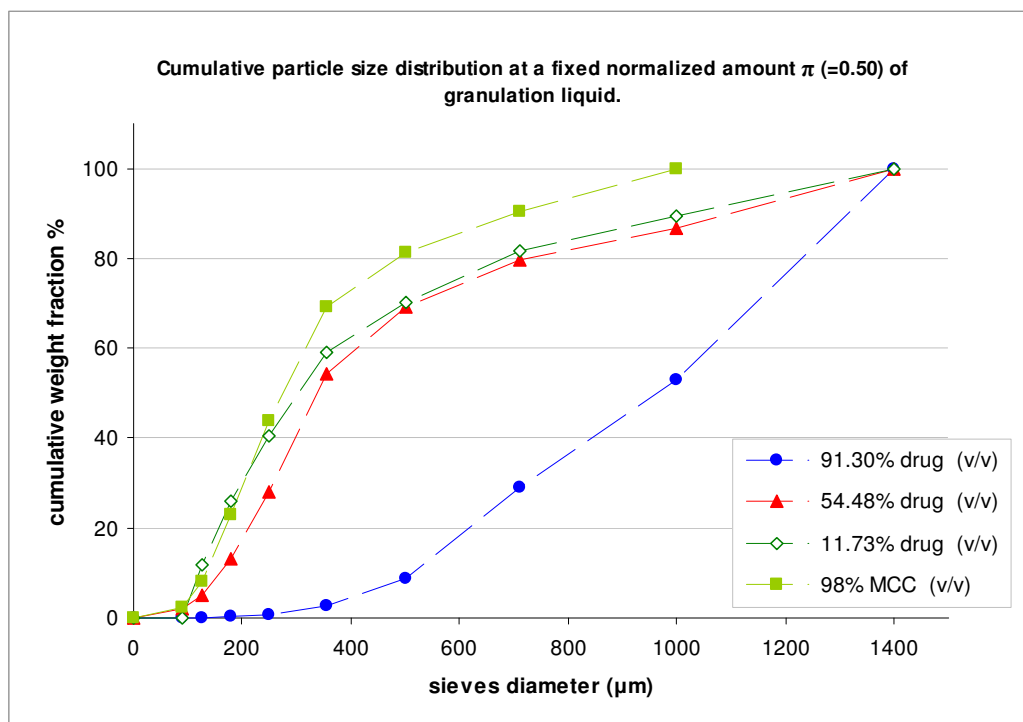


**Figure 8.6.3:** Cumulative particle size distribution at a fixed normalized amount  $\pi (=0.50)$  of granulation liquid.

The ratio of the mass of liquid binder to the mass of solid particles,  $H$ , was in the range of 0.10 to 0.17 for T.G., considering all experiments with 90%-wt. PCM, showing that a significant granule growth could happen at very low liquid saturation for this formulation (what can also be seen in figure 8.2 for  $\pi$  values). In this formulation, capillary forces were also probably acting bringing particles together and promoting their adhesion. The values of  $H$  were higher for increased amounts of MCC in the formulation. In most experiments with 10%-wt. and 50%-wt. drug formulations, the desired granules were found in the ascending slope of the profile. A non-visible well delimited plateau phase in most of those measurements could be an explanation for these findings.

For the experiments with 90%-wt drug formulations in higher mixer loads, batches of 2000 and 2400 grams, the desired granules were found in the ascent of the curve, i.e., in phase II of the profile. An exception was the experiment with higher mixer filling and a slowly liquid addition rate of 16g/min. For the smaller batch size experiments, the higher percentage of desired granules was found in the plateau phase of the P.C. profile, except for the experiment with faster liquid addition speed. For the last case, the fast addition of liquid in a small amount of powder probably promoted a premature granule agglomeration.

It is known that the coalescence of particles is characterized by the exponential growth of the mean particle size (Leuenberger and Imanidis 1986; Vonk et al., 1997), so it was expected that granules produced in the end of phase III or during phase IV would be bigger than the desired size range.

More relevant than where in the profile curve the desired granules appeared is the fact that most of them were found in the same range of power consumption value, i.e., independently of the spraying rate, for the same formulation and not so different batch sizes, the power consumption values were similar in all experiments. It means that a reproducible granulate quality can be achieved by stopping the granulation process at a defined power consumption value. In another study of process monitoring, it was also concluded that at the end of spraying, identical power consumption levels are reached not influenced by spraying rates; questioning the conventional time-control (that usually leads to large deviations in terms of granulate quality) of granulation (Carius, 1992).

For reasons of particle size, primary agglomerates made from MCC would be more resistant to rupture or breakage than agglomerates made from PCM at the same liquid saturation because liquid bridges between particles inside the agglomerates are thicker for MCC compared with PCM. Therefore, submitted to the same stress, agglomerates made of finer powder will be more fragile, what was testified by the constant increase in P.C. measurement for high MCC content formulations opposed to the long plateau phase found for high PCM content formulations.

## **8.7 Conclusion**

The drug load showed to be the most influential factor on power consumption measurement in this study. To saturate the components moisture content and to fill up the interparticulate void space with granulation liquid (reaching 100% saturation of the system) was faster with higher poor water soluble drug concentration. The powder properties are a key parameter in order to control, and predict, the process.

The range of usable granules could be found in the same range of liquid added, but not exactly in the same location in the power consumption curve. When the addition of liquid was done faster, the usable granules not anymore appeared in the plateau phase, but instead they appeared in the ascent slope of the curve, during stage II. However, the power consumption value in the moment of desired granules size was similar among experiments. If a conventional time-controlled granulation had been carried out, experiments with an under-granulated mass or an over-granulated mass would be found.

The time determination of when, i.e., in which moment during granulation process, the usable granules are formed also depends on the desired final granules size selected.

The  $S_2$  point (beginning of phase II), which is present in all profiles, indicates a well-defined, reproducible and invariant moment in the initiation of the agglomerates formation. The method of measuring the power consumption is also a useful and reliable analytical tool to define S values for different compositions, enabling the direct comparison of the agglomeration kinetics by the calculation of the dimensionless amount of granulating liquid  $\pi$ .

For a better P.C. measurement, the extremes, in all process parameters, should be avoided. It can be assumed that the prediction of a specific formulation P.C. profile can be done if enough data about the physico-chemical properties of the compounds in the formulation is available. A virtual library containing data about the physico-chemical properties of drug and excipients (as particle size, specific surface area, water affinity and uptake, residual moisture, and so on), and their interaction, could help in this process.

The application of new technologies and sciences as Artificial Neural Network can be a useful tool in the studies of prediction of the powder agglomeration behaviour. Further experiments in this area are planned. The power consumption method is a valuable monitoring tool applicable into the Process Analytical Technology - PAT Initiative (FDA, 2004) and helps to reach the "Quality by Design".

## 9 References of chapter II

- Ascanio, G., Castro, B., Galindo, E. (2004). Measurement of power consumption in stirred vessels – a review. *Chemical Engineering Research and Design*, 82(A9), 1282-1290
- Betz, G., Bürgin, P.J., Leuenberger, H. (2003). Power consumption profile analysis and tensile strength measurements during moist agglomeration. *Int. J. of Pharmaceutics*, 252, 11-25.
- Betz, G., Bürgin, P.J., Leuenberger, H. (2004). Power consumption measurement and temperature recording during granulation. *Int. J. of Pharmaceutics*, 272, 137-149
- Bier, H.P., Leuenberger, H., Sucker, H. (1979). Determination of the uncritical quantity of granulating liquid by power measurements on planetary mixers. *Pharm. Ind.*, 41, 375-380
- Buckingham, E. (1914). On physically similar systems: illustrations of the use of dimensional equations. *Physical Review*, 2<sup>nd</sup>. Series, 4, 345-376. New York.
- Cameron, I.T., Wang, F. Y., Immanuel, C. D., & Stepanek, F. (2005). Process systems modeling and applications in granulation: A review. *Chem. Eng. Science*, 60, 3723-3750
- Carius, W. (1992). Process Monitoring of Conventional Granulation. *Die Pharmazeutische Industrie*. Reprinted from vol. 54, n. 6. Aulendorf, Germany: ECV. Editio Cantor Verlag (Publisher)
- Dries, K. and Vromans, H. (2009). Quantitative proof of liquid penetration-involved granule formation in a high shear mixer. *Powder Technology*, 189, 165-171
- Ennis, B. J. (2005). Theory of Granulation: An Engineering Perspective. In: Parikh, D. M. (ed.). *Handbook of Pharmaceutical Granulation Technology*, 2<sup>nd</sup>. ed.. Boca Raton, FL: Taylor & Francis Group, 7-78
- Faure, A., Grimsey, I. M., Rowe, R. C., York, P., Cliff, M. J. (1999). Applicability of a scale-up methodology for wet granulation processes in Collette Gral high shear mixer-granulators. *Eur. J. of Pharm. Sci.*, 8, 85-93
- Faure, A., York, P., Rowe, R.C. (2001). Process control and scale-up of pharmaceutical wet granulation processes: a review. *European J. of Pharmaceutics and Biopharmaceutics*, 52, 269–277
- Food and Drug Administration - FDA (2004). *PAT - A Framework for Innovative Pharmaceutical Development, Manufacturing, and Quality Assurance* [online]. Available at: <http://www.fda.gov/downloads/Drugs/GuidanceComplianceRegulatoryInformation/Guidances/ucm070305.pdf>. Accessed on October 2006.
- Gokhale, R. (2005). High-Shear Granulation. In: Parikh, D. M. (ed.). *Handbook of Pharmaceutical Granulation Technology*, 2<sup>nd</sup>. ed.. Boca Raton, FL: Taylor & Francis Group, 191-228
- Halstensen, M., Bakker, P., Esbensen, K. H. (2006). Acoustic chemometric monitoring of an industrial granulation production process - a PAT feasibility study. *Chemometrics and Intelligent Laboratory Systems*, 84, 88 - 97

- Holm, P., Schaefer, T., Kristensen, H.G. (1985a). Granulation in high-speed mixers. Part V. Power consumption and Temperature changes during granulation. *Powder Technology*, 43, 213-223
- Holm, P., Schaefer, T., Kristensen, H.G. (1985b). Granulation in high-speed mixers Part VI. Effects of process conditions on power consumption and granule growth. *Powder Technology*, 43, 225-233
- Iveson, S.M., Litster, J.D., Hapgood, K., Ennis, B.J. (2001). Nucleation, growth and breakage phenomena in agitated wet granulation processes: a review. *Powder Technology*, 117, 3-39
- Knight, P. (2004). Challenges in granulation technologies. *Powder Technology*, 140, 156-162
- Knight, P. C., Seville, J. P. K., Wellm, A. B., Instone, T. (2001). Prediction of impeller torque in high shear powder mixers. *Chemical Engineering Science*, 56, 4457-4471
- Kopcha, M., Roland, E., Bubb, G., Vadino, W. A. (1992). Monitoring the granulation process in a high shear mixer/granulator: An evaluation of three approaches to instrumentation. *Drug Development and Industrial Pharmacy*, 18(18), 1945-1968
- Kristensen, H.G., Holm, P., Jaegerskou, A., Schaefer, T. (1984). Granulation in high speed mixers. Part 4: effect of liquid saturation on the agglomeration. *Pharm. Ind.*, 46, 763 -767
- Laicher, A., Profitlich, T., Schwitzer, K., Ahlert, D. (1997). A modified signal analysis system for end-point control during granulation. *Eur. J. Pharm. Sci.*, 5, 7-14
- Leuenberger, H. (1982). Granulation, new techniques. *Pharm. Acta Helv.*, 57, 72-82
- Leuenberger, H. (1983). Scale-up of granulation processes with reference to process monitoring. *Acta. Pharm. Technol.*, 29, 274–280
- Leuenberger, H. (1994). Moist agglomeration of pharmaceutical powders. In: Chulia, D., Deleuil, M., Pourcelot, Y. (ed.). *Powder Technology and Pharmaceutical Processes, Handbook of Powder Technology*, vol. 9. Amsterdam: Elsevier B.V., 377–389
- Leuenberger, H. (1999). The application of percolation theory in powder technology. *Advanced Powder Technology*, 10(4), 323 - 352
- Leuenberger, H. (2001). New trends in the production of pharmaceutical granules: the classical batch concept and the problem of scale-up. *Eur. J. of Pharm. and Biopharm.*, 52(3), 279-288
- Leuenberger, H. and Betz, G. (2007). Granulation Process Control - Production of Pharmaceutical Granules: The Classical Batch Concept and the Problem of Scale-Up. In: Salman, A.D., Hounslow, M.J. & Seville, J.P.K. (ed.). *Granulation, Handbook of Powder Technology*, Vol. 11. Amsterdam: Elsevier B.V., 705-733
- Leuenberger, H. and Usteri, M. (1989). Agglomeration of binary mixtures in a high-speed mixer. *Int. J. Pharm.*, 55, 135-141
- Leuenberger, H., Bier, H.P., Sucker, H. (1979). Theory of the granulation-liquid requirement in the conventional granulation process. *Pharmaceutical technology international*, 3, 61–68

- Leuenberger, H. and Imanidis, G., (1986). Monitoring mass transfer processes to control moist agglomeration. *Pharm. Technol*, March, 56-73
- Leuenberger, H., Puchkov, M., Krausbauer, E., Betz, G. (2009). Manufacturing pharmaceutical granules: Is the granulation end-point a myth?. *Powder Technology*, 189, 141-148
- Leuenberger, H., Usteri, M., Imanidis, G., Winzap, S. (1989). Monitoring the granulation process: granulate growth, fractal dimensionality and percolation threshold. *Bolletino Chimico Farmaceutico*, 128(2), 54–61
- Mort, P. (2007). Scale-up of high-shear binder-agglomeration process. In: Salman, A.D., Hounslow, M.J. & Seville, J.P.K. (ed.). *Granulation, Handbook of Powder Technology*, Vol. 11. Amsterdam: Elsevier B.V., 853-896
- Omar, W., Mohnicke, M., Ulrich, J. (2006). Determination of the solid liquid interfacial energy and thereby the critical nucleus size of paracetamol in different solvents. *Cryst. Res. Technol.*, 41, 337-343
- Pepin, X., Blanchon, S., Couarraze, G. (2001). Power consumption Profiles in high-shear wet granulation. I: Liquid distribution in relation to powder and binder properties. *J. Pharm. Sciences.*, 90, 322-331
- Pietsch, W. (2002). *Agglomeration Process. Phenomena, Technologies, Equipment*. Weinheim, Germany: Wiley-VCH Verlag GmbH
- Rowe, R.C., Sheskey, P.J., Owen S.C. (2006). *Handbook of pharmaceutical excipients*. 5th ed. London: PhP and APhA
- Schubert, H. (1984). Capillary forces - Modeling and application in particulate technology. *Powder Technology*, 37, 105 - 116
- Talu, I., Tardos, G. I., Ommen, J. R. (2001). Use of stress fluctuations to monitor wet granulation of powders. *Powder Technology*, 117, 149-162
- Tardos, G. I., Farber, L., Bika, D., Michaels, J. N. (2007). Morphology and Strength Development in Solid and Solidifying Interparticulate Bridges in Granules of Pharmaceutical Powders. In: Salman, A.D., Hounslow, M.J. & Seville, J.P.K. (ed.). *Granulation, Handbook of Powder Technology*, Vol. 11. Amsterdam: Elsevier B.V., 1213-1256
- US Pharmacopeia XXXI (2009). US Pharmacopeial Convention, Rockville, MD, pp. 2379-2380
- Vonk, P., Guillaume, C.P.F., Ramaker, J.S., Vromans, H., Kossen, N.W.F. (1997). Growth mechanisms of high-shear pelletisation. *Int. J. of Pharmaceutics*, 157, 93-102
- Walker, G.M., Bell, S.E.J., Greene, K., Jones, D.S., Andrews, G.P. (2009). Characterization of fluidised bed granulation processes using in-situ Raman spectroscopy. *Chemical Engineering Science*, 64, 91-98

Watano, S., Miyanami, K. (1995). Image processing for on-line monitoring of granule size distribution and shape in fluidized bed granulation. *Powder Technology*, 83, 55-60

Watano, S., Numa, T., Miyanami, K., Osako, Y. (2001). A fuzzy control system of high shear granulation using image processing. *Powder Technology*, 115, 124-130

Whitaker, M., Baker, G.R., Westrup, J., Goulding, P.A., Rudd, D.R., Belchamber, R.M., Collins, M.P. (2000). Application of acoustic emission to the monitoring and end point determination of a high shear granulation process. *Int. J. Pharm.*, 205, 79-92

World Health Organization, International Programme on Chemical Safety (2005). *International Chemical Safety Cards: Paracetamol (ICSC:1330)* [online]. Available at: <http://www.inchem.org/documents/icsc/icsc/eics1330.htm>. Accessed on 06 November 2009

## Third Chapter

**Artificial Neural Networks applied to  
pharmaceutical wet granulation process.****Abstract**

Pharmaceutical formulations are complex systems and are often developed empirically under a high time-pressure on the basis of 'trial and error' experiments. The situation is complicated further by the fact that many pharmaceutical processes are only poorly understood. Thus, the predictability of the manufacturing performance is suffering or completely absent. Predicting the future output of very complex systems is a difficult task. Adaptive systems however have shown themselves, trained on the right data, quite capable of producing good predictions. In this work, six formulation' and process' parameters were used as inputs, to feed an ANN, named Time, Drug concentration, MCC concentration, HPMC concentration, Batch Size and Granulation-Liquid Added. The goal was to predict the power consumption profile of a granulation process. Already in the preprocessing step, the artificial networks showed to be a helpful tool for data mining, data management and process understanding. After training trials, a network called Gamma-Recurrent Hybrid resulted in satisfactory predictions for formulations not containing high drug loads. When predicted outputs were plotted against the actual results the  $R^2$  values were 0.99, 0.95 and 0.26 for formulations of 10%, 50% and 90% (w/w) of drug, respectively; with an absolute error of 76 (Manhattan error metric). As adaptive systems learn from data inputted, and the high drug load formulations presented more irregular experimental profiles, this could result in a *difficult learning* and thus the lack of network precision in predict the behaviour of that formulation. The  $R^2$  values were better (0.99, 0.98 and 0.99 for formulations of 10%, 50% and 90% (w/w) of drug, respectively) when the network (in these cases generalized two layer and one layer) was trained using as inputs drug and excipient concentration, bulk density, residual moisture, batch size, equipment filling fraction and the granulation liquid addition rate; and it was tested the system ability in predict the relevant S2, S3, S4 and S5 points of a typical Leuenberger power consumption profile. If an operator, based on the material and process properties, could predict those 'moments' he could adjust the amount of granulation liquid and stop the process at a more precise moment. However, there is simply no substitute for domain knowledge, as any result will always need to be interpreted properly. Adaptive systems may build the model, but if wrong data is inputted or an unqualified person interprets the output, then they are of little worth.

**Keywords**

Artificial networks, adaptive systems, wet granulation process, power consumption, process and formulation design, PAT.



## 10 Introduction

Product development scientists are required to produce robust dosage forms, which may be manufactured over a range of scales with minimal time and cost. This need has encouraged the development of predictive techniques that may have benefits in reducing the time taken to develop suitable formulation and process parameters. Prediction may also have benefits in full-scale production if the causes of product variation can be identified and controlled. Predictive techniques have been used at many stages of the product development process, including selection and optimisation of formulations, prediction of process scale-up capability, control of process end-points and predicting the properties of processed material (Hardy and Cook, 2003).

Control and optimization of wet granulation process by the pharmaceutical industry is a fundamental requirement to guarantee constant product quality but since long time it is still unsettled and troublesome. Granulation still remains more 'an art', employing operator practice, than a science-based approach. More accurate methods need to be developed in order to stop granulation when the higher percentage of desired granules size is reached, since the particle size distribution is usually wider than the one specified.

Based on a series of investigations carried out by Leuenberger et al. (1979, 1982, 1986), granulation power consumption, liquid saturation level and granule particle size were inter-related, which forms a technical basis to use power consumption as a monitoring tool for the characterization of particles within a high-shear mixer. For that is essential to measure the total power consumption profile till the state of a suspension is obtained. Then, from that profile five phases can be characterized and, defining the start points for each phase, the amount of granulation liquid can be calculated. A more detailed description of this control strategy is also provided in Leuenberger (1994).

Many mathematical models had been used/created trying to explain the granulation process and consequently to model/predict its behaviour (Adetayo and Ennis, 2000; Gantt and Gatzke, 2005; Oullion et al., 2009; Tu et al., 2009; Cavinato et al., 2010), i.e. to predict powders agglomeration kinetics; a process that depends of many factors. A variety of approaches used for prediction and correlation of properties of solid dosage forms are reviewed by Hardy and Cook (2003).

One of the major problems consists of the fact that pharmaceutical formulations are complex systems and that they are often developed empirically under a high time-pressure on the basis of 'trial and error' experiments. This procedure can easily lead to a non-robust

formulation. The situation is complicated by the fact that in addition many pharmaceutical processes are only poorly understood. Thus, the predictability of the manufacturing performance is suffering or completely absent (Leuenberger and Lanz, 2005).

Predicting the future output of very complex systems is a difficult task. Adaptive systems however have shown themselves, trained on the right data, quite capable of producing good predictions. They are consistently better than more traditional methods. Adaptive systems can also be used to build a mathematical model that captures the functions and dynamics of a real-world system. Such models are very important for analysis, simulation, prediction, monitoring and control system design. The biggest difference between adaptive systems and traditional system identification methods are that adaptive systems are non-linear, giving them an order of magnitude more modelling power (Peltarion® Documentation).

One of the first talks about the application of neural network in pharmaceutical product development was done by Hussain et al. (1994). In his report is introduced the concept of formulation expert system to predict the *in vitro* drug release profile from hydrophilic matrix tablets. Prediction of a model granulation and tablet system characteristics from the knowledge of material and process variables utilizing neural networks were also the basis of the work of Kesavan and Peck (1996). They reached satisfactory predictions.

Watano et al. (1997) conducted with high accuracy a granulation scale-up using a backpropagation learning neural network, without constructing a mathematical model with a complicated non-linear relationship that use a vast amount of experimental scale-up data.

An investigation to describe the degree of data fitting and robustness of an ANN compared to classical modelling technique was carried out by Bourquin et al. (1998). Comparable results were achieved using both methodologies for data fitting. However, the robustness of the models towards outliers was clearly better for the modelling technique. Kesavan and Peck (1996) also conducted a comparison between neural networks and regression analysis. They concluded that the neural network captured more efficiently the nonlinearity of the testing data.

Other examples of using ANN in the pharmaceutical field are its application in the modelling of drug release from matrix tablets formulations (Petrovic et al., 2009), in predicting the *in vivo* behaviour of drugs (level A *in vitro-in vivo* correlation) (Parojcic et al., 2007) and also the prediction and/or optimization of microemulsion phase boundaries, in order to minimize experimental effort (Djekic et al., 2008). A generalized regression neural network was tested

and showed to be a reliable method to validate a fluid bed granulation (Behzadi et al., 2005).

The pharmaceutical formulation process is highly specialized and requires specific domain knowledge and often years of experience. Neural computing, machine learning, knowledge-based systems and expert systems, derived from research into artificial intelligence, can assist in the efficient formulation of products and increase productivity, consistency and quality (Rowe and Roberts, 1998a). Those are approaches preconized in the Quality by Design initiative that is part of the FDA's Process Analytical Technology - PAT framework. In another words, those new techniques can help companies in the understanding of the science behind its processes and demonstrate it.

Prediction of power consumption curve, and an uncritical amount of granulation liquid, on the basis of knowledge of the starting materials and process variables has not yet been successfully done, and constitute the aim of this work.

### ***Artificial Neural Networks – ANNs***

ANNs are computer-based programs that attempt to simulate certain functions of the biological brain, such as learning, generalizing, or abstracting from experience. They have the ability to discern relationships or patterns in response to exposure to facts ("learning"). Adaptive systems, such as artificial neural networks, build models that find the relationship between the inputs and the wanted output. Instead of instructing the computer how to do something, examples of what need to be done are provided. Providing it with data on numeric inputs and informing what outputs are wanted the adaptive system builds the actual function autonomously. It follows the learning-by-example paradigm (Peltarion® Documentation).

A neural network structure/architecture can be defined as a collection of *parallel processors* connected together in the form of a directed graph, organized such that the network structure lends itself to the problem being considered. The neurons in an ANN are arranged in a network architecture that may vary depending on the problem being modelled. The ANN typically consists of an input layer and output layer interconnected through one or more hidden layers, which perform the mapping functions. A typical network diagram is shown in figure 10.1. The weights of the various connections are modified through a process of training. The most common form of training used for formulation systems is supervised backpropagation training, which adjusts the weights of the connections between

neurons by back propagation of errors to bring the predicted output closer to the experimental output. Once trained, the ANN can predict the outcome of a set of formulation or process variables on product performance and vice-versa (Freeman and Skapura, 1991; Hardy and Cook, 2003; Rowe and Roberts, 1998b; Hussain et al., 1994).

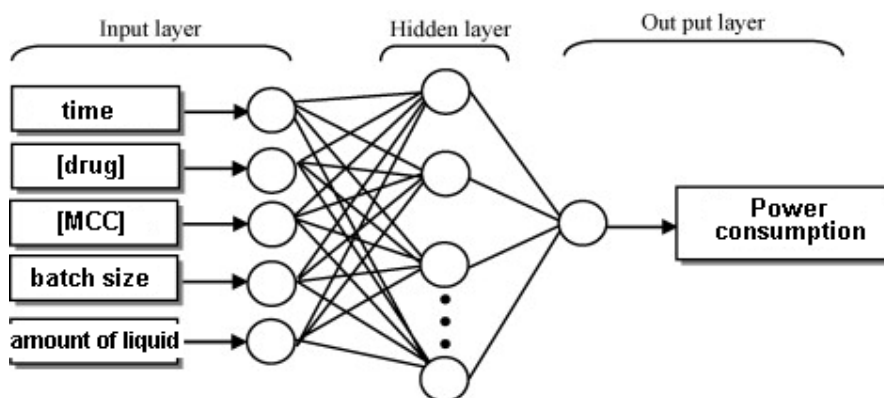


**Figure 10.1:** A schematic representation of the character-recognition problem presented in this work. In this example, application of an input pattern on the left layer of processors can cause many of the hidden-layer units to activate. The activity on the hidden layer should then cause exactly one of the output-layer units to activate – the one associated with the pattern being identified.

The multivariate nature of pharmaceutical formulations can make ANNs a useful approach.

### **Genetic Algorithms – GAs**

Holland (1975) proposed GAs as an optimization technique for minimizing multimodal functions. An optimizer is a batch processor that optimizes parameters of components such as blocks and update rules. Adaptation is the process of obtaining optimal weights while optimization is the process of finding the optimal configuration parameters for a system in order for it to be able to find a set of optimal weights.

The GA draws inspiration from the process of natural selection as seen in nature where only the fittest individuals of a population survive. It uses three processes namely, selection, reproduction and mutation. These processes work to transform one population (*generation*) into the next, as figure 10.2 shows. Any implementation of a GA begins with the generation of an initial population of points inside the given search space. Each point is referred to as a chromosome. Then, each chromosome is evaluated independently of other chromosomes using a *fitness function*. This function, which is equivalent to a cost function, assigns *fitness*

values to each chromosome such that the “healthiest” ones have larger values. The next step of the algorithm, called Selection, creates an intermediate population by selecting the fittest chromosomes of the current population. Once the intermediate population has been formed, reproduction takes place. Reproduction mimics biological mating by randomly selecting members of the intermediate population and exchanging information between them. Next, mutation takes place. The process serves to add small perturbations to the newly generated strings and ensure that all parts of the search space are reached. It also helps the algorithm escape from local minima (Ocloo and Edmonson, 2008).

GAs work best for large, unknown, search spaces. Although GA has the advantage of being able to search large domains and escaping local minimas, its primary disadvantage is its

high computational cost, due the need to compute fitness values for all chromosomes in the population during each and every iteration (Ocloo and Edmonson, 2008).

GAs can be applied alone. It is an artificial intelligence technique itself, and may be more effective than ANNs in finding solutions for certain problems. Turkoglu et al (1999) predicted the effect of formulation and process variables on tablets produced using a roll compaction process.

Nevertheless, in this work it was only applied as an optimizer batch processor.

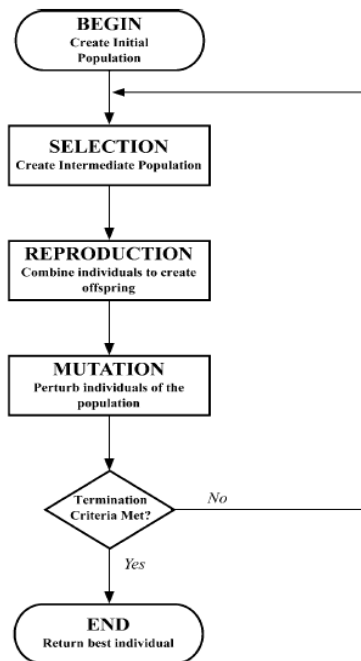


**Figure 10.2:** Flow of a Genetic Algorithm (extracted from Ocloo and Edmonson, 2008).

## 11 Materials and Methods

### 11.1 Granulation materials

Microcrystalline Cellulose (MCC101, Pharmatrans Sanaq AG), Paracetamol (Mallinckrodt Pharmaceuticals) and Hydroxypropylmethylcellulose (Methocel K100, Dow Chemical) were used to prepare three different mixtures (different ratios of drug/MCC) in different batch sizes.

### 11.2 Characterization of starting material

The particle size distribution of the starting materials was analyzed by laser diffraction (MasterSizer X Long Bed, Malvern Instruments, UK). The measurement was performed using the Manual Dry Powder Feeder, and the obscuration was set around 20%. For the moisture content, 'loss on drying' was determined thermogravimetrically (Mettler-Toledo LP16M, Mettler Instruments, Switzerland). Before and after granulation, specimens of 1 to 2 g were heated up at 105°C for 20 minutes. The loss of moisture was calculated in percent by weight. True density  $\rho_t$  was determined using a Helium Pycnometer (AccuPyc 1330, Micromeritics Instruments Corporation, USA). Bulk and Tapped Densities ( $\rho_{\text{bulk}}$  and  $\rho_{\text{tap}}$ , respectively) were determined according to U.S. Pharmacopeia 31, using the apparatus Type STAV 2003, Engelsmann AG, Germany. Powder porosity ( $\epsilon$ ) was calculated using the true and bulk densities, according to the formula  $\epsilon = 1 - \rho_{\text{bulk}}/\rho_t$ . (More detailed explanation about the methods is given in the first chapter of this thesis)

### 11.3 Granulation Design and Procedure

Three main formulations containing Microcrystalline Cellulose (MCC) and Paracetamol (PCM) in different proportions were produced. The percentage of drug in the total formulation was zero, 10%, 50% and 90% (by weight). In all formulations 2% of Hydroxypropylmethylcellulose (HPMC) was added as a dry binder into the mixture, and the granulation liquid was distilled water. A lab scale Diosna<sup>®</sup> P10 high-shear mixer (Dierks & Söhne, Osnabrück, Germany) with a volume of 10L was used. Three batch sizes were chosen: approximately 30, 50 and 70% in volume of the filling capacity of the mixer working vessel. The granulation liquid was added using a peristaltic pump under constant addition speeds, two main ones set at 38 and 50 g.min<sup>-1</sup>. The total amount of blend was mixed for 5 minutes inside the mixer with an impeller speed of 452 rpm. After the mixing time, the liquid addition and the power consumption measurement were started simultaneously. During the whole process the main impeller and chopper speeds were kept constant at 430 and 3000

rpm, respectively. The temperature inside the mixing vessel in the moment of sampling was also measured.

#### **11.4 Power consumption profile recording**

An “in process” computer calculation program was used to record the power consumption (PC) during all granulation experiments. The power consumption of the mixer motor (i.e. main impeller) is determined by the electric current consumption of the motor according to the equation  $P = U \times I$ , where  $P$  is the power (W),  $U$  the electric potential (V), and  $I$  is the electric current (A). The product of electric potential (V) times electric current (A) is measured by a measuring transducer (Sineax Type PQ 502, 0–2kW, Camille Bauer AG, Switzerland). The power consumption is converted into an electric potential signal between 0 and 10V, 10V corresponding to 2 kW and sampled by an I/O Multifunction DAQ-Card, to a laptop computer and displayed graphically by the Recorder Software (produced in cooperation with Pharmatronic Ltd, Switzerland) (Betz et al., 2003).

#### **11.5 Characterization of collected samples**

Samples were taken at predetermined time intervals and its residual moisture was immediately determined thermo-gravimetrically. The loss of moisture was calculated in percent by weight. The drawn samples were dried in a dish dryer at 40°C for around 10 hours before sieve analysis being carried out in ISO-norm sieve oscillator type equipment (Rietsch, Germany). The eight selected sieves ranged from 1000 µm to 90 µm mesh. A percentage in the particle-size distribution was calculated by the ratio of sieves cumulative and total sample weight. In this study, the desired granules particle size, also called target granules (T.G.), was set between 125µm and 710µm, i.e., cumulative weight from sieves 125µm to 500µm.

#### **11.6 Computation Methods**

From the Synapse<sup>®</sup> software library different networks were tested and a dynamic snippet called Gamma Recurrent Hybrid showed to be the best option (with reduced error) to construct the topology of the network for the PC prediction. Suitable for simple dynamic problems it is a dynamic neural network that combines gamma and infinite impulse response (IIR) memories. The *gamma memory block* is used in dynamic systems to remember past signals. It enables the usage of past information to predict current and future states. *IIR* is infinite and used for applications where linear characteristics are not of concern, it operates on current and past input values and current and past output values.

Dynamic snippets use memory structures and are for processing time series. It follows a supervised learning rule. In supervised learning, each example is a *pair* consisting of an input object and a desired output value (also called the *supervisory signal*). A supervised learning algorithm analyzes the training data and produces an inferred function. As mentioned in the introduction, a supervised training adjusts the weights of the connections between neurons by back propagation of errors to bring the predicted output closer to the experimental output.

The steps implicated in a network design until its deployment are described in the figure 11.6.1.

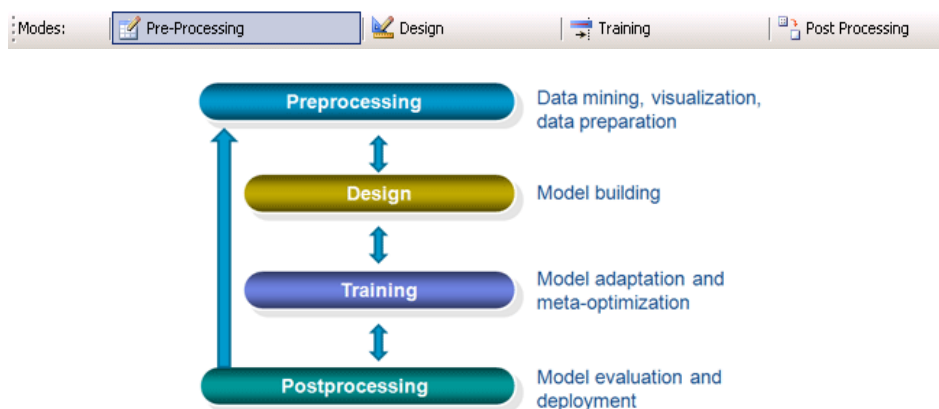


**Figure 11.6.1:** Steps of network construction (From <http://www.peltarion.com/doc/images/ModesChart.png>).

As inputs, six formulation properties and process parameters had been used, namely Time (minutes), Drug (paracetamol) concentration (% by weight of total formulation), MCC concentration (% by weight of total formulation), HPMC concentration (% by weight of total formulation), Batch Size (grams) and Granulation-Liquid Added (grams). The output was the absolute power value itself (watts). Each feature represents one column and the data/values were arranged in the rows and sorted in an ascending order (time sequence). As the experimental values were a time series, i.e. they are in time sequence, the order of the data is important to avoid that the software when taking a value doesn't break the sequence, leading to a misunderstanding/misinterpretation of the data. Consequently the obtained network architecture consisted of six units in the input layer and one output unit.

All experiments were collated in a single excel sheet and converted to a CVS file. From the overall data (20 experiments) an amount equivalent to 14.25% was selected for validation of the system, it corresponded to 3 experiments. Other 3 experiments (one for each formulation) were kept out of the inputted data set in order to be used to test the trained system.



The presented network was trained by the software Peltarion Synapse® Version 1.3.5 (Peltarion® Corporation, 2010). It is very important for the training how many samples to take in to account for each update of the system parameters, i.e. the batch length; as well as the amount of times that the collection of all available samples (rows) enter the system, called *epoch* or *iteration* (repetition). Preferably the batch length should be chosen so that the full length is a multiple of the batch length. Failing to have it can result in samples being cropped. Many epochs are usually required to fully train the system. However, for small amount of samples the system can become over-trained easily and hence not being able to execute reliable generalizations.

The final network topology/architecture is shown in the figure 11.6.2. After conclusion of designing step the model was optimized using a Genetic Algorithm optimizer followed by further training.

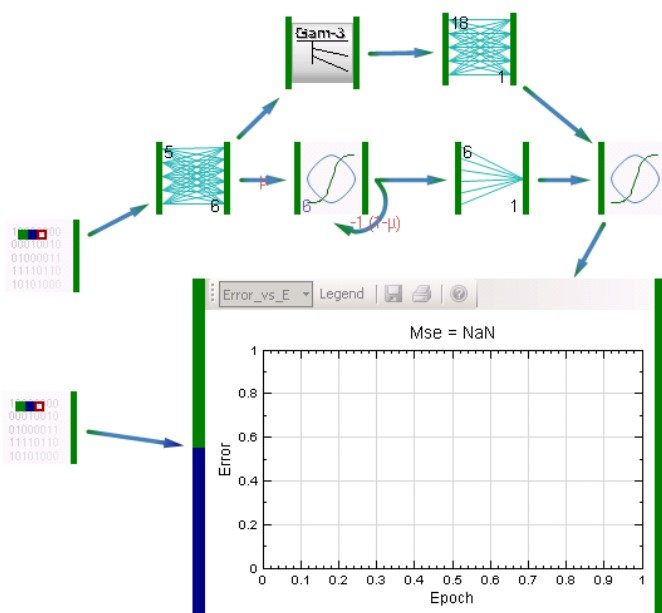


**Figure 11.6.2:** Gamma-Recurrent Hybrid network topology/architecture (before training).

On a second moment, other *static* networks were tested submitting as inputs formulation properties and process parameters such as drug concentration, excipient concentration, bulk density and residual moisture of the power mixture, batch size and equipment filling fraction as well as the granulation liquid addition rate. It was tested the ability of an adaptive system to predict the relevant S2, S3, S4 and S5 points of a typical Leuenberger power consumption profile (Leuenberger and Usteri, 1989; Leuenberger and Betz, 2007). The networks that resulted in higher values in the  $R^2$  coefficient are shown.

## 12 Results and Discussion

The power consumption profiles, of all 20 experiments, are not shown here (some of them can be seen in the chapter II of this thesis). However, as their absolute values were used as outputs in this study, it is relevant to mention that for formulations containing 90% (w/w) drug the PC curves exhibited wider variation among the experiments compared with other formulations.

During the preprocessing step, the correlation visualizer showed the linear correlation between features. The correlation between the output and input features is shown in the Figure 12.1. This procedure can be seen as a triage stage to see what features affect the desired output, as well as to get an overview of the system general behaviour.

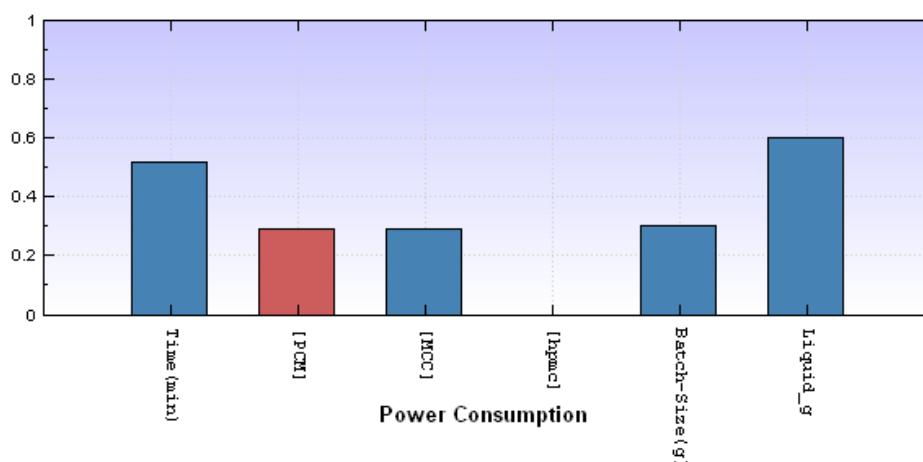


**Figure 12.1:** Correlation between the output (absolute power consumption) and the inputs (all six features). The higher the bar goes, the more the features are correlated. Blue bars indicate a positive correlation while red bars indicate a negative correlation.

As can be seen in the figure 12.1 the HPMC concentration has zero relevance over the output. That happened due its constant value in all experiments; for that reason it was removed from the inputted features since it can only slow down the system. The MCC and PCM concentrations had the same level of correlation with the output (PC) but the drug concentration was the only feature that affects the output negatively.

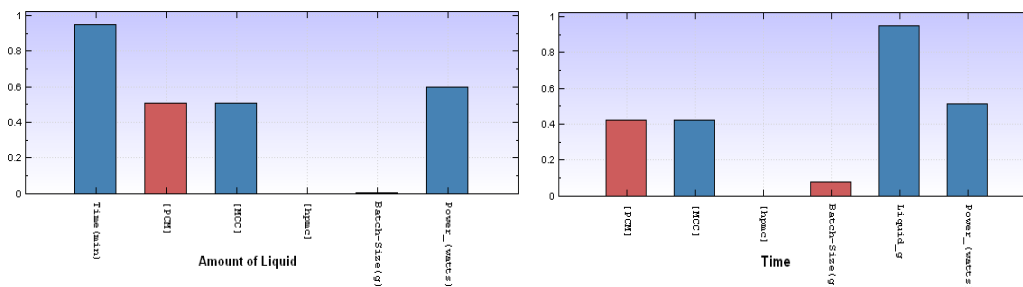


**Figure 12.2:** Correlation between the applied amount of liquid and other features (left). And correlation between the expended time and other features (right).

In both cases shown in the figure 12.2, the MCC and PCM concentrations had the same level of correlation with the amount of granulation liquid and the experiment time; however the amount of drug presented an inverse correlation with them, as experimentally measured. Time was the feature more correlated with the amount of liquid and *vice versa*.

After optimization and training (batch length of 1 and short training time, resulting in a Mse of  $3.84e^{-002}$ ), the system was tested and the predicted values for the power consumption are plotted in the figures 12.3.a, b and c together with the respective experimental values.

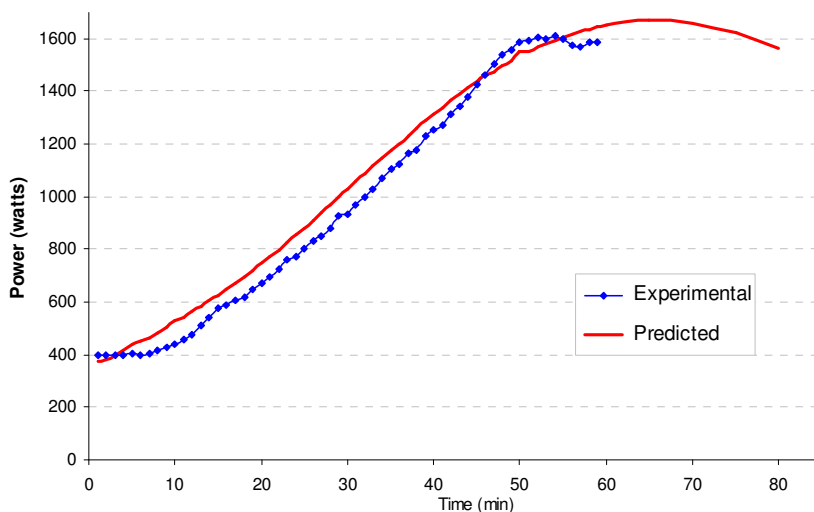


**Figure 12.3.a)** Predicted and Experimental values of power consumption versus time for a wet granulation process of a formulation containing 10% (w/w) of drug.

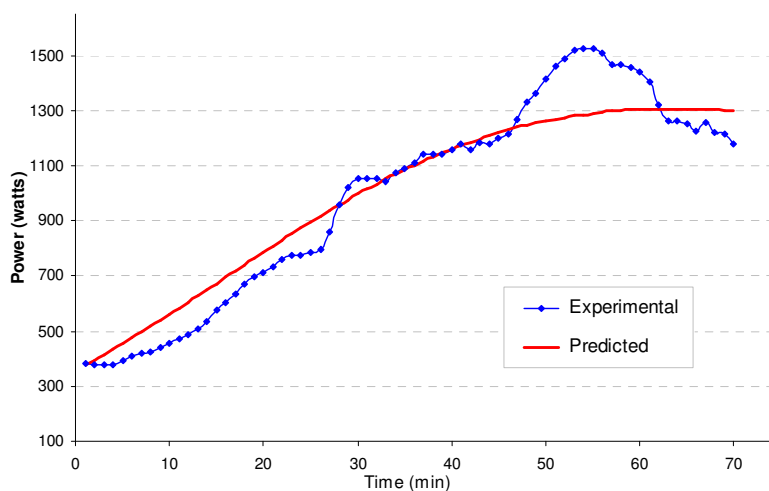


**Figure 12.3.b)** Predicted and Experimental values of power consumption versus time for a wet granulation process of a formulation containing 50% (w/w) of drug.

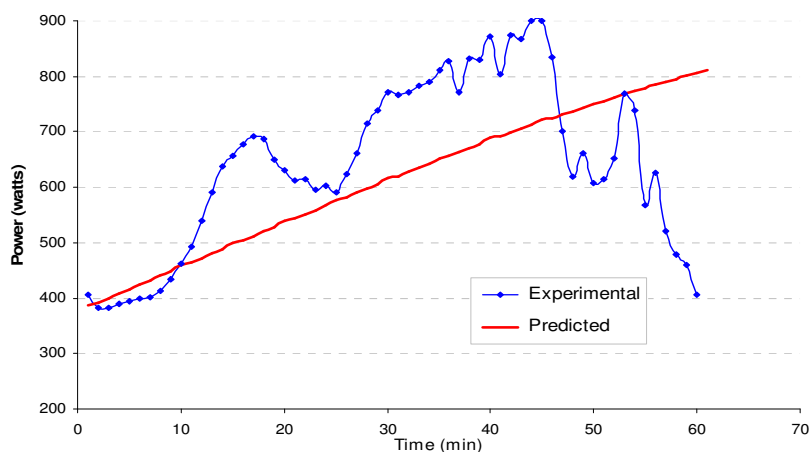


**Figure 12.3.c)** Predicted and Experimental values of power consumption versus time for a wet granulation process of a formulation containing 90% (w/w) of drug.

The neural network model produced smoother curves compared with the experimental measured ones, what is not so good or intended. As it ‘learns’ from the data supplied, it did better prediction for the formulations containing higher amounts of MCC (the ones that were more robust during granulation and resulted in more similar energy consumption profiles). It was not possible to predict the accentuated slope, plateau and faster drop in the power consumption for the higher dose of paracetamol formulations (which ones presented more irregular measured profiles what could result in a *difficult learning*). However, the network did predict the decreased absolute values of power for this formulation. The non-linear prediction of power consumption could be better if there were other sets of data in the training set to indicate such tendency of fast overwetting with the increase in PCM concentration, i.e. for a better *learning* other experiments with additional/intermediate drug loads would enclose the design space.

It could also be noticed that extended training times led to an over-trained network (over-training was identified when the errors of training set and validation set starts to diverge in the error visualizer window). An over-trained network loses its ability to make generalizations and leads to a bad prediction. Another observation was that bigger batch lengths tend to produce smaller errors but not better predictions.

The  $R^2$  correlation coefficients between the experimentally measured and the network predicted output values are depicted on the figure 12.4.

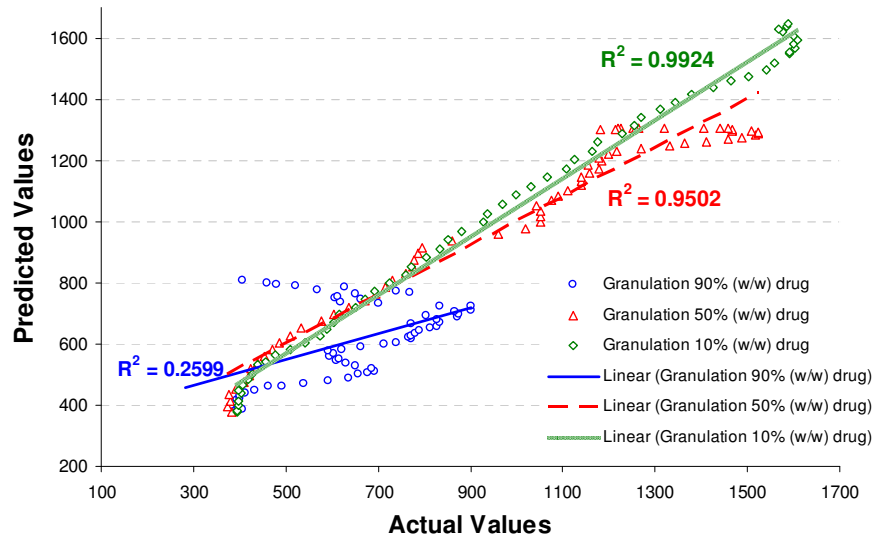


**Figure 12.4:** Predicted output values plotted against the experimentally measured (actual) values. The three different formulations used in the prediction studies are shown in the legend.

From the  $R^2$  values it is observed that the predicted values for the formulations of 10% and 50% (w/w) drug were in good agreement with the actual measured values. When predictions inside the domain of 90% (w/w) drug formulation were attempted, network performance was poor, as shown in the figures 12.3.c and 12.4 (low  $R^2$  value). As commented above the granulation process for that formulation generated more irregular power consumption curves/profiles and that wide variability among the input samples can be the reason for the lack of network precision in predict the behaviour of this formulation. However, it must be highlighted that a different network, properly trained, may be more successful in the power consumption prediction for that formulation.

To test the performance of the trained adaptive system (its statistical validity) the 'Error Analyzer Postprocessor' tool was used. It also provides a connection to preprocessing allowing you to use the information gained by training a system to better understand the data. The error has been measured using the Manhattan error metric. Whereby the mean absolute error is an average of the absolute errors  $E = \text{abs}(S_2 - S_1)$ , where  $S_2$  is the prediction and  $S_1$  the true value. The absolute error for the prediction of the power consumption value was 76,35 when the system was trained with a batch length of 1 for 1500 epochs (iteration). The output prediction accuracy of +/- 201.34 (the smallest among all networks tested) was within the desired 95% confidence, as shown in the figure 12.5.

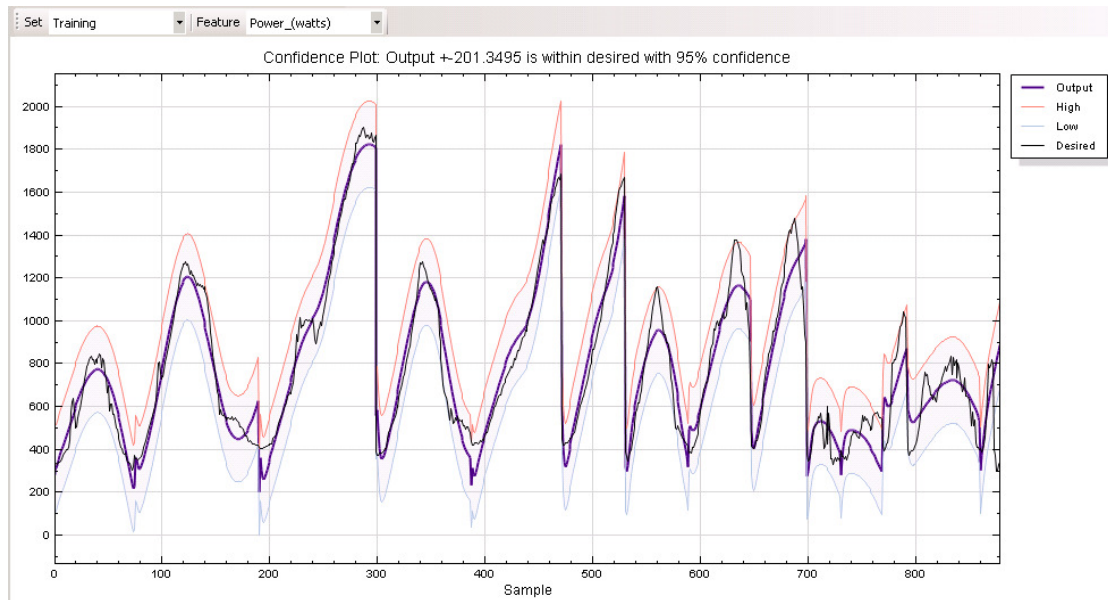


**Figure 12.5:** Confidence plot. The purple line is the output of the system; the black line is the desired output. The two other lines that enclose the shaded area are the confidence limits.

The exact resulted values will vary depending on the random order of data and initial weights. As systems are initialized with random values they converge to different solutions. And *problem space* not covered by the data can result in great variance in output between models (Peltarion® Documentation, 2010).

So the values looked nearly as good as the theoretical limit. Hence the system was quite acceptable for its purposes (to predict as the PC profile looks like) with the confidence level set to 95% (it means that 95% of the desired outputs should be within the gray area). As it starts with random weights when the training starts, it is expected the results will vary.

The measurement of how important a feature is at a certain level is given by a 'sensitivity analyses'. In another words this means that it is possible to see how much the output changes if an input feature is changed at certain percentage. In the Figure 12.6.a can be seen that a 10% increase in the paracetamol concentration can give a stronger output change than a 10% of MCC increase; and the output change is even stronger (quote y-scale) if the parameters are changed 25% (figure 12.6.b) and 50% (figure 12.6.c).

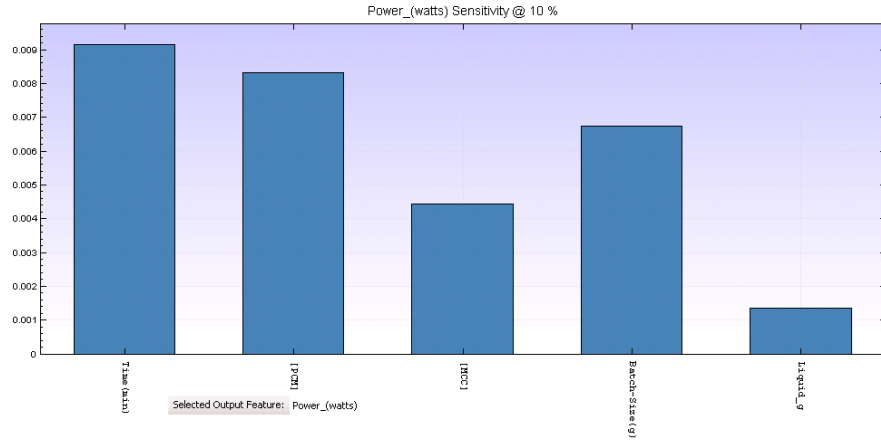


**Figure 12.6.a:** Sensitivity of the output (power consumption) when the inputs (features) are dithered in 10%. The height of the bars is the absolute value of the difference between  $Error_{original} - Error_{dither}$ .

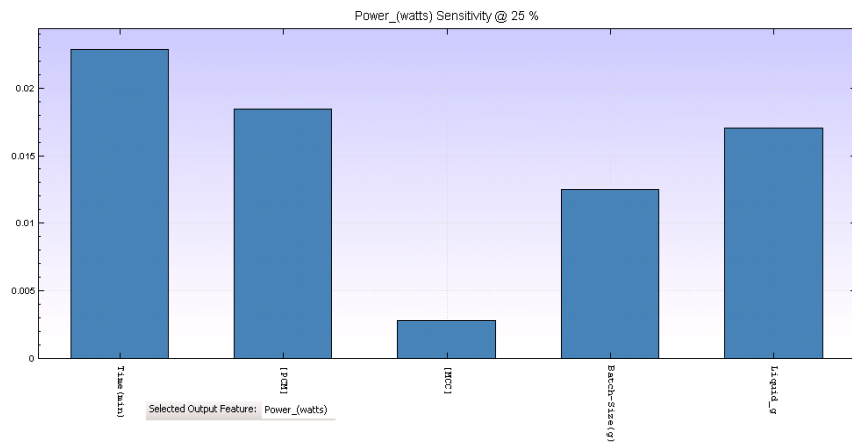


**Figure 12.6.b:** Sensitivity of the output (power consumption) when the inputs (features) are dithered in 25%. The height of the bars is the absolute value of the difference between  $Error_{original} - Error_{dither}$ .

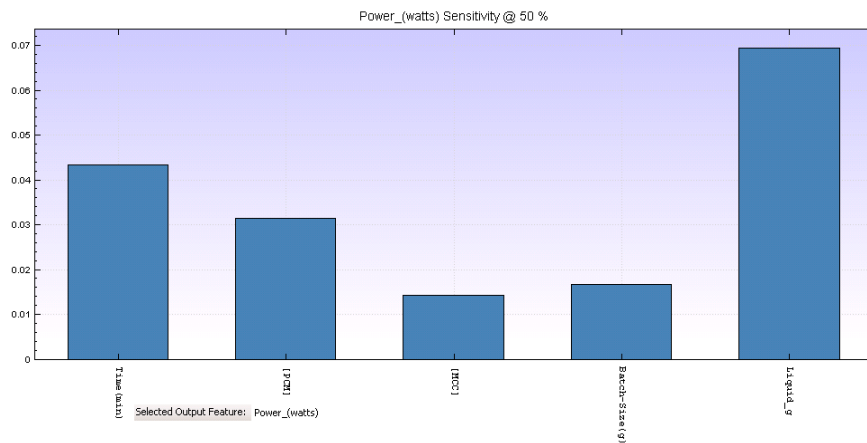


**Figure 12.6.c:** Sensitivity of the output (power consumption) when the inputs (features) are dithered in 50%. The height of the bars is the absolute value of the difference between  $Error_{original} - Error_{dither}$ .

Being careful with the interpretation, sensitivity analysis can give a lot of information about the model. Higher sensitivity differences lead to increased error. For example, a change from 10 to 25% in MCC concentration did not show a big relevance as a change from 25 to 50%. Considering the applied liquid variable in this model, the sensitivity analysis states that if the changing in concentration is 10% it does not make a big difference, but if it is 25% or 50% does and so on.

It is important to understand that sensitivity is per model as long as input variables are correlated (and in this case, inputs are complex and non-linear). A neural net can choose which information it wishes to extract from what features, and that depends on many factors, the initial random weights in the network being a major one. This directly impacts the sensitivity and two models trained on the same data are unlikely to have equal sensitivity (Peltarion® Documentation). In such a way, it would be incorrect to state that PCM variable is more important than MCC variable, because this system is non-linear.

Another way to work with the granulation power consumption using an ANN was tested. Submitting as inputs some formulation properties as drug concentration, excipient concentration, bulk density and residual moisture of the power mixture, batch size and equipment filling fraction as well as the granulation liquid addition rate, it was tested the ability of an adaptive system to predict the relevant S2, S3, S4 and S5 points of a typical Leuenberger power consumption profile. Those points were characterized from the experimental PC profiles by its respective time values (in minutes).

As these points/values do not represent a long time series, static networks were tested once they are less complex and faster. The ones that gave the higher values in the  $R^2$  coefficient are shown in the table 1. They are the generalized one layer and generalized two layer. They are extensions of the standard Multi-Layer Perceptron (MLP), a basic static feedforward backpropagation neural network. The systems were trained for a very short time and using small batches. No optimization was necessary.

The experimental values and their corresponding predicted values are given in Table 12.1.



**Table 12.1:** Powder properties and/or process parameters used as inputs and their corresponding experimental measured and predicted results [(time points (in minutes))].

inputs	formulation*	outputs				$R^2$	network
		S2	S3	S4	S5		
[drug]	A	8	18	29	54	--	<i>experimental results</i>
[MCC]		8	18	33	57	0.995	Generalized Two Layer
bulk density	B	4	30	45	54	--	<i>experimental results</i>
residual moisture		6	27	43	57	0.982	Generalized Two Layer
batch size	C	7	14	26	44	--	<i>experimental results</i>
filling fraction		9	14	24	39	0.999	Generalized One Layer

\*Formulation A, B and C correspond to formulations containing 10%, 50% and 90% (w/w) of drug, respectively.

From the  $R^2$  values it could be concluded that the prediction of important points (ones that represent moments of changes in the agglomeration process) in the power consumption curve can be reasonably done. If an operator could predict these moments he could adjust the granulation liquid amount to them and to stop the process in a more precise moment. A prediction of time moments means a prediction in the amount of liquid to add, if the liquid is added at constant rates.

Finalizing, a word of caution should be highlighted. If a person is not qualified to evaluate the input variables and to interpret the output variables, then chances of making a mistake are big. If not enough domain knowledge about the studied subject is present, can be difficult to spot some probe combinations that could never happen in the real world and for which the model will give out nonsense. The results for impossible combinations vary greatly from model to model. There is simply no substitute for domain knowledge, as the results need to be interpreted properly. Adaptive systems may build the model, but if wrong data is inputted or an unqualified person interprets the output, then they are of little worth.

## 13 Conclusion

Predicting the future output of very complex systems is a difficult task. Adaptive systems however have shown themselves, trained on the right data, quite capable of producing good predictions. They are consistently better than more traditional methods.

The optimum structure/topology of the neural network was chosen by its error convergence behaviour and its correlation factor with the data obtained by laboratory experiments. The prediction of the non-linear curve of power consumption could have been better for the high drug load formulation if there were available more sets of data in the training set, i.e. experiments with broader ratios of drug concentration. ANN effectiveness is limited by the training data selected as well as how the data is introduced to the system and trained. Training parameters as batch length and number of epochs makes a big influence in the network capacity of generalization.

Another limitation is that, in most of cases, ANNs lack explanation capability and there is difficulty in obtaining justification for results. However, such systems can shorten development time, simplify formulations, provide the rationale for decisions taken in arriving at a formulation, serve as excellent teaching tools for novices, and accumulate and preserve the knowledge and experience of experts (Augsburger and Zellhofer, 2007).

ANN's are valuable tools that fulfil into the PAT framework, helping in data mining, data management and process understanding.

## 14 References of chapter III

- Adetayo, A. A. and Ennis, B. J. (2000). A new approach to modeling granulation processes for simulation and control purposes. *Powder Technology*, 108, 202-209
- Augsburger, L.L., Zellhofer, M.J. (2007). Tablet Formulation. In: Swarbrick, J. (ed.). *Encyclopedia of Pharmaceutical Technology*, third edition. New York: Marcel Dekker, 2710
- Behzadi, S.S., Klocker, J., Hüttlin, H., Wolschann, P., Viernstein, H. (2005). Validation of fluid bed granulation utilizing artificial neural network. *International Journal of Pharmaceutics*, 291, 139-148
- Betz, G., Bürgin, P.J., Leuenberger, H. (2003). Power consumption profile analysis and tensile strength measurements during moist agglomeration. *Int. J. of Pharmaceutics*, 252, 11-25
- Bourquin, J., Schmidli, H., Hoogevest, P., Leuenberger, H. (1998). Pitfalls of artificial neural networks (ANN) modelling technique for data sets containing outlier measurements using a study on mixture properties of a direct compressed dosage form. *European Journal of Pharmaceutical Sciences*, 7 (1), 17-28
- Cavinato, M., Bresciani, M., Machin, M., Bellazzi, G., Canu, P., Santomaso, A.C. (2010). Formulation design for optimal high-shear wet granulation using on-line torque measurements. *International Journal of Pharmaceutics*, 387, 48-55
- Djekic, L., Ibric, S., Primorac, M. (2008). The application of artificial neural networks in the prediction of microemulsion phase boundaries in PEG-8 caprylic/capric glycerides based systems. *International Journal of Pharmaceutics*, 361, 41-46
- Freeman, J.A., Skapura, D.M. (1991). *Neural networks. Algorithms, applications, and programming techniques*. Chapter 1: Introduction to ANS Technology. Addison-Wesley Pub (Sd)
- Gantt, J.A. and Gatzke, E.P. (2005). High-shear granulation modelling using a discrete element simulation approach. *Powder Technology*, 156, 195-212
- Hardy, I.J. and Cook, W.G. (2003). Predictive and correlative techniques for the design, optimisation and manufacture of solid dosage forms. *Journal of Pharmacy and Pharmacology*, 55, 3-18
- Holland, J. H. (1975). *Adaptation in Natural and Artificial Systems*. Cambridge, MA: MIT Press
- Hussain, A.S.; Shivanand, P. and Johnson, R.D. (1994). Application of Neural Computing in Pharmaceutical Product Development: Computer Aided Formulation Design. *Drug Development and Industrial Pharmacy*, 20(10), 1739-1752
- Kesavan, J.G. and Peck, G.E. (1996). Pharmaceutical Granulation and Tablet Formulation Using Neural Networks. *Pharmaceutical Development and Technology*, 1(4), 391-404
- Leuenberger, H. (1982). Granulation, new techniques. *Pharm. Acta Helv.*, 57, 72-82

- Leuenberger, H. (1994). Moist agglomeration of pharmaceutical powders. In: Chulia, D., Deleuil, M., Pourcelet, Y. (eds.). *Powder Technology and Pharmaceutical Processes, Handbook of Powder Technology*, vol. 9. Amsterdam: Elsevier B.V., 377–389
- Leuenberger, H. and Betz, G. (2007). Granulation Process Control - Production of Pharmaceutical Granules: The Classical Batch Concept and the Problem of Scale-Up. In: Salman, A.D., Hounslow, M.J. & Seville, J.P.K. (eds.). *Granulation, Handbook of Powder Technology*, Vol. 11. Amsterdam: Elsevier B.V., 705-733
- Leuenberger, H. and Imanidis, G., (1986). Monitoring mass transfer processes to control moist agglomeration. *Pharm. Technol*, March, 56-73
- Leuenberger, H. and Lanz, M. (2005). Pharmaceutical powder technology - from art to science: the challenge of the FDA's Process Analytical Technology initiative. *Advanced Powder Technol.*, 16(1), 3-25
- Leuenberger, H. and Usteri, M. (1989). Agglomeration of binary mixtures in a high-speed mixer. *Int. J. Pharm.*, 55, 135-141
- Leuenberger, H., Bier, H.P., Sucker, H. (1979). Theory of the granulation-liquid requirement in the conventional granulation process. *Pharmaceutical technology international*, 3, 61–68
- Ocloo, S., Edmonson, W. (2008). IIR Filter Adaptation Using Branch-and-Bound: A Novel Approach. *IEEE Transactions on Circuits and Systems - I: Regular Papers*, 55 (11), 3393-3403
- Oullion, M., Reynolds, G.K., Hounslow, M.J. (2009). Simulating the early stage of high-shear granulation using a two-dimensional Monte-Carlo approach. *Chemical Engineering Science*, 64, 673-685
- Parojčić, J., Ibrić, S., Djurić, Z., Jovanović, M., Corrigan, O.I. (2007). An investigation into the usefulness of generalized regression neural network analysis in the development of level A in vitro–in vivo correlation. *European Journal of Pharmaceutical Sciences*, 30, 264-272
- Peltarion® Documentation. Applications of adaptive systems [online]. Available at: <http://www.peltarion.com/doc> Accessed on 7 July 2010
- Petrović, J., Ibrić, S., Betz, G., Parojčić, J., Đurić, Z. (2009). Application of dynamic neural networks in the modeling of drug release from polyethylene oxide matrix tablets. *European Journal of Pharmaceutical Sciences*, 38 (2), 172-180
- Rowe, R.C. and Roberts, R.J. (1998a). Artificial intelligence in pharmaceutical product formulation: knowledge-based and expert systems. *PSTT*, 1, 153-159
- Rowe, R.C. and Roberts, R.J. (1998b). Artificial intelligence in pharmaceutical product formulation: neural computing and emerging technologies. *PSTT*, 1, 200–205
- Tu, W., Ingram, A., Seville, J., Hsiau, S. (2009). Exploring the regime map for high-shear mixer granulation. *Chemical Engineering Journal*, 145, 505–513

Turkoglu, M., Aydin, I., Murray, M., Sakr, A. (1999) Modelling of roller-compaction process using neural networks and genetic algorithms. *Eur. J. Pharm. Biopharm*, 48, 239-245

Watano, S., Sato, Y., Miyanami, K. (1997). Application of a neural network to granulation scale-up. *Powder Technology*, 90, 153-159

---

## 15 Thesis Outlook

Regarding Chapter I, for a better assumption that cellulose type II can be used in pulsatile drug release systems further studies using more proportions of it in the core composition, being directly compressed or granulated, with different model drugs (including high water-soluble drugs), as well as dissolution tests representing more precisely the environment of drug release, should be done. Stability tests could be realized to guarantee efficiency during product shelf-life. The disintegration efficiency/performance of cellulose type II after pass through a wet granulation process can also be deeper investigated, as well as its performance as a super-disintegrant in the presence of different types and amounts of binder, i.e. interactions with other embedding excipients. Experiments with increased number of ratios drug/excipients can also help in the investigation of the percolation thresholds for this new excipient. Furthermore, the influence of commercial available coating suspensions (with its chemical adjuvants) in the water permeation through the coating layer can become another study. To increase the accuracy of dissolution models, more data points in the first few minutes after coating rupture should be generated.

At Chapter II, the high-shear mixer walls, lid and blade could have been covered with a teflon lining to guarantee no powder adhesion. The measurement of all sampled granules densities would have offered a more complete monitoring of the changes in density and porosity during the granulation process. It was reinforced that the PC method is an efficient method of monitoring the agglomeration process. Powder physicochemical properties showed to be an intrinsic part of the PC method and deserve special attention. Inversely, measuring the PC can provide scientist with extra information about the powder properties. As much as information you collect from a material or process more you are able to understand it.

Regarding the use of ANNs in granulation process, on chapter II, it was concluded that its functionality has a wide applicability, once that same data can be inputted in different ways and/or one can predict same output by using different inputs. For a better network *learning* further experiments with additional drug loads may enclose the entire design space. ANNs have some drawbacks such as the lack of explanations and different solutions can be generated as the system initialize with random values and weights (the last can be overcome, in a close future, by software optimization). ANNs are coming to pharmaceutical field to stay as it showed to be not only a tool for prediction but also an interesting and useful tool for storage and mining of data.